

***Optimization of the water
photodetoxification process by
modified and unmodified TiO₂***

***Von der
Naturwissenschaftlichen Fakultät der
Gottfried Wilhelm Leibniz Universität Hannover***

Zur Erlangung des Grades

***Doktorin der Naturwissenschaften
Dr. rer. nat.***

***genehmigte Dissertation
von***

***Marta Pilar Bello Lamo, Licenciada en Ciencias
geboren am 20. Februar 1978 in Zaragoza, Spanien***

April 2009

Referee: Prof. Dr. T. Scheper
Co-referee: Prof. Dr. B. Hitzmann
Day of PhD exam: 09.06.09

Hiermit erkläre ich an Eides statt, dass ich die vorliegende Arbeit selbständig angefertigt und nur die angegebenen Hilfsmittel verwendet habe.

Hannover, April 2009

Marta P. Bello Lamo

Acknowledgements

I would like to thank Prof. Dr. Bahnemann for the possibility to do my PhD work in this institute and to take part in such an interesting project with the collaboration of BASF AG. I owe special thanks to Dr. Dillert for the supervision of this work and his help in research area.

I thank to all members of the BASF AG- project: Dr. Schindler, Mrs. Dr. Freitag, Mrs. Dr. Seeber and Mrs. Dr. Patchkas for their enthusiasm, scientific discussions, financial support and of course for the supplied of Elemental analysis and XRD- measurements.

To Prof. Dr. Scheper, Angelika, Martina, Martin, Ivo, Michael, Thorleif and Burghard (electrical Workshop); Wilhelm, Thorsten and Fiddi (mechanical Workshop) and of course not only my colleges from my research group but also all the people who I “met” in the labs, presentations (and other places such as “auf der Terraze”, “Sozialraum”, “Sommerfest”, etc) during the last three years...It was really a pleasure to work with you. Thanks for your help, suggestions, advices and your patience. The atmosphere of work could not be better.

To “mi Maestro” Prof. Dr. Laguna because he trusted in me and helped to come to Germany.

To Dr. Dan Driscoll and Steffi for helping me with the language corrections.

To my friends for being there in good and especially in bad moments: You gave me force to go ahead !!! (Mago, you are **of course** included ;-)))

To my parents, Andrés, Bea, Ana, m & m for your support, love...

*„Während ich esse, tue ich nichts weiter als essen.
Wenn ich laufe, dann mache ich nichts außer
laufen.*

*Und wenn ich kämpfen muss, dann wird dieser Tag
zum Sterben ebenso gut sein wie jeder andere.*

*Denn ich lebe weder in der Vergangenheit noch in
der Zukunft. Ich habe nur die Gegenwart, und nur
diese interessiert mich.*

*Wenn du immer in der Gegenwart leben kannst,
dann bist du ein glücklicher Mensch.*

*Dann wirst du bemerken, dass die Wüste lebt,
dass der Himmel voller Sterne ist und dass die
Krieger kämpfen, weil dies Teil des Menschen ist.*

*Dann wird das Leben zu einem großen Schauspiel,
zu einem Fest, denn es ist immer und
ausschließlich der Moment, den wir gerade
erleben.“*

Paulo Coelho

Contents

1	Kurzfassung.....	7
2	Abstract	8
3	Aim of the work	9
4	Introduction	10
5	Fundamentals	12
5.1	Heterogeneous photocatalysis	12
5.2	Direct photocatalysis	12
5.3	Indirect photocatalysis.....	14
5.3.1	Color compounds: dyes.....	15
5.3.2	Surface complexation.....	16
5.4	Advantages and disadvantages of aqueous heterogeneous photocatalysis	17
5.5	Extrinsic and intrinsic semiconductors	18
5.6	TiO ₂ as photocatalyst	20
5.7	Modification of Titanium (IV) dioxide	22
5.8	DCA as model compound	24
5.9	Escherichia coli as model Microorganism	27
6	Experimental	30
6.1	Synthesis of materials.....	30
6.1.1	Synthesis of the undoped –TiO ₂ photocatalysts	30
6.1.2	Synthesis of sulfur-doped TiO ₂	31
6.1.3	Synthesis of lanthanum-doped TiO ₂	34
6.2	Commercial photocatalysts	35
6.3	Characterisation of the new materials	35
6.3.1	X- ray diffraction (XRD).....	35
6.3.2	Elemental analysis.....	36
6.3.3	Absorbance- and Transmission- measurements.....	36
6.3.4	Reflection Measurements	36
6.3.5	Photonic Efficiency	39
6.4	Experimental procedure	41
6.4.1	Photocatalytic degradation of dichloroacetic acid (DCA)	41
6.4.1.1	Study of DCA-degradation under UV (A)-illumination	41
6.4.1.2	Study of DCA- degradation by pH-Stat Titration System	41
6.4.1.3	Study of DCA-degradation under outdoor solar illumination.....	44
6.4.1.4	Study of DCA under indoor solar illumination.....	44
6.4.1.5	Study of DCA-degradation under artificial visible illumination.....	46
6.4.2	Photocatalytic Disinfection of E. coli	48

7	Results and Discussion.....	51
7.1	Characterisation of materials.....	51
7.1.1	Unmodified- TiO ₂	51
7.1.2	Sulfur- doped TiO ₂	51
7.1.3	Lanthanum-doped TiO ₂	60
7.2	Photocatalytic activity study of sulfur doped TiO ₂	61
7.2.1	Study of undoped samples under UV (A)- illumination	61
7.2.2	Degradation of DCA by pH-Stat titration system	64
7.2.3	Degradation of DCA under outdoor solar illumination	68
7.2.3.1	Indoor solar illumination photoactivity test by DCA-degradation.....	70
7.2.3.2	Dependence on the relative position of the reactor	74
7.2.3.3	Study of sulfur-concentration and calcination temperature	77
7.2.3.4	Study of the dependence of different heating rates	79
7.2.4	Degradation of DCA under artificial visible illumination	82
7.2.4.1	Study of standard catalyst	82
7.2.4.2	Study of heating- profiles dependency.....	84
7.2.4.3	Dependence on sulfur molar ratio	86
7.3	Photocatalytic activity study of lanthanum-doped TiO ₂	89
7.4	Photocatalytic disinfection of E. coli and microbiological analysis concerning the amount of microorganisms (C.F.U.)	92
7.4.1	Study of different UV-irradiation sources.....	92
7.4.2	Study of flow rate dependency.....	95
7.4.3	Study of different catalyst loadings.....	97
8	Conclusions and Outlook	100
9	Literature	105
10	List of Abbreviations and Symbols.....	113
11	Appendix	116
11.1	Additional data	116
11.2	List of figures	120
11.3	List of tables.....	128
11.4	Curriculum Vitae.....	132

1 Kurzfassung

Heterogene Photokatalyse ist eine sehr effiziente Methode in der Wasserbehandlung. Der Schwerpunkt dieser Dissertation lag in der photokatalytischen Oxidation der organischen Verbindung Dichloressigsäure (DCA) und der photokatalytischen Inaktivierung von *Escherichia coli*.

Schwefel- und Lanthandotierte TiO₂-Photokatalysatoren wurden in einem Sol-Gel-Verfahren durch Dotierungs-Vorstufen mit Thioharnstoff bzw. Lanthannitrat hergestellt und anschließend durch Röntgendiffraktometrie (XRD), Elementaranalyse und Reflexionsmessungen (DRS) charakterisiert. Die Ergebnisse deuten darauf hin, dass Anatas-TiO₂ dabei der günstigste Kristalltyp ist. Im Vergleich mit nicht dotierten und kommerziellen Photokatalysatoren wie Sachtleben Hombikat UV 100, Kronos VLP 7001 und Toho legt Schwefel-dotiertes TiO₂ eine signifikante Absorption in einem Wellenlängenbereich von 400 bis 470 nm. Die Messungen der photokatalytischen Aktivität sowohl der selbstsynthetisierten als auch der kommerziellen Photokatalysatoren, welche bei den Messungen als Standards dienten, wurden anhand der Zersetzung von Dichloressigsäure (DCA) unter unterschiedlichen Beleuchtungs-Bedingungen wie Sonnenlicht, Innenraumbeleuchtung und künstlichen Licht durchgeführt.

Die photokatalytische Desinfektion eines ampicillinresistenten *E. Coli*-Stammes dienten dazu, das grundsätzliche Desinfektions-Potenzial zu überprüfen. Hierbei wurden unterschiedliche Parameter überprüft, wie der Einfluss des Lichts, die Photokatalysator-Beladung und die Durchflussrate. Es stellte sich heraus, dass die photokatalytische Inaktivierung einer Kinetik erster Ordnung folgt. Eine 2-log Inaktivierung von *E. Coli* wurde dabei unter künstlichem UV (A)- Licht im Mittel nach 90 Minuten erreicht.

Stichworte

Heterogene Photokatalyse, Dotierung, photokatalytische Aktivität, Sol-Gel Verfahren, TiO₂-Photokatalysator, Reflexionsmessungen, Elementaranalyse, Röntgendiffraktometrie, Dichloressigsäure, *Escherichia Coli*.

2 Abstract

Heterogeneous photocatalysis is a very efficient tool for water treatment. This PhD-work has focused on the photocatalytic oxidation of an organic compound, dichloroacetic acid (DCA), and the photocatalytic inactivation of *Escherichia coli*.

Sulfur doped TiO₂ and Lanthanum doped TiO₂ photocatalysts were prepared by a sol-gel process with doping precursors of thiourea and lanthanum nitrate, respectively, and characterized by X-ray diffraction (XRD), Elemental Analysis and Reflection measurements (DRS). The results indicate that anatase TiO₂ is the dominant crystalline type. The sulfur doped TiO₂ exhibits significant absorption within the range of 400 – 470 nm compared to the non-doped and commercial photocatalysts Sachtleben Hombikat UV 100, Kronos VLP 7001 and Toho. The photocatalytic activity of the new synthesized photocatalysts and commercial photocatalysts, which were chosen as standards, has been carried out by degradation of dichloroacetic acid (DCA) under different illumination conditions: sunlight; indoor illumination; and artificial illumination.

The photocatalytic disinfection of an *E. coli* strain, which is resistant against an antibiotic (Ampicillin) has been used to test disinfection efficiencies. Different parameters have been tested, such as the effect of the light, photocatalyst loading and flow rate. Photocatalytic inactivation of bacteria was found to follow first order kinetics. Approximately 90 minutes were required to achieve two-log inactivation of *E. coli* under UV (A)-light.

Key words

Heterogeneous photocatalysis, doping, photocatalytic activity, sol-gel process, TiO₂-photocatalyst, reflection measurements, elemental analysis, X-ray diffraction, dichloroacetic acid, *Escherichia coli*.

3 Aim of the work

The aim of this work is the development of new, visible light active photocatalysts for the application of water treatment. These materials, sulfur- and lanthanum- doped TiO₂, were prepared by a sol-gel method using different titanium precursors such as titanium (IV) isopropoxide and titanium (IV) butoxide and different dopant atoms by addition of thiourea (sulfur) and lanthanum nitrate (lanthanum), respectively, with the aim of forming new energy levels.

The influence of physical parameters during the preparation of the new materials, such as heating profile, calcination temperature and molar ratio, have been deeply studied in order to optimize the photocatalytic activity of the photocatalysts, especially under visible light conditions.

- In each series of experiments, commercial photocatalysts such as Sachtleben Hombikat UV 100, Kronos VLP 7001 and Toho (sulfur doped TiO₂ photocatalyst) were measured as references.
- As a model chemical pollutant dichloroacetic acid (DCA) was used because this molecule absorbs light only at wavelengths $\lambda \leq 250$ nm, avoiding the problem of catalyst sensitization e.g.: dyes, specially at longer wavelengths $\lambda \geq 400$ nm and catalyst surface complexes e.g. phenolic compounds.
- As a model biological pollutant *E. coli* was chosen for microorganism disinfection with Degussa P25 under UV-illumination. The selection of an *E. coli* strain which is resistant to Ampicillin negates the presence of other microorganisms.

4 Introduction

Water is a scarce resource and the contamination of ground- and wastewaters is an environmental problem, which requires a lot of effort to resolve. Different solutions have been proposed: air scrubbing, adsorption, activated carbon, etc., but some of them only remove the pollutant from one phase to another as well as requiring additional processes to eliminate toxic compounds. Heterogeneous Photocatalysis by TiO_2 is a potential solution that has been the subject of intense research efforts since the early 1970s. Photocatalytic oxidation has the advantage that usually pollutants in water are transformed into carbon dioxide and mineral acids. Thus one of its most noticeable qualities is the absence of selectivity allowing the treatment of very complex mixtures, that are transformed via oxidative or reductive paths. Hence, phenols, organic chloroderivatives, volatile organic pollutants (from washing towers), monomers or short chain polymer residuals, different leftover byproducts from the pharmaceutical industry - in particular some that (being biocides) cannot be treated in conventional biological reactors - pesticides, chlorine disinfecting byproducts, reduced metallic ions, *Escherichia Coli* cells, etc. can be effectively treated¹. Furthermore, UV/ TiO_2 has been chosen as one of the best disinfection technologies for bacteria and viruses because it is not dangerous for humans, and no malodorous halogenated compounds are formed in comparison to other disinfection procedures which use halogenated reagents.

The principle of photocatalysis, using TiO_2 as the photocatalyst, consists of the irradiation of TiO_2 particles with light of corresponding wavelengths until 387 nm for anatase ($E_g = 3.2$ eV) and 410 nm for rutile ($E_g = 3.0$ eV), creating electron-hole pairs. The electron transfers from the valence band to the conduction band and the hole remaining on the valence band reacts with hydroxyl groups on the surface, producing OH^\bullet radicals. The OH^\bullet radicals might react either with an adsorbed pollutant (heterogeneous photocatalysis) or desorb into the solution and react with the pollutant in solution phase (homogeneous photocatalysis). Titanium dioxide is the most widely used photocatalyst in environmental purification. However, TiO_2 is a semiconductor, which can only be activated with light of energy larger than the bandgap ($E_g = 3.2$ eV for anatase) limiting its application under solar light illumination or artificial visible light illumination. Moreover, traditional visible light catalysts are unstable under illumination (such as CdS and CdSe) or have very low activity (such as WO_3 and Fe_2O_3)².

Due to all of these reasons it is necessary to develop new photocatalysts which effectively absorb visible light. Many different attempts have been carried out to prepare solar active photocatalysts by modifying the TiO_2 surface with transition metals, by dye-sensitization or to couple titanium (IV) dioxide with narrow band gap semiconductors. Another more promising approach is doping TiO_2 with non metals to achieve narrower band gaps, extending the photocatalytic activity of TiO_2 into the visible light range.

Photocatalysis presents a wide spectrum of applications, which are described in Table 1.

Table 1. Overview of different photocatalysis applications³⁻⁵.

<i>Property</i>	<i>Category</i>	<i>Application</i>
Self-cleaning	Materials for residential and office buildings	Exterior tiles, kitchen and bathroom components, interior furnishings, plastic surfaces, building stone
	Indoor and outdoor lamps and related systems	Translucent paper for indoor lamp covers, coatings on fluorescent lamps and highway tunnel lamp cover glass
	Materials for roads	Tunnel wall, soundproofed wall, traffic signs and reflectors
	Others	Tent material, clothes for hospital garments and uniforms and spray coating for cars
Air-cleaning	Indoor air cleaners	Room air cleaner, photocatalyst-equipped air conditioners and interior air cleaner for factories
	Outdoor air purifiers	Concrete for highways, roadways and footpaths, tunnel walls, soundproofed walls and building walls
Water purification	Drinking water	River water, groundwater, lakes and water storage tanks
	Others	Fish feeding tanks, drainage water and industrial wastewater
Antitumor activity	Cancer therapy	Endoscopic-like instruments
Self-sterilizing	Hospital	Tiles to cover the floor and walls of operating rooms, silicone rubber for medical catheters and hospital garments and uniforms
	Others	Public rest rooms, bathrooms

5 Fundamentals

5.1 Heterogeneous photocatalysis

Heterogeneous photocatalysis involves redox reactions initiated by the excitation of a semiconductor. This excitation results from the absorption of photons which exhibit enough energy to induce the transfer of electrons from the valence band to the conduction band subsequently forming holes (positively charged vacancies) in the valence band. As a prerequisite for photocatalytic degradation, the pollutant must first be absorbed onto the TiO_2 surface, before the photodegradation process will occur.

5.2 Direct photocatalysis

In a semiconductor the energy difference between the lower edge of the conduction band and the upper edge of the valence band is defined as the band gap energy, E_g . The band gap of a semiconductor is smaller in comparison to an insulator thus the electrons can be excited by absorbed photons to the conduction band, leaving holes in the valence band.

The following mechanism of heterogeneous photocatalysis at the titania surface for the photo-mineralization of organic compounds was proposed⁶ (as shown Fig. 1).

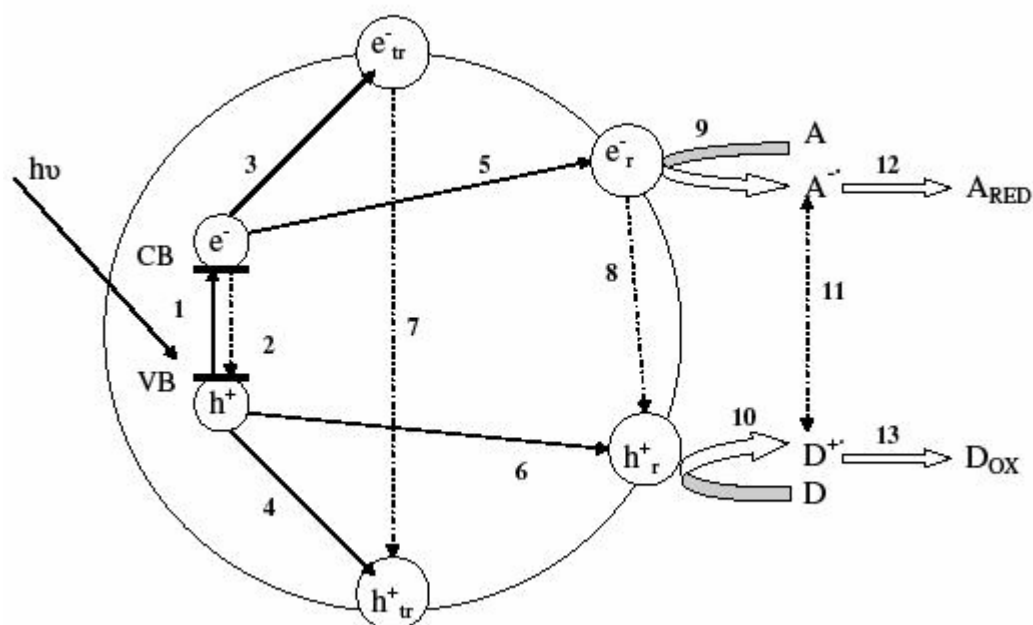


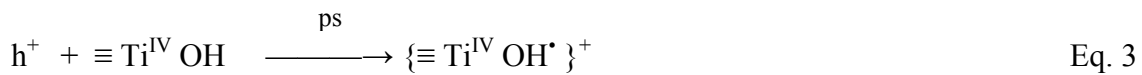
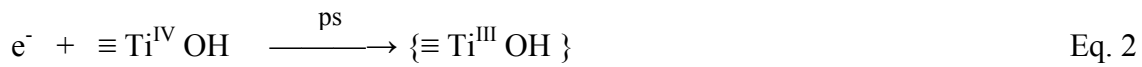
Fig. 1. Scheme of the elementary processes at a semiconductor particle upon irradiation⁷.

Electron hole pair formation (Step 1 in Fig. 1):

An electron can be excited into the conduction band from the valence band if it absorbs a photon that corresponds to the energy difference between the filled and the unfilled state. Any such photon must have an energy that is greater than or equal to the band gap between the valence band and the conduction band.



Charge carrier trapping (Step 3 and 4 in Fig. 1):



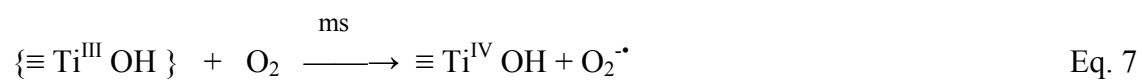
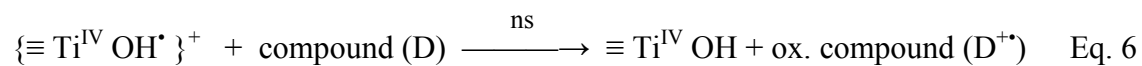
Recombination (Step 2, 7 and 8 in Fig. 1):

The opposite process to the creation of an electron-hole pair is called recombination. This occurs when an electron drops down in energy from the conduction band to the valence band. Just as the creation of an electron-hole pair may be induced by a photon, recombination can produce a photon.



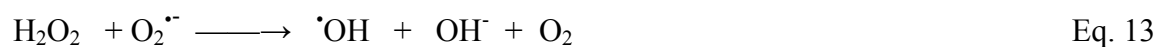
Interfacial electron transfer (IFET) (Step 5, 6, 9 and 10 in Fig. 1):

The overall quantum efficiency for interfacial charge transfer is determined by two critical processes. They are the competition between charge-carrier recombination and trapping (picoseconds to nanoseconds) followed by the competition between trapped carrier recombination and interfacial charge transfer (microseconds to milliseconds) ⁶.



It is assumed that organic pollutants, after photoexcitation of TiO₂ could be either oxidized directly by the holes, h⁺, or via surface bond hydroxyl radicals {≡ Ti^{IV} OH[•]}⁺.

Several different species result from the reduction of oxygen, such as: superoxide anion O₂^{•-} (Eq.8, 10 and 13); hydrogen superoxide radical HO₂[•] (Eq. 8, 9 and 10); hydrogen peroxide H₂O₂ (Eq. 9, 11, 12, 13 and 14); and hydroxyl radicals [•]OH (Eq. 12, 13 and 14) contributing to the oxidation of organic pollutants⁶.



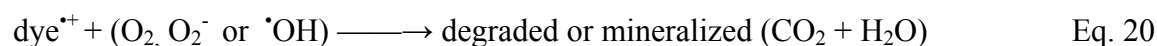
5.3 Indirect photocatalysis

Another photocatalytic mechanism was recently identified for the photodegradation of organic dyes⁸. Due to this mechanism, it is possible to carry out any visible light induced reactions on pure TiO₂.

Two different ways of sensitization of the titania surface can be defined:

- Sensitization by color compounds: dyes.
- Sensitization by colorless compounds via substrate –catalyst surface complexes.

The following mechanism of TiO₂ sensitization by dyes was proposed by Wu et al.⁹ As a prerequisite, the dye must be adsorbed onto the titania surface.



5.3.1 Color compounds: dyes

As a prerequisite, it is necessary for a dye (D) such as methylene blue, rhodamine B, etc that is able to absorb light (UV or visible) to be absorbed at the surface of TiO₂. The mechanism can be described as the transfer of an electron from an excited state of the dye (D^{*}) into the conduction band of the semiconductor (see Fig. 2). The oxidized molecule transforms further leading to self-degradation¹⁰.

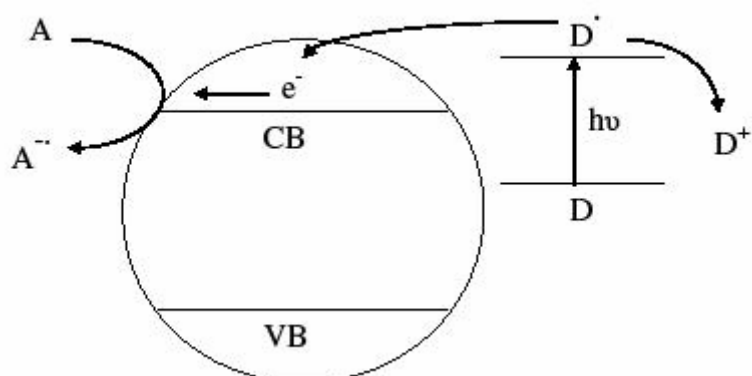


Fig. 2. Scheme of simplified mechanism of indirect photocatalysis upon irradiation¹⁰.

5.3.2 Surface complexation

The same prerequisites are necessary as for dyes sensitization: a compound, e.g. phenol, which can absorb light (UV or visible) and has been absorbed at the TiO_2 surface. This mechanism takes place between a surface complex-mediated path (ligand and the Ti (IV) site on the surface). As shown Fig. 3¹¹.

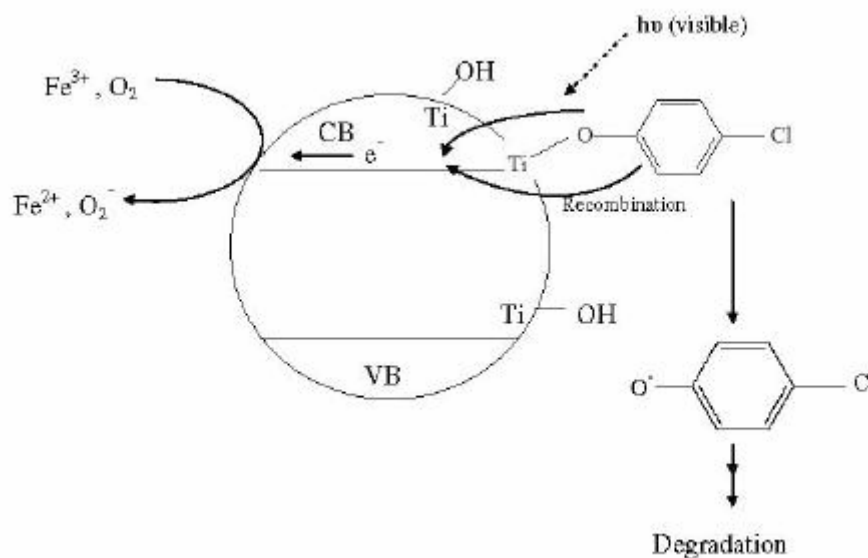


Fig. 3. Photodegradation of 4-Chlorophenol (4-CP) on pure titania by visible light illumination in the presence of Fe^{3+} or oxygen as electron acceptors¹¹.

Kim et al.¹¹ have also studied dichloroacetate as a model compound and they concluded that no photodegradation was observed in the visible light range for pure TiO₂ contrary to phenolic compounds which form complexes on the TiO₂ surface that absorb visible light in the region of $\lambda > 400$ nm.

5.4 Advantages and disadvantages of aqueous heterogeneous photocatalysis

An overall view of the potential of photocatalytic oxidation, taking into account the advantages and disadvantages for successful application of the process, has been discussed.¹²⁻¹⁴

- Chemical stability of TiO₂ in aqueous media and at a wide range of pH ($0 \leq \text{pH} \leq 14$)
- Low cost of TiO₂
- No additives required (only oxygen from air)
- Process applicable at low pollutant concentrations
- Process operation at ambient temperature and pressure conditions
- Possibility for natural resources utilization, e.g. solar radiation
- Total mineralization achieved for many organic pollutants
- Efficient with halogenated compounds even for bacteria in biological water treatment
- Possible combination with other water treatment procedures

There are also some disadvantages for the photocatalytic oxidation process application on an industrial scale for wastewater treatment, which were also summarized as follows:

- Necessity for treated water to be transparent at the spectral region, where the catalyst absorbs UV-light
- Contamination of the catalyst
- Competitive adsorption/ oxidation of co-pollutants
- Need for an effective and economic separation technique for suspended catalyst reactors
- Operation strategies need to be developed for the industrial scale: minimisation of incident light losses due to light scattering, solution to get uniform catalyst irradiation with the same incident intensity

Despite the reported drawbacks, research and development in this field are still very active e.g. the solar photocatalytic treatment of pesticides used in the food industry and agriculture, which is under study at Plataforma Solar de Almería (Spain) and is a very good example of the successful application of solar water photodetoxification.

Nevertheless, water purification has lagged behind air purification as a commercial process. The main problems in the practical application of water treatment as compared to air purification can be summarized as follows: the degradation efficiency is slower in water; pollutant concentration in water is higher than in air; pollutants have less contact with the photocatalyst due to its slower diffusion in water; and recovery of powder photocatalyst from water causes engineering difficulties in automatic operation³.

5.5 Extrinsic and intrinsic semiconductors

A semiconductor free of impurities is termed intrinsic while those doped with impurities are called extrinsic.

Intrinsic semiconductors

An intrinsic (pure) semiconductor has no impurities and the number of electrons, n , in the conduction band are the same as the number of holes, p , in the valence band. The number of electrons or holes is termed the intrinsic carrier concentration, n_i . The Fermi energy (E_F) is a concept used to describe the energy of the highest occupied electron energy level at absolute zero temperature, with intrinsic semiconductors this is near the middle of the energy gap.

Extrinsic semiconductors

Impurities that are added to control the carrier concentrations are named dopants. When a dopant has the same basic electronic structure as the atom it replaces the change in bonding behaviour is insignificant. However, if the atom then has one more or one fewer electron than the atom it replaces, this state has an extra electron or hole in it, not present in the intrinsic semiconductor. The extra electron or hole can move through the semiconductor causing a change in conductivity. Semiconductors doped with donor impurities are termed n-type, while those doped with acceptor impurities are called p-type. The n and p designations indicate which charge carrier acts as majority carrier. A donor atom creates excess negative charge carriers (electrons), while an acceptor atom creates excess positive charge carriers (holes).

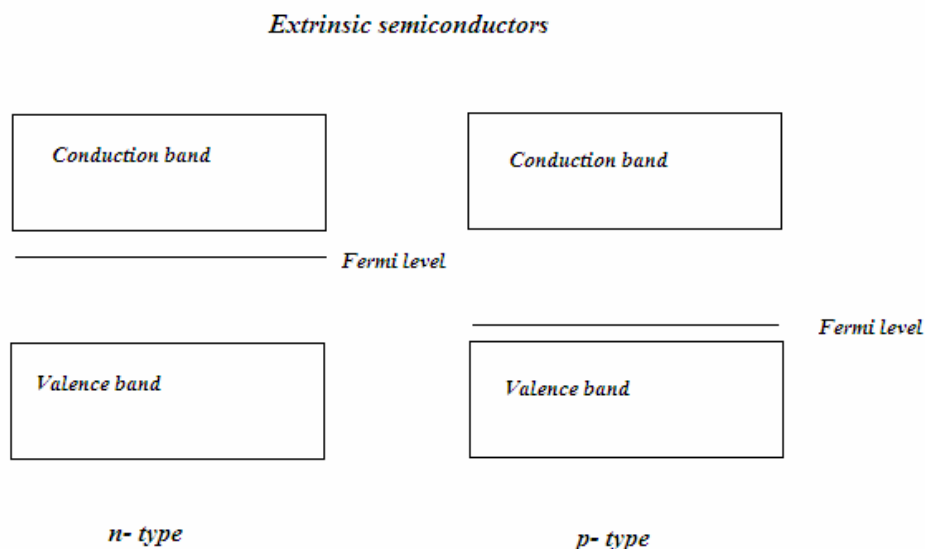


Fig. 4. Simplified schematic of newly formed extra energy levels for doped semiconductors¹⁵.

5.6 TiO_2 as photocatalyst

The photocatalysts have to fulfill some requirements⁶:

- Mechanical stability
- Long term stability
- Environmentally benign
- Chemically and biologically inert
- Resistant against photocorrosion and chemical corrosion
- Easily and cheaply available
- Active, by oxidation, against different pollutants

The band gap is not only an important property for a photocatalyst but also the position of the band edge. The values for band edge positions and band gap energies are shown in Fig. 5 for TiO_2 and other semiconductors.

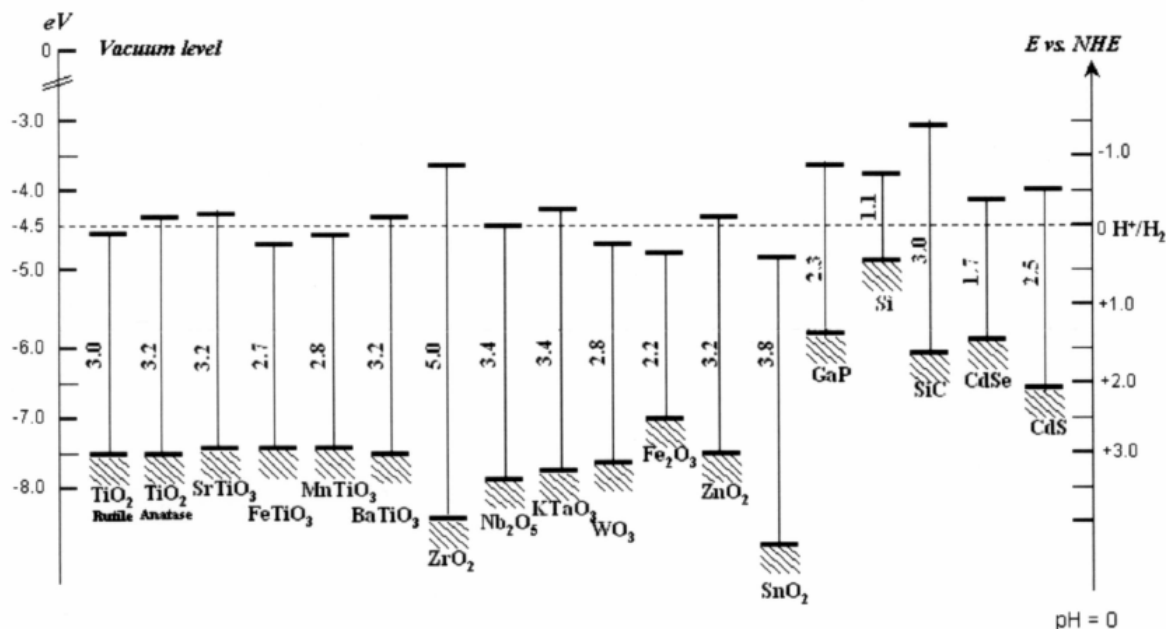


Fig. 5. Energetic positions of valence band, conduction band and band gap energies of semiconductors vs. NHE and Vacuum level in aqueous solution at $\text{pH} = 7$ ³⁷.

The aim for photodetoxification of water is the degradation of pollutants, thus the semiconductors which are of interest for this purpose must possess very powerful oxidant characteristics from the generated holes. Its valence band electrons have a very low reduction potential of -0.1 eV (anatase crystal) (the reduction potential of $E^{\circ}_{\text{H}_2/\text{H}^+} = -0.1$ eV) but the oxidation potential of the holes, in reference to the normal hydrogen electrode (NHE), is very high, 3.1 eV (the oxidation potential of $E^{\circ}_{\text{OH}^-/\text{O}_2} = 1$ eV and $E^{\circ}_{\text{H}_2\text{O}_2/\text{OH}^-} = 1.5$ eV). Therefore, TiO_2 is able to partially or totally degrade organic molecules to carbon dioxide, oxidize a number of inorganic molecules⁵ and kill bacteria such as *E. coli*.

The photocatalytic properties of TiO_2 can be probably ascribed to a favourable combination between very good absorption of UV- light and very high adsorption capacity. Other semiconductors can also be used as photocatalysts, e.g. ZnO , CdS , etc, but they do not comply with all the necessary requirements explained in section 5.6.

TiO_2 is a n- type semiconductor, which can be found in three different crystalline forms anatase, rutile and brookite (see Fig. 6), but mostly anatase and rutile are used for photocatalytic applications.

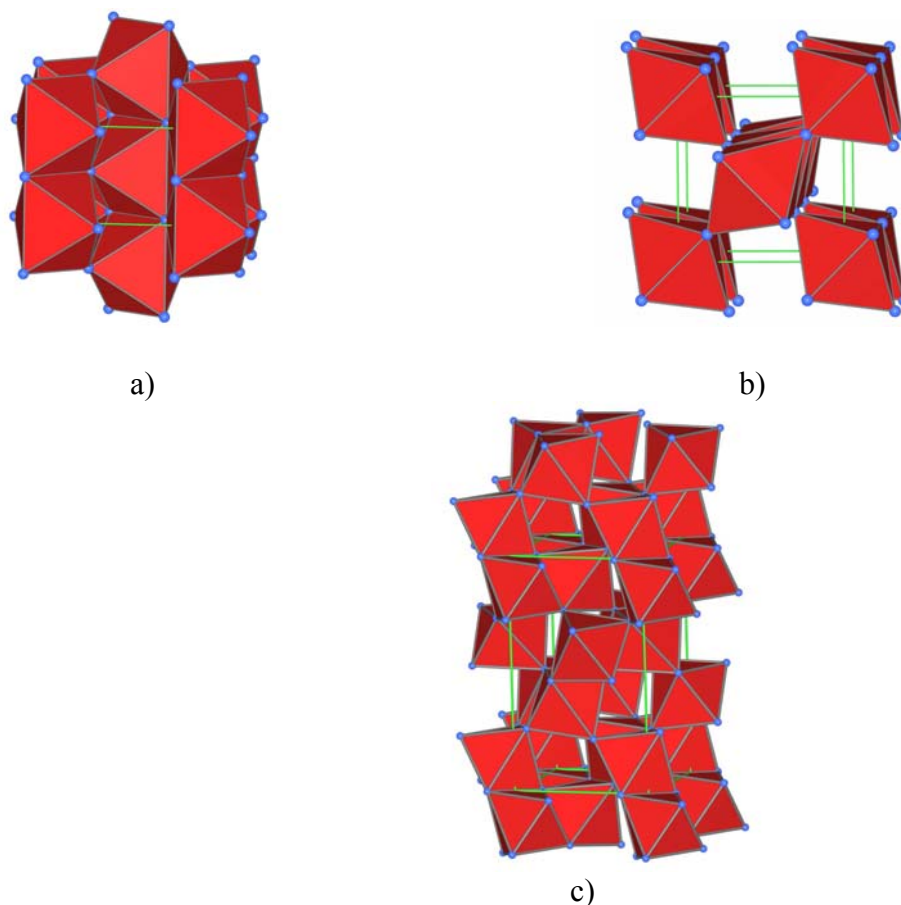


Fig. 6. Crystal structure of the three TiO_2 - modifications: a) rutile, b) anatase and c) brookite.

Thermodynamically, anatase is less stable than rutile. Therefore, anatase is formed at lower temperatures (below 600 °C). Anatase is the most photocatalytically active form of TiO₂, one reason can be the slower recombination of charge carriers than in rutile¹⁶. The band gap energy for anatase is about 3.2 eV, which corresponds with quantum of irradiation with a wavelength of 387 nm, whereas for rutile it is 413 nm (with a band gap energy of 3 eV).

5.7 Modification of Titanium (IV) dioxide

One method employed to activate TiO₂ in the visible light region consists of the modification of its physical or chemical structure, giving a shift in its absorption spectrum into the visible light region.

Various processes are cited in the literature: e.g. ion implantation methods, which require sophisticated and expensive equipment; chemical methods, which are more economical and can be carried out at or near room temperature. The first approach was doping titanium (IV) dioxide with transition metal ions, e.g. Choi et al.¹⁷ carried out a systematic study of metal ion doping for 21 metal ions. They found that doping with Fe³⁺, Mo⁵⁺, Ru³⁺, Os³⁺, Re⁵⁺, V⁴⁺ and Rh³⁺ significantly increased the photoactivity for both redox processes (oxidation and reduction) while Co³⁺ and Al³⁺ doping decreased the photoreactivity for carbon tetrachloride reduction and chloroform oxidation. It is also well known that the modification of TiO₂ with noble metals such as Ag, Au and Pt improved the photocatalytic properties of the photocatalysts, especially under UV-light conditions.

The modification of TiO₂ by doping forms intra band gap states close to the conduction or valence band edges which provoke visible light absorption at the sub-bandgap energies $h\nu_2$ and $h\nu_3$. Intra band gap states can also be created by lattice defects and trace amounts of impurities.

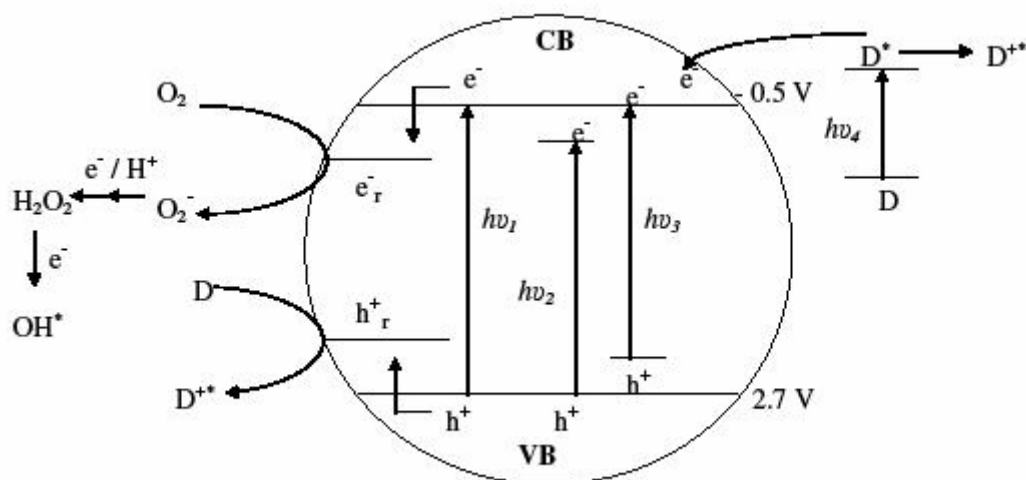


Fig. 7. Simplified schematic of different methods to activate titanium (IV) dioxide in the visible light region: sensitized ($h\nu_4$ explained in section 5.3.), doping with transition metals or non metal ion doping ($h\nu_2$ and $h\nu_3$)^{10, 18}.

These materials absorb visible light only in a few cases but rather suffer from photocorrosion, thermal instability and low quantum efficiency of the photoinduced charge carriers. In order to reduce recombination of photogenerated electrons and holes and to extend its light absorption into the visible light region, a second generation approach has been carried out by doping TiO₂ with non metal ions such as carbon, nitrogen, phosphorus, sulfur and fluorine.^{8, 10, 19-41} These photocatalysts, depending on the ion doping, could increase the lifetime of the so called photoinduced charge carriers in such a way that it predominates over the fast charge carrier recombination process, resulting in an enhanced reactivity. The photoreactivity of doped TiO₂ depends on several parameters¹⁸ such as dopant concentration, energy level of dopant with the TiO₂ lattice, their electronic configuration, distribution of dopants, electron donor concentration and light intensity.

A literature review of sulfur doped TiO₂ photocatalysts has been carried out to see the beginnings and the new discoveries in this field. The first reports about sulfur doped TiO₂ were published by Umebayashi et al.³⁴ They synthesized sulfur modified TiO₂ materials by calcination of TiS₂ at 500 °C and 600 °C under air. The sulfur doped TiO₂ photocatalysts were obtained in anatase form. It was detected by X-ray photoelectron spectra (XPS) that the sulfur atoms occupied oxygen sites in the TiO₂ lattice, forming Ti-S bonds. The color of the samples were white for the samples calcined at 500 °C and 600 °C, respectively. The photocatalyst, calcined at 500 °C for 90 min., had good photocatalytic properties by methylene blue degradation under visible light illumination conditions.

Prof. Ohno et al.²⁷ have prepared chemically sulfur modified titanium dioxide photocatalysts in which S (S^{4+}) substitutes for some of the lattice titanium atoms. The powders were calcined at different temperatures 400 °C, 500 °C, 600 °C and 700 °C. They showed strong absorption for visible light and high activities for degradation of methylene blue and 2- propanol in aqueous solution and partial oxidation of adamantane under irradiation at wavelengths longer than 440 nm. Photoabsorption in the visible region was strongest when the powder was calcined at 500 °C. The oxidation state of the sulfur atoms incorporated into the TiO_2 particles is determined to be mainly S^{4+} from XPS.

5.8 DCA as model compound

Dichloroacetic acid (DCA) is a typical by-product of chlorine disinfection. In aqueous solution at $pH > 2$ ($pK_s = 1.48$) it is mostly present as dichloroacetate. It was chosen due to its physical properties such as a high solubility in water, low volatility and its relevance as an industrial pollutant. Also, aliphatic compounds such as DCA absorb only light corresponding to wavelengths $\lambda \leq 250$ nm, this is a very important factor for experiments which are carried out under visible light illumination conditions.

The oxidation process depends on the pH. It can be expected that two different reaction paths for the dichloroacetate ion photocatalytic degradation (mono- and bi- dentate complexes) occur. Obviously, the type of the DCA coordination should strongly influence its activation and further photocatalytic degradation. A simplified scheme for DCA photocatalytic degradation is described below at acidic pH⁴².





Bahnemann et al.^{16, 42-45} reported the direct oxidation of dichloroacetic acid at acidic pH, by the hole forming the dichloroacetate radical (Eq. 22). By decarboxylation, carbon dioxide and the dichloromethyl radical are formed (Eq. 23). Adsorbed molecular oxygen reacts with the formed radical to create the dichloromethylperoxil radical (Eq. 24). The combination of two molecules of this radical gives hydrogen peroxide and phosgene^{42, 46} (Eq. 25) that hydrolyzes to hydrogen chloride and carbon dioxide (Eq. 26).

Hufschmidt et al.⁴⁷ have studied the DCA-degradation for three commercially available TiO₂ catalysts, Degussa P25, Sachtleben Hombikat UV 100 and Millennium TiONA PC50, which were platinised by a photochemical impregnation method in two ratios of platinum deposits (0.5 and 1 wt. %) under UV-light illumination conditions. The photonic efficiency for DCA-degradation increased from 6.1 % for pure Hombikat UV 100 (for a pH value of 3) to 16.05 % for Hombikat UV 100 (0.5 wt. % Pt) and to 21.35% for Hombikat UV 100 (1 wt. % Pt). No immediate relationship was found between the photocatalytic activity of the catalyst samples and their physical properties (surface area, adsorption of pollutants, absorption of light).

Bahnemann et al.⁴³ have tested DCA as a model compound to predict the light intensity dependence of the degradation processes, concluding that a linear dependency, i.e., an intensity independent quantum yield of the mineralization, is observed at pH 2.6, 7 and 11. Only at pH 5, they found that the rate of DCA degradation increased with the square root of the light intensity. The work showed that when illuminations were carried out with light intensities below 1.2 E-06 mol*photons/L*s, e.g., between 0.015E-06 mol*photons/L*s and 1.1E-06 mol*photons/L*s, even at pH 5 the quantum yield of DCA photodegradation no longer depended upon the irradiation intensity.

Lindner⁴⁸ has performed some studies with Hombikat UV 100 as the catalyst taking DCA as a model compound in order to check the dependency of parameters such as catalyst loading, pollutant concentration, pH, light intensity, on DCA-degradation (see Fig. 8)

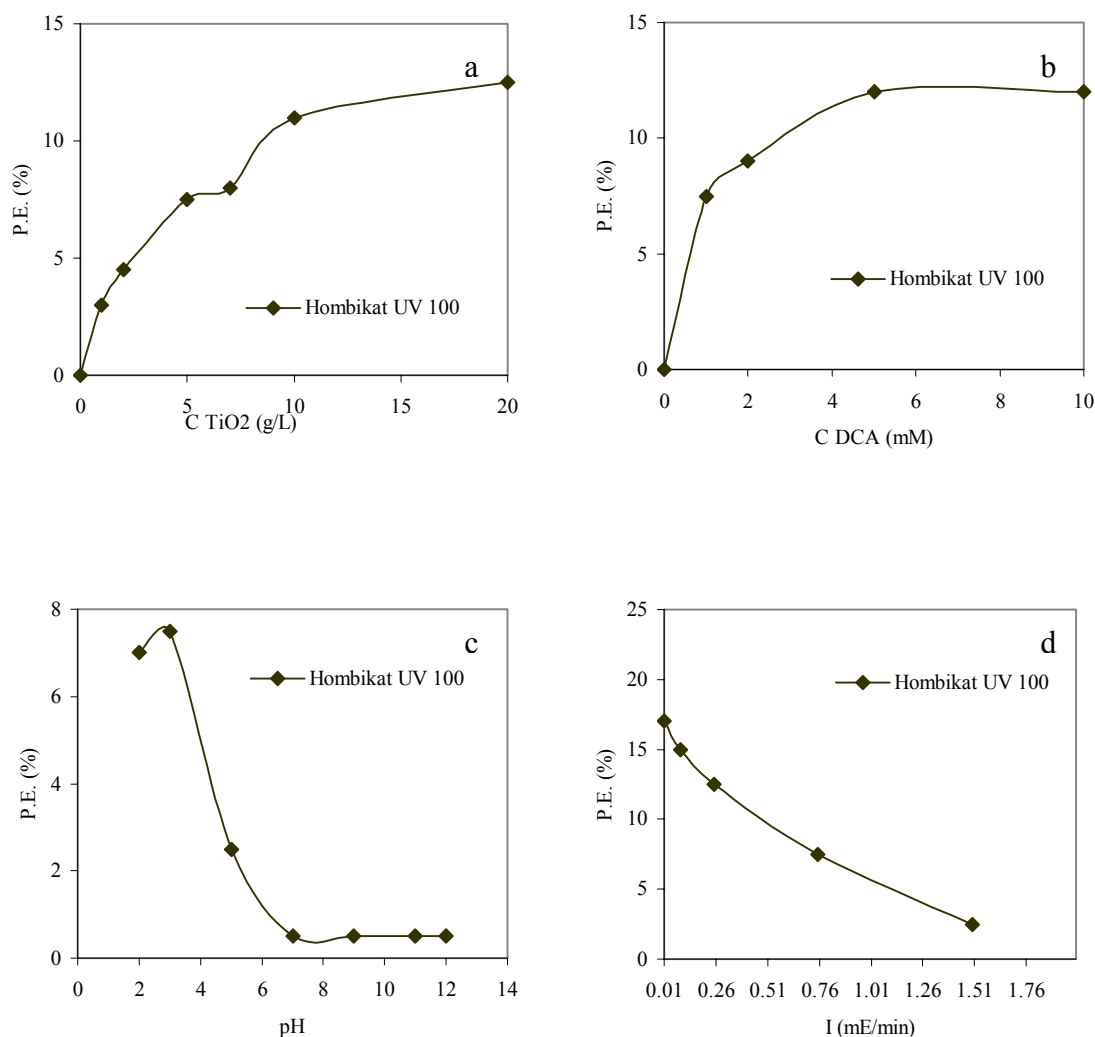


Fig. 8. Photonic efficiencies (%) of Hombikat UV 100⁴⁸ as function of a) catalyst loading, b) pollutant concentration, c) pH value, d) light intensity for the DCA- degradation (1 mM). *Experimental conditions:* 1 mM DCA, pH = 3, catalyst loading 5 g/L, 10 mM KNO₃, $\lambda > 320$ nm.

In relation to the dependency on catalyst loading, it is observed that, an exponential increase of the photonic efficiency value occurs when the catalyst concentration increases until about 10 g/L. A similar behaviour appears in the case of DCA –concentration, getting a maximum value of 5 mM. For Hombikat UV 100 the optimal pH value is 3, then the photonic efficiency decreases drastically at pH values ≥ 5 . There is a linear dependency (at pH 3) with the light intensity as concluded by Bahnemann et al.⁴³ and the photonic efficiency decreases, when the light intensity increases.

5.9 *Escherichia coli* as model Microorganism

In order to prevent human contact with pathogenic bacteria, large amounts of drinking water are daily chlorinated to inactivate pathogens in water treatment systems. However, numerous studies have reported the disadvantages of chlorination, because of recolonization and health hazards, especially the damage due to disinfection byproducts including trihalomethanes, haloacetic acids, bromate and chlorite formed during the reaction of chlorine with natural organic matter in the source water.^{1, 49, 50} Photocatalytic disinfection of *E. coli* has been studied as one of the alternative methods to chlorination in water disinfection.^{51,52,53}

Wei et al.⁵³ have reported that the irradiation of suspensions of *Escherichia coli* and TiO₂ (anatase) with UV-visible light of wavelengths longer than 380 nm resulted in the killing of the bacteria within 90 min. Oxygen was found to be a prerequisite for the bactericidal properties of the photocatalyst. Bacterial killing was found to adhere to first order kinetics.

Ibáñez et al.⁵⁴ have tested the bactericidal action of heterogeneous photocatalysis (UV-A/TiO₂) on representative strains of indicative bacilli of bacterial contamination *E. coli* and *S. typhimurium* and common soils and aquatic rods *E. cloacae* and *P. aeruginosa* cells. The TiO₂ photocatalytic technology can inactivate bacteria resistant to oxidative membrane damage caused by direct UV irradiation. They have found a high efficiency in the case of the studied microorganisms, particularly for the very resistant *E. cloacae*, which can not be inactivated in the absence of TiO₂.

Rincón et al.⁵⁵ have studied the effect of some parameters such as light intensity, extent of continuous irradiation, catalyst concentration and temperature on photocatalytic disinfection of *E. coli*. They concluded that intermittent illumination resulted in an increase in the time required for *E. coli* inactivation. No bacterial growth was observed after illumination of a contaminated TiO₂ suspension. In contrast, without catalyst, illuminated bacteria recovered its initial concentration after 3 h in the dark. TiO₂ concentrations higher than 1 g/L did not significantly increase the initial inactivation rate. Water turbidity negatively affects the photocatalytic inactivation of bacteria.

Coleman et al.⁵⁶ have determined the photocatalytic disinfection of *E. coli* by various catalysts. Degussa P25 was found to be the most effective catalyst and cell destructions followed first order kinetics. Non-buffered samples displayed a greater bactericidal efficiency which was attributed to an elevated stress on *E. coli* at acidic pH. Samples buffered with NaHCO₃ showed a decrease in bactericidal efficiency due to HCO₃⁻ ions competing with oxidising species and blocking (by adsorption) the TiO₂ particles. The optimum catalyst loading for Degussa P25 was 1 g/L.

Dillert et al.⁵⁷ have carried out experiments with pure bacteria *E. coli* and with pretreated municipal wastewater. Higher bactericidal efficiencies were found for pure bacteria *E. coli* systems than for pretreated municipal wastewater, thus they concluded that the disinfection is a consequence of both, the direct action of the light on the microorganisms as well as the photocatalytic action of the excited photocatalyst particles. The lower disinfection rates observed in the catalyst containing suspensions, when compared with catalyst free systems can be explained with the shadowing effect as well as by the competition between the microorganisms and the organic wastewater contaminants for the holes or surface bound hydroxyl radicals generated at the photocatalyst surface upon irradiation. In the municipal wastewater transformation products of the organic pollutants present, formed by photolysis and/or photocatalysis, can also act as germicides.

E. coli is an indicator bacteria generally used as a measure of faecal pollution of water and should not be present in any water used for drinking.^{52, 58} *E. coli* is the most important indicator organism within the group (Gram- negative bacteria) because it is found in large numbers and is relatively “easy to grow”. The mechanism of disinfection of *E. coli* is still unknown. However, there are some suggestions and evidence of the steps leading to cell inactivation. Recent studies attribute the TiO₂ photocatalytic action to promote peroxidation of phospholipid components of the lipid membrane, inducing cell membrane disorder, followed by loss of essential functions such as respiratory activity and cell death.^{53, 54, 59}

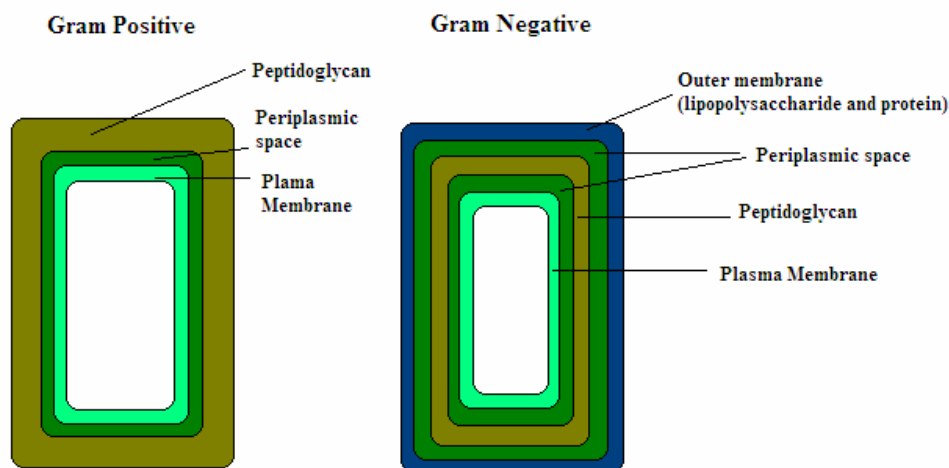


Fig. 9. Scheme of difference between Gram -positive and -negative bacteria's cell wall structure.^{60, 61}

The important chemical constituent of the bacterial cell wall is peptidoglycan. The cell walls of Gram- positive and Gram-negative bacteria differ considerably. In Gram- positive bacteria, the peptidoglycan layer is about 25 nm wide and contains an additional polysaccharide called teichoic acid, by contrast, Gram-negative bacteria have a peptidoglycan layer that is only 3 nm wide without any evidence of teichoic acid. The cell wall of Gram-negative bacteria contains various polysaccharides, proteins and lipids and so it is much more complex than the cell wall of Gram-positive bacteria. Also the cell wall is surrounded by an outer membrane barely separated from the cell wall by a so called periplasmic space. On the inner side of the cell wall the periplasmic space is wider. Bacterial toxins and enzymes apparently remain in this space and destroy antibacterial substances before they can affect the cell membrane. The multiple layers of the Gram-negative cell also afford protection by restricting the passage of chemicals such as antibiotics, salts, and dyes to the cell. The cell wall holds the cell together.^{62, 63} Moreover, the lipopolysaccharide layer (see Fig. 9) (not present in Gram-positive) plays a protective role in Gram-negative organisms. When antimicrobial substances act on the cell membrane (also called the plasma membrane) however, bacterial death usually follows.⁵⁹

The chosen *E. coli* strain for this work, is resistant against an antibiotic Ampicillin by means of a plasmid. A plasmid is an extra piece of DNA, usually much smaller than the chromosome, which can replicate independently. Plasmids exist apart from the chromosome as independent units in the cytoplasm. They are not essential to the life of the cell, but they may confer selective advantages for those organisms that have them. Plasmids encode various functions. Some encode enzymes which inactivate particular antibiotics; such R plasmids (resistance plasmids) usually make the host cell resistant to the relevant antibiotic(s).^{62, 63} For this work, a selected *E. coli* strain (resistant against Ampicillin) was taken in order to avoid the presence of other microorganisms.

6 Experimental

6.1 *Synthesis of materials*

Sulfur doped TiO₂ photocatalysts were prepared by a sol-gel process with titanium (IV) isopropoxide and thiourea as a doping precursor. Lanthanum doped TiO₂ photocatalysts were synthesized with titanium (IV) butoxide and lanthanum nitrate. Meanwhile, the undoped TiO₂ photocatalysts were synthesized with titanium precursors titanium (IV) isopropoxide and titanium (IV) butoxide, respectively, but without the addition of dopants.

6.1.1 Synthesis of the undoped –TiO₂ photocatalysts

The undoped TiO₂- photocatalysts were synthesized in order to study the photocatalytic activity of the different titanium precursors titanium (IV) isopropoxide and titanium (IV) butoxide without the presence of the dopant atoms (sulfur and lanthanum).

Titanium isopropoxide (50 g, 0.70 mol) was dissolved in 500 mL ethanol. The solution was stirred at room temperature overnight and concentrated under reduced pressure. After evaporation of ethanol, a white slurry was obtained. The slurry was kept overnight in a furnace at 80°C to eliminate the excess of organic compounds.

Titanium (IV) butoxide Ti(OBu)₄ (10 mL) in ethanol (40 mL) was added dropwise to a stirred solution of water (10 mL), ethanol (10 mL) and 70 % HNO₃ (2 mL) at room temperature. After stirring overnight, the transparent sol was concentrated under reduced pressure and dried at 80°C overnight. Finally, TiO₂ samples were gained by thermal treatment at different temperatures for three hours.

After both of these treatments, white powders were obtained. The powders were calcined at different temperatures (500°C, 600°C and 700 °C) for three hours, each (as shown Table 2).

Table 2. List of the synthesized undoped photocatalysts and their different calcination temperatures.

<i>Name</i>	<i>Ti- precursor</i>	<i>Calc. T (°C)</i>	<i>Calc. Time (h)</i>
TiI1	Ti-isopropoxide (IV)	500	3
TiI2	Ti-isopropoxide (IV)	600	3
TiI3	Ti-isopropoxide (IV)	700	3
TiB1	Ti-butoxide (IV)	500	3
TiB2	Ti-butoxide (IV)	600	3
TiB3	Ti-butoxide (IV)	700	3

6.1.2 Synthesis of sulfur-doped TiO₂

To prepare sulfur doped TiO₂ powder, the procedure described by Prof. Ohno et. al.²⁷ was followed: (50 g, 0.175 mol) titanium isopropoxide (Fluka, purity of 97 %) was mixed with (53.6 g, 0.70 mol) thiourea (Fluka, purity of 98%) at a molar ratio of 1:4 in ethanol (500 mL, Roth). Other molar ratios have been also tested 1:2 and 1:6. The solution was stirred at room temperature overnight and concentrated under reduced pressure. After evaporation of ethanol, a white slurry was obtained. The slurry was kept overnight in a furnace at 80°C to eliminate the excess of organic compounds. After this treatment, a white powder was obtained.

This powder was calcined at different temperatures from 300 to 700 °C for three and seven hours, and yellow powders were obtained. The intensity of the yellow color depends on the calcination temperatures. The intensity of the color increases with the temperature until 600 °C, after that the intensity of the colour is less strong.

Table 3 summarizes the different preparation conditions for the sulfur doped TiO₂ photocatalysts. Different parameters have been studied such as several molar ratios of titanium isopropoxide (IV) to thiourea (1:2, 1:4 and 1:6), different calcination rates (10 °C/h, 50 °C/h, 100 °C/h, 200 °C/h, 300 °C/h and 400 °C/h) and different calcination temperatures from 300°C to 750°C at two different calcination times of 3 hours and 7 hours.

Table 3. The different molar ratios and calcination temperatures chosen for the synthesis of the sulfur- doped TiO₂ photocatalysts.

<i>Name</i>	<i>Molar ratio</i>		<i>Calc. rate(°C/h)</i>
	<i>Tiisop./TU</i>	<i>Calc. T (°C)</i>	
KS1	1:4	300 °C (3h)	~ 150 °C/h
KS2	1:4	500 °C (3h)	~ 150 °C/h
KS3	1:4	550 °C (3h)	~ 150 °C/h
KS4	1:4	575 °C (3h)	~ 150 °C/h
KS5	1:4	600 °C (3h)	~ 150 °C/h
KS6	1:4	625 °C (3h)	~ 150 °C/h
KS7	1:4	650 °C (3h)	~ 150 °C/h
KS8	1:4	700 °C (3h)	~ 150 °C/h
KS9	1:4	750 °C (3h)	~ 150 °C/h
KS10	1:4	500 °C (7h)	~ 150 °C/h
KS11	1:4	600 °C (7h)	~ 150 °C/h
KS12	1:4	650 °C (7h)	~ 150 °C/h
KS13	1:4	750 °C (7h)	~ 150 °C/h
KW1	1:2	500 °C (3h)	~ 150 °C/h
KW2	1:2	600 °C (3h)	~ 150 °C/h
KW3	1:2	650 °C (3h)	~ 150 °C/h
KW4	1:2	750 °C (3h)	~ 150 °C/h
KW5	1:2	500 °C (7h)	~ 150 °C/h
KW6	1:2	600 °C (7h)	~ 150 °C/h
KW7	1:2	650 °C (7h)	~ 150 °C/h
KW8	1:2	750 °C (7h)	~ 150 °C/h
KM1	1:6	500 °C (3h)	~ 150 °C/h
KM2	1:6	600 °C (3h)	~ 150 °C/h
KM3	1:6	650 °C (3h)	~ 150 °C/h
KM4	1:6	750 °C (3h)	~ 150 °C/h
KM5	1:6	500 °C (7h)	~ 150 °C/h
KM6	1:6	600 °C (7h)	~ 150 °C/h
KM7	1:6	650 °C (7h)	~ 150 °C/h
KM8	1:6	750 °C (7h)	~ 150 °C/h

Table 3 (continuation). The different molar ratios, calcination temperatures and calcination rates for the synthesis of the sulfur- doped TiO₂ photocatalysts.

<i>Name</i>	<i>Molar ratio</i>		<i>Calc. T (°C)</i>	<i>Calc. rate(°C/h)</i>
	<i>Tiisop./TU</i>			
KT1	1:4		550 °C (3h)	400 °C/h
KT2	1:4		575 °C (3h)	400 °C/h
KT3	1:4		600 °C (3h)	400 °C/h
KT4	1:4		625 °C (3h)	400 °C/h
KT5	1:4		550 °C (3h)	300 °C/h
KT6	1:4		575 °C (3h)	300 °C/h
KT7	1:4		600 °C (3h)	300 °C/h
KT8	1:4		625 °C (3h)	300 °C/h
KT9	1:4		550 °C (3h)	200 °C/h
KT10	1:4		575 °C (3h)	200 °C/h
KT11	1:4		600 °C (3h)	200 °C/h
KT12	1:4		625 °C (3h)	200 °C/h
KT13	1:4		550 °C (3h)	100 °C/h
KT14	1:4		575 °C (3h)	100 °C/h
KT15	1:4		600 °C (3h)	100 °C/h
KT16	1:4		625 °C (3h)	100 °C/h
KT17	1:4		550 °C (3h)	50 °C/h
KT18	1:4		575 °C (3h)	50 °C/h
KT19	1:4		600 °C (3h)	50 °C/h
KT20	1:4		625 °C (3h)	50 °C/h
KT21	1:4		550 °C (3h)	10 °C/h
KT22	1:4		575 °C (3h)	10 °C/h
KT23	1:4		600 °C (3h)	10 °C/h
KT24	1:4		625 °C (3h)	10 °C/h
KT21A	1:6		550 °C (3h)	10 °C/h
KT22A	1:6		575 °C (3h)	10 °C/h
KT23A	1:6		600 °C (3h)	10 °C/h
KT24A	1:6		625 °C (3h)	10 °C/h

6.1.3 Synthesis of lanthanum-doped TiO₂

The preparation of lanthanum-doped TiO₂ nanoparticles was performed by a sol-gel procedure with 10 mL titanium (IV) butoxide (Aldrich, purity of 98 %) as the starting material. Ti(OBu)₄ was mixed with 40 mL ethanol (Roth). The mixed Ti(OBu)₄: ethanol solution was then added dropwise into a mixture consisting of 10 mL water and 10 mL ethanol as well as the appropriate amount of La₂O₃ (Fluka, purity of 99.9 %) dissolved in 70 % HNO₃ (Fluka, purity of 70 %) at room temperature with stirring to carry out the hydrolysis. After stirring overnight, the transparent sol was concentrated under reduced pressure and dried at 80°C overnight⁶⁴. Finally, TiO₂ samples were gained by thermal treatment at different temperatures: 400 °C, 500 °C, 600 °C and 700 °C for three hours.

Table 4 summarizes the different preparation conditions for the lanthanum- doped TiO₂ photocatalysts. Several parameters have been studied such as different lanthanum concentrations (0.4 % and 0.9 %) and different calcination temperatures in the range 400°C to 700°C with a corresponding heating rate of 400 °C/h.

Table 4. The experimental conditions of different lanthanum-concentrations, calcination temperatures and heating rates for the preparation of lanthanum- doped TiO₂ photocatalysts.

<i>Name</i>	<i>La-Conc. (%)</i>	<i>Calc. T (°C)</i>	<i>Calc. rate(°C/h)</i>
KL1	0.4 %	400 °C (3h)	400 °C/h
KL2	0.4 %	500 °C (3h)	400 °C/h
KL3	0.4 %	600 °C (3h)	400 °C/h
KL4	0.4 %	700 °C (3h)	400 °C/h
KL5	0.9 %	400 °C (3h)	400 °C/h
KL6	0.9 %	500 °C (3h)	400 °C/h
KL7	0.9 %	600 °C (3h)	400 °C/h
KL8	0.9 %	700 °C (3h)	400 °C/h

6.2 Commercial photocatalysts

Four different commercial photocatalysts (see Table 5) have been tested. Hombikat UV 100 and Degussa P25 are established worldwide as standard photocatalysts and they are very active catalysts specially under UV-light conditions. Meanwhile, Kronos (batch was produced in 2005) and Toho are also active under visible light conditions. Toho is a sulfur doped TiO₂ photocatalysts, synthesized from titanium isopropoxide (IV) and thiourea. These data were kindly supplied by BASF AG.

Table 5. Physical properties of different types of commercial TiO₂ catalysts used in this study.

Name	Type	Composition	Size of crystallites (nm)	Surface area (m ² *g ⁻¹)	Band gap (eV)
Sachtleben Hombikat	UV 100	Anatase	5	300 ± 15	3.2
Evonik Degussa	P25	A/R 70/30	20	55 ± 15	3.1
Kronos ¹	VLP 7001	Anatase	15	225 ± 15	3.0
Titanium Co. Toho ²⁷	NS-51	A/R	-	6.5 ± 15	2.9

6.3 Characterisation of the new materials

6.3.1 X- ray diffraction (XRD)

XRD- patterns were collected using a D4 Endeavor Diffractometer. Crystalline sizes were estimated using Scherrer's equation:

$$\beta_{hkl} = \frac{K * \lambda}{L_{hkl} * \cos \theta_{hkl}} \quad \text{Eq. 27}$$

¹ Data supplied by Kronos company

where,

β_{hkl}	width of the peak of a specific phase (hkl)
K	constant that varies with the method of taking the breadth ($0.89 < K < 1$)
λ	wavelength of incident X-rays
θ	center angle of the peak
L_{hkl}	crystallite length

6.3.2 *Elemental analysis*

Elemental analysis of the titania samples were carried out with two different instruments: a CHN- Analyser (Vario El Cube from the Elementar company) and an S- Analyser (Euro EA 3000, Eurovector company). The measurement principle in both cases consists of the calcination of the sample at 1000 °C in the presence of molecular oxygen. The newly formed carbon dioxide or sulfur dioxide, respectively, were determined by gas chromatography (Helium as carrier gas). The values are given in weight percent.

6.3.3 *Absorbance- and Transmission- measurements*

The measurements were carried out with an UV-Spectrometer (Varian Cary 100).

6.3.4 *Reflection Measurements*

The UV- Spectrometer (Varian Cary 100) equipped with an integrating sphere from Labsphere was used to analyze the reflectance spectra of the powders ranging from 200 to 600 nm.⁶⁵⁻⁶⁷

Cover glasses for optical microscopy (0.2 mm in thickness) were cut in rectangles with a width of 0.9 cm and a length of 4.3 cm employing a diamond- tip glass cutter. They were first cleaned with acetone, then with methanol and finally with distilled water. A thin layer of the respective TiO_2 particles was deposited onto the thin glass panes. The TiO_2 layers were prepared from a suspension of 70 mg photocatalyst in 10 mL isopropanol. In the case of the commercial catalysts it was considerably easier to obtain this coating on the glass. For the sulfur- doped powders more than one hour sonication in an ultrasonic bath was required to obtain stable coating suspensions. Reflectance measurements of Degussa P25, Hombikat UV 100 and Kronos were carried out as standards in order to compare the values of the sulfur-doped TiO_2 catalysts to those of known materials.

For this study a modification of the commercially available integrating sphere set- up has been constructed in order to probe the samples (on glass) placed in a quartz cuvette. For this purpose, a supporting stand for the cuvette was made of polytetrafluoroethylene (Teflon). This material is normally used as a reference standard for reflectance measurements.

The reflectance factor of Teflon found for the hemispherical accessory is close to unity. For the measurements an empty cuvette was taken as a standard. Fig. 10 shows the values of reflectance in percent (R %) corresponding to the commercial catalyst Hombikat UV 100 (as an example).

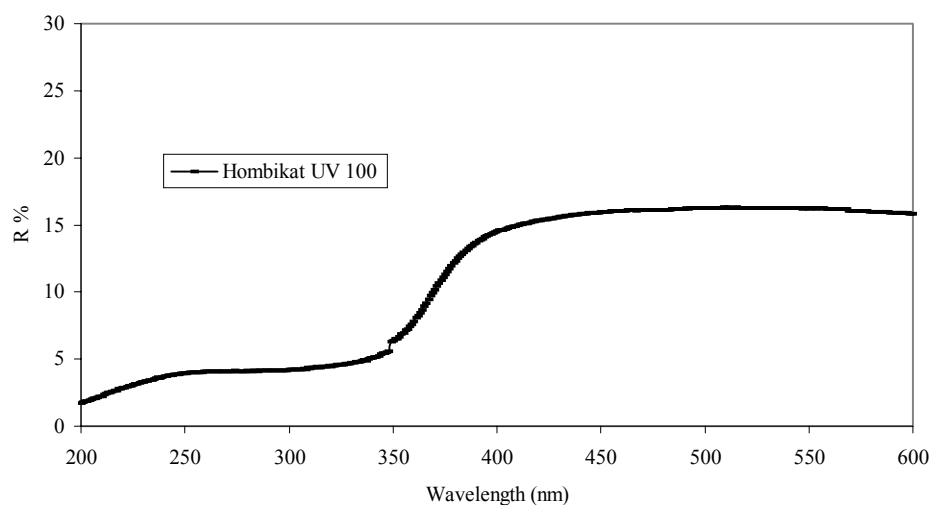


Fig. 10. Plot of the Reflectance spectra of the commercial titania powder Hombikat UV 100 as a function of wavelength.

Generally, for the calculation of the band gap energy, the diffuse reflectance R is expressed in terms of $F(R)$, the so-called Kubelka-Munk (KM) function⁶⁵⁻⁶⁷. The diffuse reflectance R of the sample is related to the Kubelka-Munk function by:

$$F(R) = \frac{(1-R)^2}{2R} = \frac{\alpha}{S} \quad \text{Eq. 28}$$

where α and S represent the absorption coefficient and the scattering coefficient, respectively. To evaluate the influence of sulfur doping, the Kubelka-Munk model is frequently used to estimate the absorption band gap from the diffuse reflection spectra⁶⁵⁻⁶⁷. The plot of $[F(R) \cdot h\nu]^{1/\eta}$ versus $h\nu$ can be applied to determine the band gap energy. In the Kubelka-Munk plot, $h\nu$ is the energy of the incident photon and the exponent η depends on the type of optical transition caused by photon absorption. In crystalline semiconductors, where crystal momentum is conserved and the electron transitions obey well-defined selection rules, η is $1/2$, $3/2$, 2 and 3 when the transitions are direct-allowed, direct-forbidden, indirect-allowed, and indirect-forbidden, respectively. In our case, the energy was obtained using this method ($\eta = 2$), e.g., assuming the transition to be indirect and allowed⁶⁸ for the undoped TiO_2 , sulfur-doped and lanthanum-doped TiO_2 . The experimental band gap is usually obtained from the X-axis intercept of the slope. (see Fig. 11).

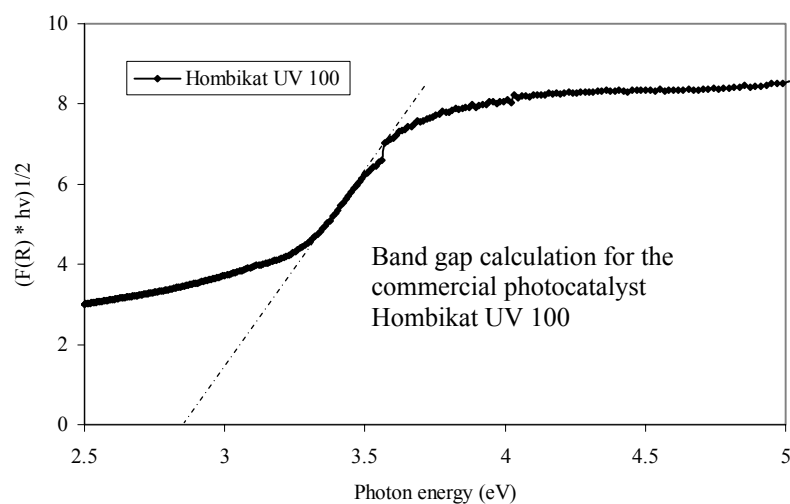


Fig. 11. Plot of transformed Kubelka Munk function versus Photon energy (eV) for the commercial catalysts Hombikat UV 100.

As shown in Fig. 11, the experimental band gap energy calculated by means of the Kubelka Munk function for Hombikat UV 100 is 2.9 ± 0.1 eV. In the literature the band gap energy value for anatase is 3.2 eV, which corresponds with a wavelength of 388 nm. It follows that anatase can only be activated in the range of UV (A) irradiation from 280 nm to 388 nm¹⁶.

6.3.5 Photonic Efficiency

The photodegradation of DCA proceeds in only one step without the formation of intermediate products, as shown in the following equation:



$$-\frac{\Delta C_{\text{DCA}}}{\Delta t} = \frac{\Delta C_{\text{H}^+}}{\Delta t} = \frac{1}{2} \frac{\Delta C_{\text{Cl}^-}}{\Delta t} = \frac{1}{2} \frac{\Delta C_{\text{TOC}}}{\Delta t} \quad \text{Eq. 30}$$

From the TOC- values, the degradation rates for each studied catalyst were calculated. This parameter is defined as,

$$\frac{\Delta C_{\text{TOC}}}{\Delta t} = \text{Rate}_{\text{TOC}} \quad \text{Eq. 31}$$

The photonic efficiency ζ_{TOC} , can be calculated using the equation given below:
($\zeta_{\text{TOC}} = 2 \zeta_{\text{DCA}}$)

$$\zeta_{\text{TOC}} (\%) = \frac{\text{Rate}_{\text{TOC}}}{I_{\text{hv}} (\text{vol})} * 100 \quad \text{Eq. 32}$$

with the rate ($\text{mol} \cdot \text{l}^{-1} \cdot \text{s}^{-1}$) and I_{hv} (vol) being the incident UV-A photon flux ($\text{mol} \cdot \text{l}^{-1} \cdot \text{s}^{-1}$).

I_{hv} (for monochromatic light) is defined as:

$$I_{hv} = \frac{I * \lambda}{N * h * c} \text{ (mol/m}^2\text{*s)} \quad \text{Eq. 33}$$

where,

I = Intensity of the light (W/m^2)

λ = lambda value (m)

N = Avogadro number $6.02\text{E}+23$ (mol^{-1})

h = Planck's constant $6.63\text{E}-34$ (J*s)

c = speed of light $3\text{E}+08$ (m*s^{-1})

The value of I_{hv} is limited by the window-surface of the reactor (A), which depends on the set-up size. The I_{hv} -value must be related to the reactor volume (V) (in this study $V = 200$ mL).

$$I_{hv}(\text{vol}) = \frac{I_{hv} * A}{V} \text{ (mol/m}^3\text{*s)} \quad \text{Eq. 34}$$

where,

I_{hv} = (Einstein/ $\text{m}^2\text{*s}$)

$A = \pi * r^2 = 4.42\text{E}-03$ m^2

$V = 2\text{E}-04$ m^3

$I = 1.55$ W/ m^2

6.4 Experimental procedure

6.4.1 Photocatalytic degradation of dichloroacetic acid (DCA)

Dichloroacetic acid (DCA) has been chosen as a model compound (for more details see section 5.8.) due to its physical properties such as very good solubility in water and no volatile compounds. Moreover, aliphatic compounds only absorb light with wavelengths lower than 250 nm, that it is a very interesting point, especially for experiments which are carried out under visible light illumination conditions.

6.4.1.1 Study of DCA-degradation under UV (A)-illumination

The photocatalytic activity of the undoped samples for the degradation of DCA was studied under UV-illumination conditions. Each reactor contained 1mM DCA dissolved in 200 mL distilled water in the presence of KNO₃ (10 mM). At the beginning of the experiment a value of pH = 3 was noted. The photocatalytic activity test has been used here but for these experiments, the illumination (for three hours) was carried out using Philips R-UV A 100 W lamps with an emission maximum of 351 nm and an intensity of 1.55 mW/cm² measured with an UV (A)-light Meter instrument at the upper reactor windows.

6.4.1.2 Study of DCA- degradation by pH-Stat Titration System

The overall stoichiometry of the photocatalytic degradation of dichloroacetic acid in a suspension of semiconductor particles is:



$$-\frac{\Delta C_{\text{DCA}}}{\Delta t} = \frac{\Delta C_{\text{H}^+}}{\Delta t} = \frac{1}{2} \frac{\Delta C_{\text{Cl}^-}}{\Delta t} = \frac{1}{2} \frac{\Delta C_{\text{TOC}}}{\Delta t} \quad \text{Eq. 30}$$

Therefore, the complete photocatalytic oxidation of dichloroacetic acid leads to the formation of carbon dioxide which (as detailed below) depending upon the pH, will react with water to form bicarbonate or carbonate. The protons formed in the latter reaction (see Eq. 29) are measured during the photocatalytic tests with a pH-electrode (pH- values were measured with a Metrohm 605 pH-meter and Metrohm 6.0259.100 electrode).

The so-called pH-stat titration technique, which allows the in-situ measurement of H^+ formed during photolysis experiments with sufficient sensitivity even at low light intensities, is used. The corresponding experimental set-up is shown in Fig. 12.

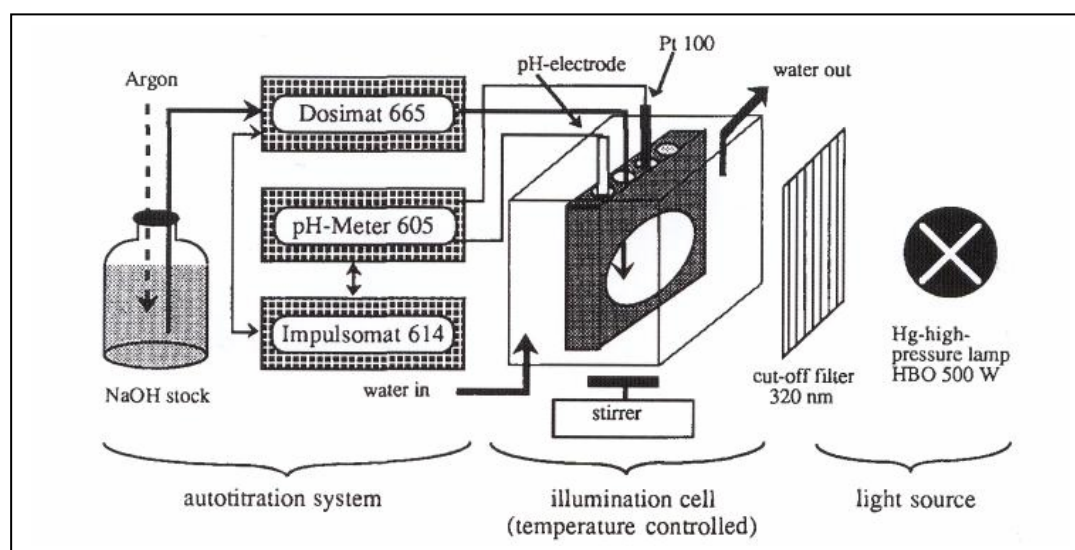


Fig. 12. The pH-stat titration system employing Metrohm instruments⁶⁹.

In order to keep the pH- value constant, the Dosimat adds precisely the required amount of base (NaOH 0.1 M), which is governed by the Impulsomat, into the reaction solution. The data (quantity of NaOH added) from the dosimat are transferred to a PC. The reactor consists of UV(A)-transparent glass (volume is 250 mL) with a cooling jacket to avoid heating. A Xenon lamp is used to irradiate the reactor. During the degradation of dichloroacetic acid CO_2 is formed, but between pH 6.3 and 10.2 it is converted to HCO_3^- and at higher pH the formation of CO_3^{2-} must be considered too. Therefore, the amount of NaOH consumed rises with increasing pH- value because it is necessary to neutralize the protons, which do not result from the primary stoichiometry but are formed by the reaction of carbon dioxide with water. $(NaOH)_{real} = (H^+) + (HCO_3^-) + (CO_3^{2-})$.

The amount of organic carbon converted into carbon dioxide was measured employing a Shimadzu TOC-5000 analyzer with NDIR optical system detector. The sample passes through a tube into the oven and is then calcined at 680 °C, obtaining the total carbon by IR-measurements of carbon dioxide. The inorganic carbon, which can be found in the form of carbonate and hydrogen carbonate, first passes through a fresh phosphoric acid solution and then continues along initial route. Organic carbon is calculated as the difference between total carbon and inorganic carbon (HCO_3^- and CO_3^{2-} species). In our case, taking into account that pH =3 was maintained, total organic carbon (TOC) values were directly measured. All carbon in the sample was converted to carbon dioxide and measured by infrared detection. The concentration of carbon dioxide was directly proportional to the peak intensity.

To determine the photocatalytic activity of the powders, the degradation of DCA was studied by measuring the TOC- content. Photocatalytic reactions were carried out in a Duran glass reactor containing 0.5 g/L of the photocatalytic powder and an aqueous solution of KNO_3 with 1mM DCA. The pH- value was adjusted to pH 3 and a cooling system was used to maintain the temperature at 20 °C. The experiments were carried out for 4 hours and every hour a sample was assayed to measure its TOC content. To limit the irradiation wavelength, the light beam was passed through a WG 320, a GG 420, or a GG 495 filter to cut off the wavelengths shorter than 320 nm, 420 nm and 495 nm, respectively (see Fig. 13).

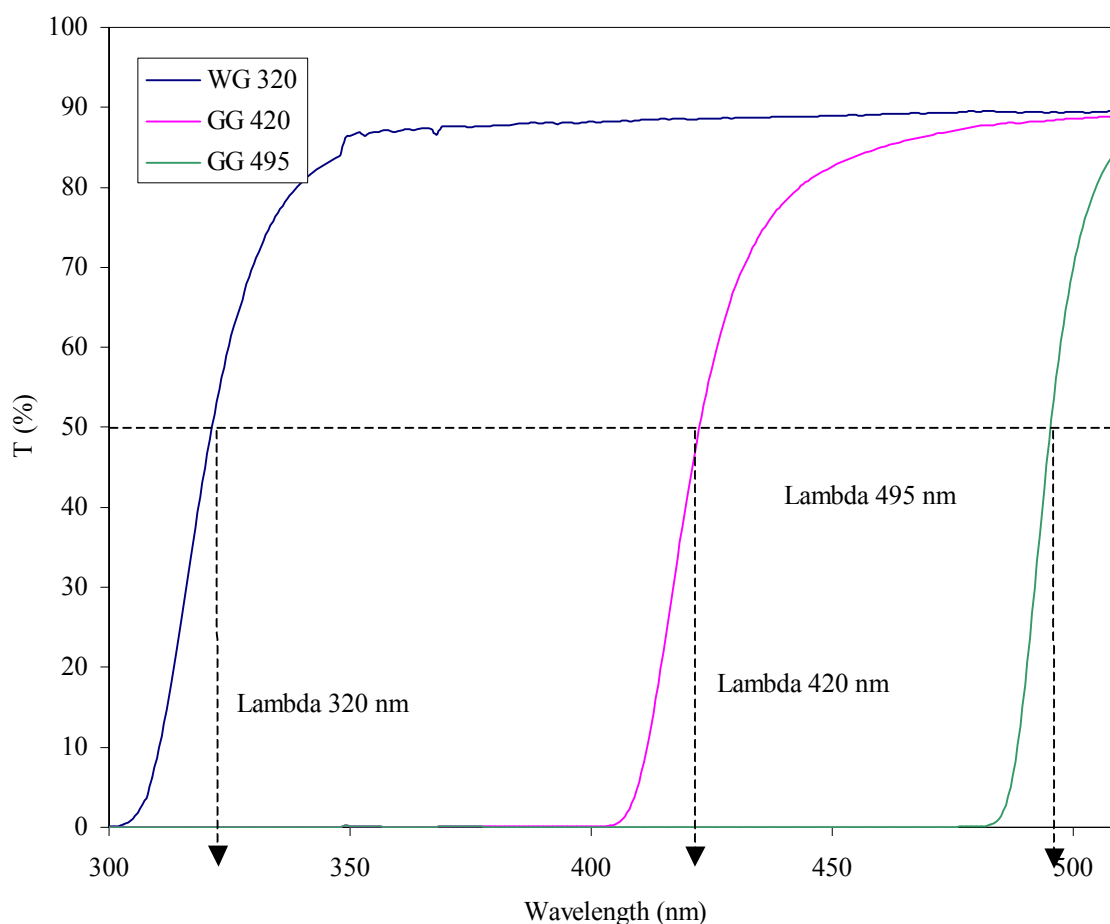


Fig. 13. Spectra of the filters WG 320, GG 420, GG 495, showing the transmission as a function of the wavelength.

As shown in Fig. 13, to determine the lambda-value: a horizontal line is drawn at 50 % transmission calculating the corresponding lambda (λ) - value. In the case of absorbance, it is known that a value of 1 absorbance corresponds to 10 % transmission, while 50 % transmission is equal to an absorbance of 0.3.

$$A(\lambda) = \log\left(\frac{1}{T}\right) \quad \text{Eq. 35}$$

6.4.1.3 Study of DCA-degradation under outdoor solar illumination

To check the activity of the sulfur-doped TiO₂ catalysts under sun light illumination with a UV (A) light intensity of 9.9 W/m² (Hannover, May 2007), the degradation of DCA has been studied. A Duran glass reactor (see Fig. 14) was put outside for 4 hours with 1mM DCA dissolved in 200 mL distilled water containing KNO₃ (10 mM). The concentration of the catalyst was 0.5 g/L and every hour a sample was taken to measure its TOC- content. Neither stirring nor bubbling of oxygen was carried out during these experiments, the reactors were closed to prevent evaporation during the whole experiment.

6.4.1.4 Study of DCA under indoor solar illumination

The photocatalytic activity of the sulfur doped TiO₂ catalysts for the degradation of DCA was studied again under indoor conditions to test the effect of indoor sunlight. Six reactors (as shown below in Fig. 14) were placed near the window for 5 days containing 1mM DCA dissolved in 200 mL distilled water in the presence of KNO₃ (10 mM). At the beginning of the experiment a value of pH= 3 was noted for each reactor.

During the first three days a polycarbonate box was put over the six reactors (see Fig. 14) to avoid any UV (A)-light, after that time the experiments were carried out for 2 further days without the box.

The concentration of the catalyst was 0.5 g/L and every day one sample was taken to measure its TOC- content. Also, the light intensity (mW/cm²) was measured with a UV (A)- Light Meter instrument three times per day, the measured values were between 0.01 and 0.04 mW/cm².

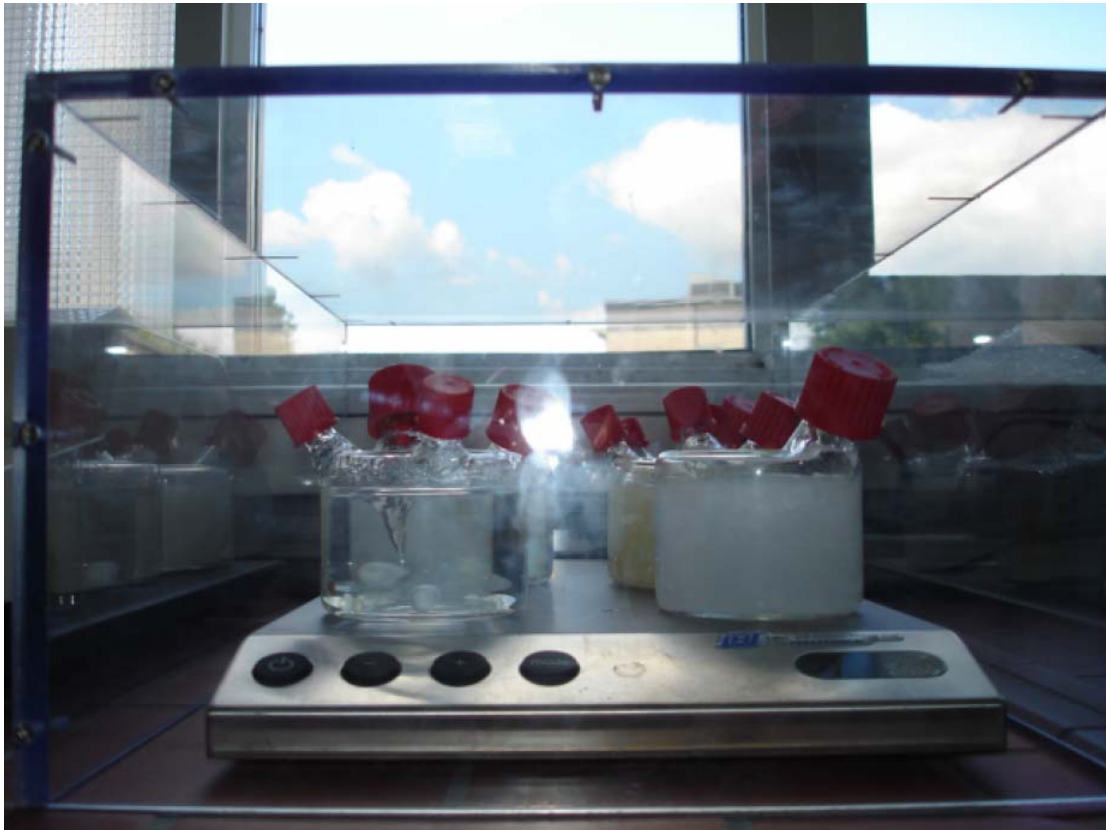


Fig. 14. DCA- degradation set-up for indoor experiments.

Fig. 15 Transmittance-spectra of the polycarbonate material employed for the cover, measured using an UV- Spectrometer (Varian Cary 100).

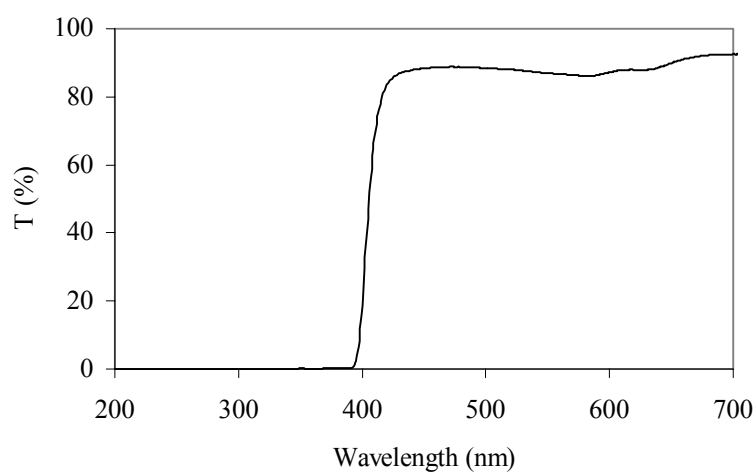


Fig. 15. Transmittance- spectra of polycarbonate material employing UV- Spectrometer. Only visible light can penetrate this material.

6.4.1.5 Study of DCA-degradation under artificial visible illumination

A new illumination chamber (as shown in Fig. 16) was equipped with six lamps (type of lamp: ibv L18W742 Coolwhite, electric power: 18 W each) for artificial illumination experiments in order to achieve more reproducible experimental illumination conditions.

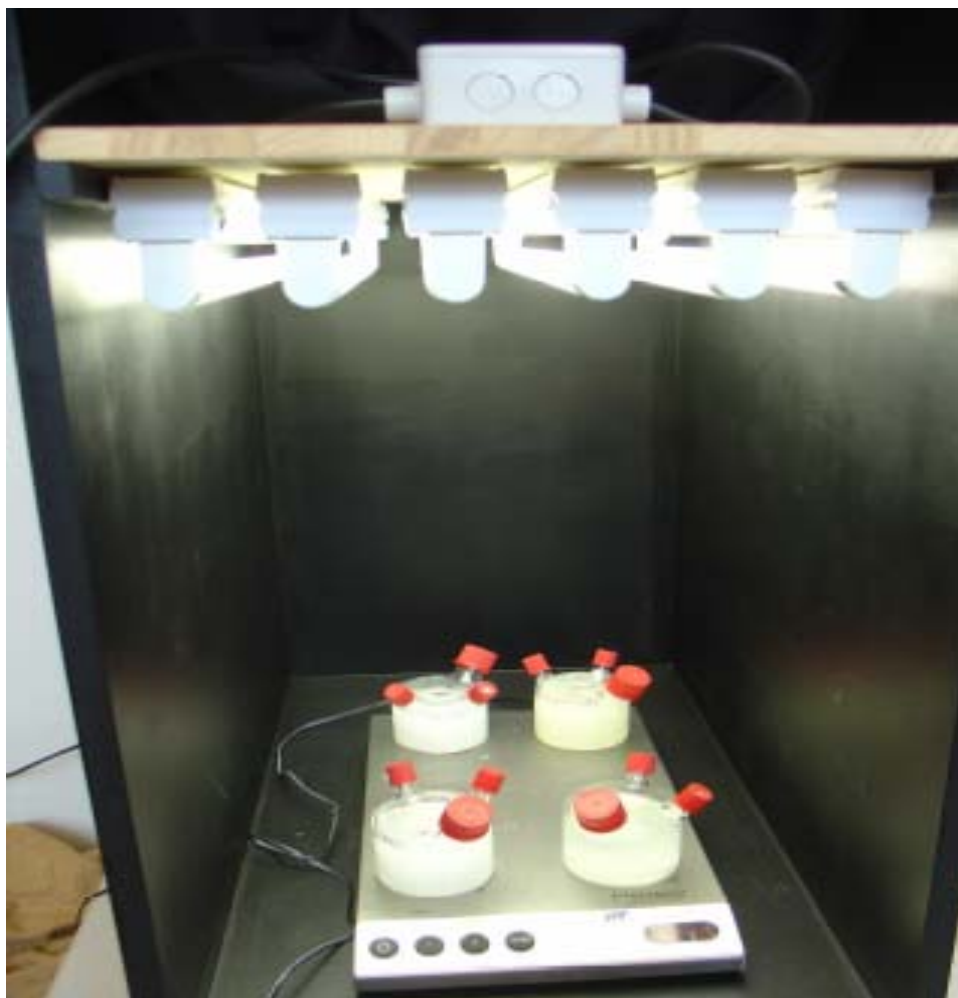


Fig. 16. Picture of the illumination chamber

The emission spectrum of the lamps was measured² and plotted as shown in Fig. 17.

² Thanks to Dr. Proft from Sachtleben for the Emission spectrum measurement of the lamp ibv L18W742 Coolwhite.

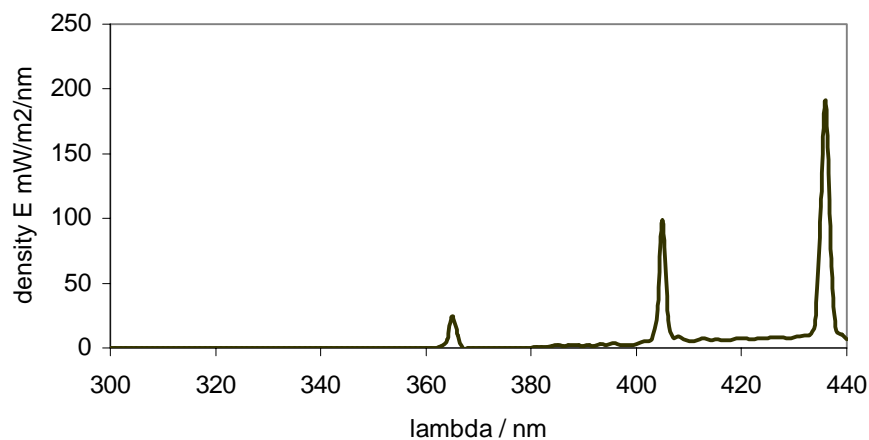


Fig. 17. Emission spectrum of the lamp ibv L18W742 Coolwhite measured at a distance of 20 cm., with three maxima emissions by the corresponding wavelengths of 365 nm, 406 nm and 439 nm. The incident photon fluxes (I_{hv}) were calculated by the integrated wavelengths values obtaining $2.77E-07 \text{ mol/ m}^2*s$, $7.40 E-07 \text{ mol/ m}^2*s$ and $2.06 E-05 \text{ mol/ m}^2*s$, respectively.

Four reactors were placed in the newly designed black chamber for 19 hours containing 1mM DCA dissolved in 200 mL distilled water in the presence of KNO_3 (10 mM). At the beginning of the experiment a value of $\text{pH} = 3$ was achieved for each reactor. The four reactors were illuminated for 1 hour, containing only 10 mM KNO_3 solution and the catalysts in order to eliminate possible impurities. After that, the DCA aliquot was added and allowed to equilibrate under dark conditions for 1 hour. Prior to light illumination a sample was assayed and later at six, thirteen, sixteen and nineteen hours to measure its TOC- content. The UV(A) light intensity (mW/m^2) was also obtained by the emission spectrum and the integrated value was found to be 83 mW/m^2 at the position of 20 cm, corresponding with an integrated lambda value of 400 nm (values of wavelengths were found in the range from 362 to 400 nm).

6.4.2 Photocatalytic Disinfection of *E. coli*

These experiments were carried out using a membrane pump recirculating at a rate of 18 L/h, with suspensions containing *E. coli* and TiO_2 (5 g/L) in 5 L of a physiological salt solution (0.9 g/L NaCl, pH = 7.3). The experimental set-up (see Fig. 18) consisted of an annular immersion lamp reactor (1200 mL) and a reservoir (5 L), both were vigorously stirred. UV-irradiation was performed by employing either a Heraeus mercury high-pressure lamp TQ718, which emits illumination in the UV (B) region ($280 \text{ nm} \leq \lambda \leq 315 \text{ nm}$) and in the UV (C) ($100 \text{ nm} \leq \lambda \leq 280 \text{ nm}$) region, or a Heraeus mercury high-pressure lamp TQ 718Z4, which emits predominantly in the UV (A) region ($315 \text{ nm} \leq \lambda \leq 380 \text{ nm}$), in both cases the lamps were sheathed by a Jena quartz glass tube.



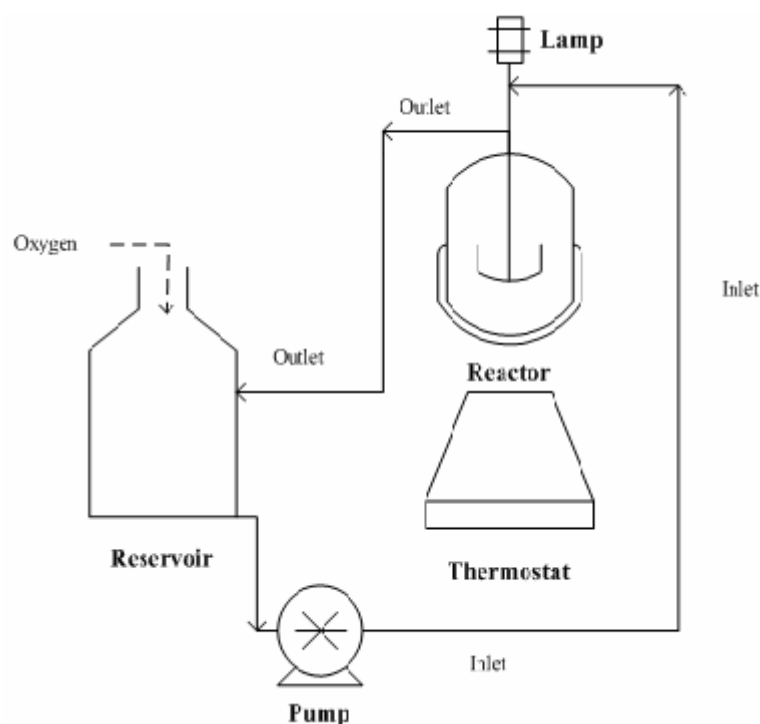


Fig. 18. Photocatalytic disinfection *E. coli* -set- up and -scheme.

The selected strain of *E. coli* was resistant to the antibiotic Ampicillin.

5000 mL of a TiO_2 suspension in a physiological salt solution of NaCl, also containing a concentration of ampicillin of 75 mg/L, was first circulated for 2 hours to disinfect the system described above. After that, an aliquot of an *E. coli* broth (about 30 mL) was added.

Before the photocatalytic experiment was started, the suspension was recirculated in the dark for 30 min, during the entire duration of the experiment, the suspension was oxygenated by bubbling molecular oxygen through the reservoir.

An aliquot was sampled before the light was switched on and afterwards a sample was taken every thirty minutes of illumination for a total experimental time of three hours.

To determine the concentration of *E. coli*, 1 mL of sample solution was withdrawn at each sampling time and was diluted to 1/10, 1/100 and 1/1000 with physiological salt solution.

Different experiments were carried out to study the effect of several parameters, such as the effect of TiO_2 concentration, flow rate and intensity of light.

Organism and growth

All materials were autoclaved prior to use at 121°C for 30 min to ensure sterility.

Liquid cultures of *E. coli* were grown in a complex medium (the composition of the medium is given in Table 6), containing the antibiotic: Ampicillin (75 mg/L, Sigma), at 37°C on a rotary platform at 123 rpm⁷⁰.

Table 6. Complex mediums recipe.

<i>Complex Medium</i>	
<i>Compound</i>	<i>Concentration</i>
Yeast extract (Fluka)	24 g/L
Phosphate buffer (Riedel de Haën)	50 mM
<i>after Autoclave:</i>	
Thiamin* HCl (Fluka)	10 mg/L
Glycin (Sigma)	100 mg/L
Ampicillin (Sigma)	75 mg/L
Glucose (Sigma)	1000 mg/L

Cell density of the liquid cultures was measured by its optical density at 580 nm.

In order to determine the Colony formed units (C.F.U.) an LB-Endo Agar Medium (the recipe of the LB-Endo Agar medium is given in Table 7) was used for the Agar plates, which also contained 75 mg/L Ampicillin.

Table 7. LB-Endo Agar Mediums recipe

<i>LB-Endo Agar</i>	
<i>Compound</i>	<i>Concentration</i>
Trypton (Fluka)	10 g/L
Yeast extract (Fluka)	5 g/L
NaCl (Merck)	10 g/L
Agar (Fluka)	15 g/L

7 Results and Discussion

7.1 Characterisation of materials

Sulfur doped TiO₂ photocatalysts were synthesized by a sol-gel process with titanium isopropoxide (IV) and thiourea. Lanthanum doped TiO₂ photocatalysts were prepared by a sol-gel process with titanium butoxide (IV) and lanthanum nitrate. Sulfur- and lanthanum-doped TiO₂ photocatalysts were characterized by different techniques such as Diffuse Reflectance Spectroscopy (DRS), X-ray Diffraction (XRD) and Elemental Analysis.

7.1.1 Unmodified- TiO₂

The undoped TiO₂ photocatalysts have been characterized by Elemental analysis and the band gap values determined by means of diffuse reflectance spectroscopy.

Table 8. Elemental analysis and band gap values of the undoped TiO₂ materials.

<i>Titanium-precursor</i>	<i>Notation</i>	<i>Calc. T</i>	<i>Ti %</i>	<i>C %</i>	<i>E_g (eV)</i>
<i>Titanium (IV) isopropoxide</i>	TiI1	500	n.d.	n.d.	3.2
	TiI2	600	60	0.23	3.1
	TiI3	700	60	0.06	3.2
<i>Titanium (IV) butoxide</i>	TiB1	500	60	0.15	3.1
	TiB2	600	60	0.11	3.2
	TiB3	700	60	0.02	3.2

The band gap values for the undoped TiO₂ photocatalysts are in the same range as standard UV- photocatalysts such as Hombikat UV 100 (pure anatase, E_g = 3.2 eV). The Elemental analysis data suggests that higher calcination temperatures leads to a drastic decrease in the percentage of carbon present.

7.1.2 Sulfur- doped TiO₂

About fifty sulfur-modified TiO₂ photocatalysts were synthesized (see section 6.1.2.) and tested (see section 7.2.) under different illumination conditions to study the dependency of their photoactivity on different sulfur-concentrations, calcination temperatures and calcination profiles. The elemental analysis of these powders are listed below in Table 9.

Table 9. Elemental analysis of the prepared sulfur doped TiO₂ samples from Table 2.

<i>Name</i>	<i>Molar ratio</i>		<i>Calc. T (°C)</i>	<i>Calc. rate(°C/h)</i>	<i>Ti %</i>	<i>S %</i>	<i>C %</i>
	<i>Tiisop./TU</i>						
KS1	1:4		300 °C (3h)	~ 150 °C/h	n.d.	n.d.	n.d.
KS2	1:4		500 °C (3h)	~ 150 °C/h	56	0.57	0.27
KS3	1:4		550 °C (3h)	~ 150 °C/h	56	0.37	0.32
KS4	1:4		575 °C (3h)	~ 150 °C/h	-	0.18	0.14
KS5	1:4		600 °C (3h)	~ 150 °C/h	59	0.25	0.16
KS6	1:4		625 °C (3h)	~ 150 °C/h	59	0.13	0.08
KS7	1:4		650 °C (3h)	~ 150 °C/h	59	0.09	0.1
KS8	1:4		700 °C (3h)	~ 150 °C/h	59	0.05	0.06
KS9	1:4		750 °C (3h)	~ 150 °C/h	59	0.03	0.06
KS10	1:4		500 °C (7h)	~ 150 °C/h	58	0.49	0.19
KS11	1:4		600 °C (7h)	~ 150 °C/h	59	0.11	0.11
KS12	1:4		650 °C (7h)	~ 150 °C/h	59	0.07	0.08
KS13	1:4		750 °C (7h)	~ 150 °C/h	60	0.02	0.04
KW1	1:2		500 °C (3h)	~ 150 °C/h	58	0.54	0.49
KW2	1:2		600 °C (3h)	~ 150 °C/h	60	0.17	0.17
KW3	1:2		650 °C (3h)	~ 150 °C/h	60	0.11	0.18
KW4	1:2		750 °C (3h)	~ 150 °C/h	60	0.04	0.05
KW5	1:2		500 °C (7h)	~ 150 °C/h	57	0.56	0.46
KW6	1:2		600 °C (7h)	~ 150 °C/h	58	0.52	0.39
KW7	1:2		650 °C (7h)	~ 150 °C/h	60	0.11	0.17
KW8	1:2		750 °C (7h)	~ 150 °C/h	60	0.03	0.04

Table 9 (continuation). Elemental analysis values of the synthesized sulfur doped TiO₂ samples from Table 2.

<i>Name</i>	<i>Molar ratio</i>		<i>Calc. T (°C)</i>	<i>Calc. rate(°C/h)</i>	<i>Ti %</i>	<i>S %</i>	<i>C %</i>
	<i>Tiisop./TU</i>						
KM1	1:6		500 °C (3h)	~ 150 °C/h	57	0.62	0.33
KM2	1:6		600 °C (3h)	~ 150 °C/h	59	0.16	0.21
KM3	1:6		650 °C (3h)	~ 150 °C/h	59	0.1	0.12
KM4	1:6		750 °C (3h)	~ 150 °C/h	60	0.04	0.11
KM5	1:6		500 °C (7h)	~ 150 °C/h	57	0.62	0.36
KM6	1:6		600 °C (7h)	~ 150 °C/h	59	0.13	0.22
KM7	1:6		650 °C (7h)	~ 150 °C/h	59	0.11	0.18
KM8	1:6		750 °C (7h)	~ 150 °C/h	60	0.02	0.08
KT1	1:4		550 °C (3h)	400 °C/h	59	0.54	0.16
KT2	1:4		575 °C (3h)	400 °C/h	59	0.35	0.1
KT3	1:4		600 °C (3h)	400 °C/h	59	0.29	0.12
KT4	1:4		625 °C (3h)	400 °C/h	59	0.21	0.1
KT5	1:4		550 °C (3h)	300 °C/h	n.d.	n.d.	n.d.
KT6	1:4		575 °C (3h)	300 °C/h	n.d.	n.d.	n.d.
KT7	1:4		600 °C (3h)	300 °C/h	n.d.	n.d.	n.d.
KT8	1:4		625 °C (3h)	300 °C/h	n.d.	n.d.	n.d.
KT9	1:4		550 °C (3h)	200 °C/h	60	0.42	0.2
KT10	1:4		575 °C (3h)	200 °C/h	58	0.34	0.06
KT11	1:4		600 °C (3h)	200 °C/h	60	0.23	0.06
KT12	1:4		625 °C (3h)	200 °C/h	60	0.14	0.04
KT13	1:4		550 °C (3h)	100 °C/h	60	0.36	0.16
KT14	1:4		575 °C (3h)	100 °C/h	57	0.16	0.1
KT15	1:4		600 °C (3h)	100 °C/h	58	0.37	0.12
KT16	1:4		625 °C (3h)	100 °C/h	60	0.1	0.06
KT17	1:4		550 °C (3h)	50 °C/h	60	1.2	0.24
KT18	1:4		575 °C (3h)	50 °C/h	57	0.85	0.22
KT19	1:4		600 °C (3h)	50 °C/h	59	0.62	0.06
KT20	1:4		625 °C (3h)	50 °C/h	59	0.44	0.06
KT21	1:4		550 °C (3h)	10 °C/h	n.d.	n.d.	n.d.
KT22	1:4		575 °C (3h)	10 °C/h	n.d.	n.d.	n.d.
KT23	1:4		600 °C (3h)	10 °C/h	n.d.	n.d.	n.d.
KT24	1:4		625 °C (3h)	10 °C/h	n.d.	n.d.	n.d.
KT21A	1:6		550 °C (3h)	10 °C/h	n.d.	n.d.	n.d.
KT22A	1:6		575 °C (3h)	10 °C/h	n.d.	n.d.	n.d.
KT23A	1:6		600 °C (3h)	10 °C/h	n.d.	n.d.	n.d.
KT24A	1:6		625 °C (3h)	10 °C/h	n.d.	n.d.	n.d.

From the data given in Table 9 it is obvious that the calcination temperature is influencing the amount of sulfur and carbon in the TiO_2 matrix. At higher calcination temperatures the concentration of sulfur and carbon decreased drastically. The more active yellowish powder, which was calcined for 3 hours at 600 °C (KS5), has a relatively high sulfur and low carbon concentration in comparison to the photocatalysts (KS6, KS7 and KS12) calcined at about the same temperature range from 600 °C to 650 °C. It is also noticeable that the powders calcined at the same temperature but different times, 3 hours (KS2, KS5, KS7 and KS9) or 7 hours (KS10- KS13), do not show any major change in the concentration of sulfur or carbon content (in %).

Fig. 19 shows the sulfur doped powders which were calcined at different temperatures: 550 °C (KS3); 625 °C (KS6); 650 °C (KS7) and 700 °C (KS8).

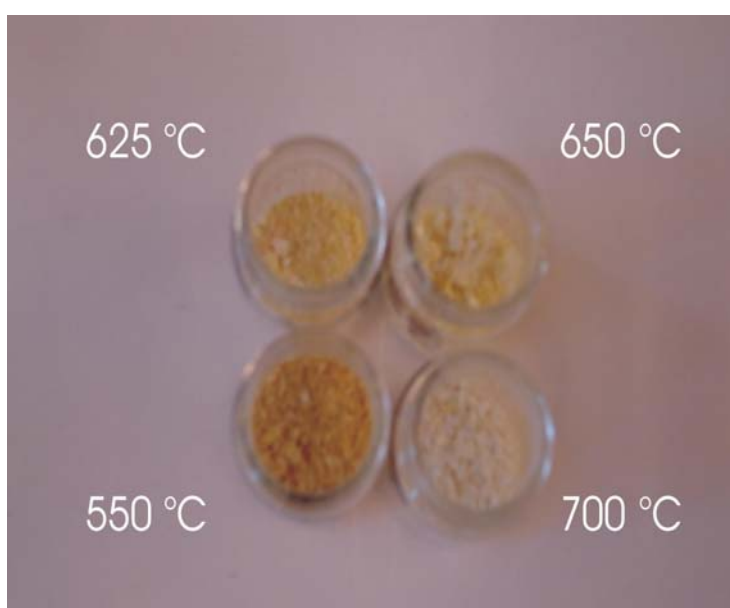


Fig. 19. Sulfur doped TiO_2 photocatalysts calcined at different temperatures 550 °C (KS3) 625 °C (KS6), 650 °C (KS7) and 700 °C (KS8), prepared following the synthesis in section 6.1.2.

The intensity of the yellow color depends on the calcination temperature. The intensity of the color increases with temperature until 600°C, after that the intensity of the color is less strong. The sulfur content is found to decrease with an increase of the calcination temperature. This can be explained by oxidation of sulfur followed by the migration of the reaction product to the surface of the catalyst forming sulfates, which were removed upon suspension of the catalyst in water. The rate of this process increases with the calcination temperature. In the case of the different heating profiles study, it can be summarized that by slower heating profiles (KT21 - KT24) the concentration of sulfur and carbon (in percent) is higher than by faster profiles (KT1 - KT4).

A selection of the prepared sulfur doped TiO₂ photocatalysts were characterized by X-ray Diffraction (XRD) as depicted in Fig. 20. The photocatalysts (KS2, KS3, KS4, KS5, KS6, KS7, KS8, KS9 and KS12) were calcined at different calcination temperatures in the range 500 °C to 750°C, with a molar ratio of titanium (IV) isopropoxide to thiourea 1:4 (the corresponding notation of these photocatalysts are given in Table 2).

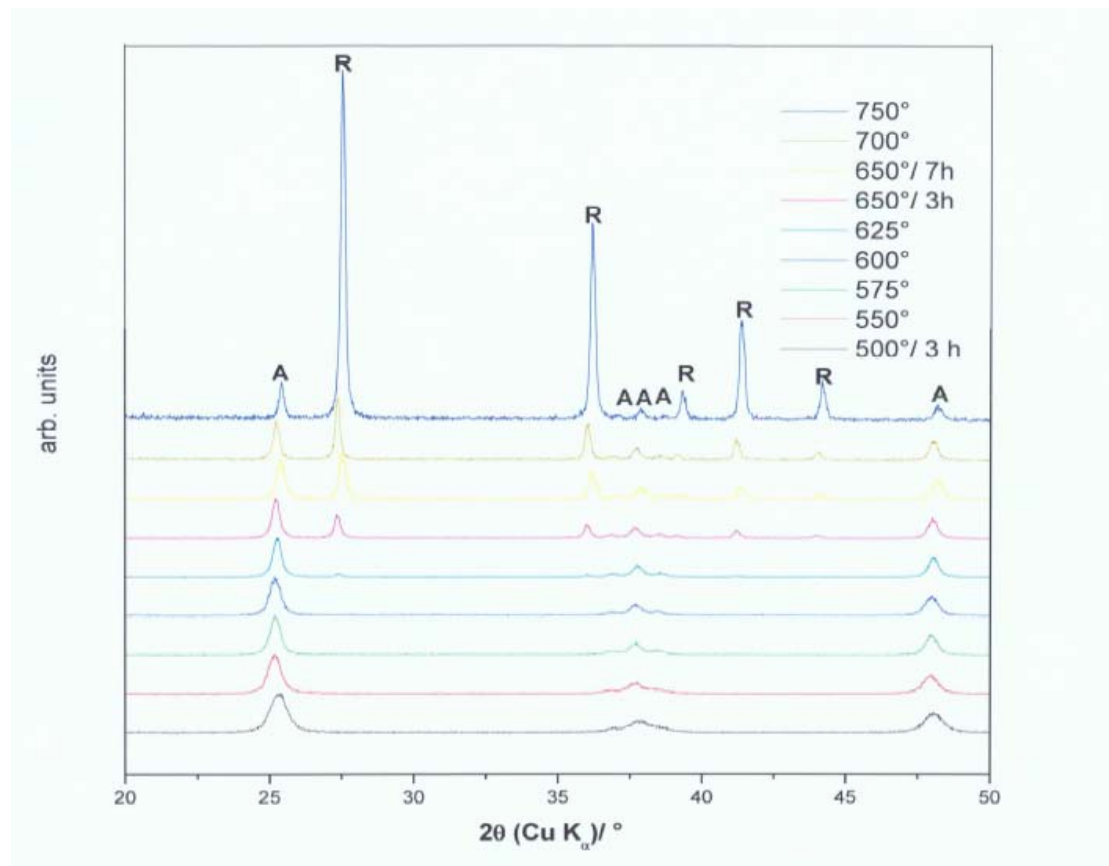


Fig. 20. XRD patterns for the sulfur doped TiO₂ photocatalysts.

The XRD patterns of the titania samples show the presence of both anatase and rutile phases. The crystalline properties of the materials increases with higher calcination temperatures such as the transformation from anatase to rutile. The rutile phase appears from $T \geq 650^\circ\text{C}$, the calcined powders at these temperatures are no longer photocatalytically active (see Fig. 23). Until 625°C , the anatase phase is predominant and the sulfur doped catalysts still show photocatalytic activity.

Diffuse reflectance spectra (DRS) of the sulfur doped photocatalysts studied were carried out to determine the band gap energies by the calculated Kubelka Munk functions. Section 6.3.4. explains how it is possible to calculate the experimental band gap values from the diffuse reflectance spectra by means of Kubelka Munk. The samples were measured as powders and BaSO₄ was taken as the background reflectance spectrum.

Table 10. Summary of the experimental band gaps obtained for the sulfur doped TiO₂ photocatalysts.

<i>Molar ratio</i>			
<i>Name</i>	<i>Tiisop./TU</i>	<i>Calc. T (°C)</i>	<i>Eg_{exp.}(eV)</i>
KS1	1:4	300 °C (3h)	3.2
KS2	1:4	500 °C (3h)	3.2
KS3	1:4	550 °C (3h)	3.2
KS4	1:4	575 °C (3h)	3.2
KS5	1:4	600 °C (3h)	2.8
KS6	1:4	625 °C (3h)	3.2
KS7	1:4	650 °C (3h)	3.2
KS8	1:4	700 °C (3h)	3.2
KS9	1:4	750 °C (3h)	3.2
KS10	1:4	500 °C (7h)	3.2
KS11	1:4	600 °C (7h)	3.2
KS12	1:4	650 °C (7h)	3.2
KS13	1:4	750 °C (7h)	3.2
KW1	1:2	500 °C (3h)	3.2
KW2	1:2	600 °C (3h)	3.2
KW3	1:2	650 °C (3h)	3.2
KW4	1:2	750 °C (3h)	3.2
KW5	1:2	500 °C (7h)	3.2
KW6	1:2	600 °C (7h)	3.2
KW7	1:2	650 °C (7h)	3.2
KW8	1:2	750 °C (7h)	3.2

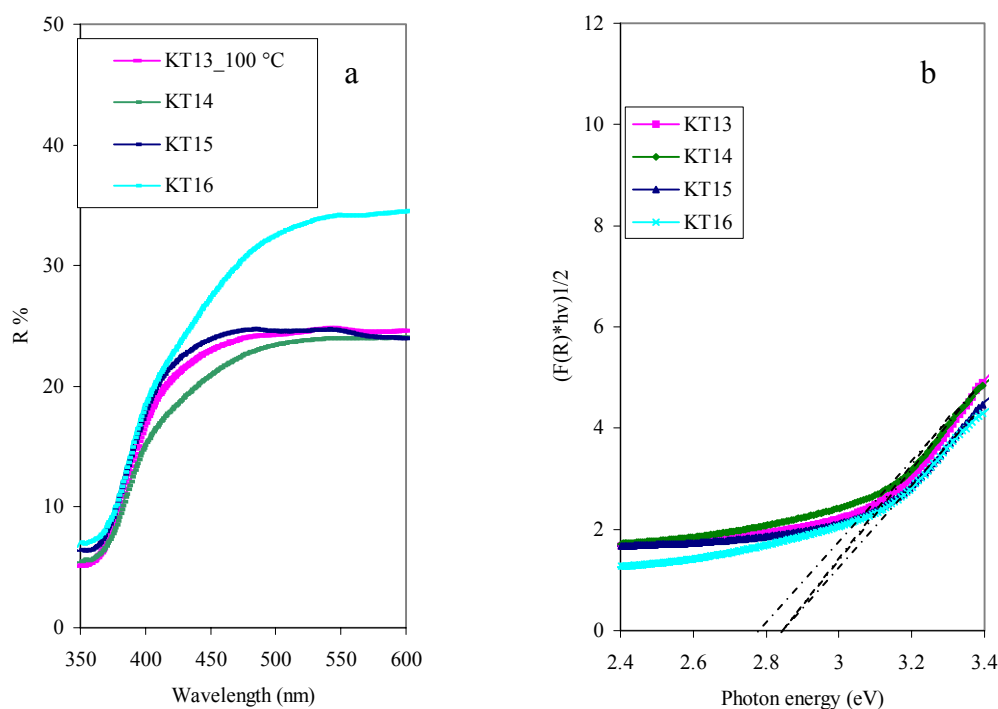
Table 10 (continuation). Summary of the experimental band gaps obtained for the sulfur doped TiO₂ photocatalysts.

<i>Molar ratio</i>			
<i>Name</i>	<i>Tiisop./TU</i>	<i>Calc. T (°C)</i>	<i>E_{g,exp.} (eV)</i>
KM1	1:6	500 °C (3h)	3.2
KM2	1:6	600 °C (3h)	3.2
KM3	1:6	650 °C (3h)	3.2
KM4	1:6	750 °C (3h)	3.2
KM5	1:6	500 °C (7h)	3.2
KM6	1:6	600 °C (7h)	3.2
KM7	1:6	650 °C (7h)	3.2
KM8	1:6	750 °C (7h)	3.2
KT1	1:4	550 °C (3h)	3.2
KT2	1:4	575 °C (3h)	3.2
KT3	1:4	600 °C (3h)	3.2
KT4	1:4	625 °C (3h)	3.2
KT5	1:4	550 °C (3h)	3.2
KT6	1:4	575 °C (3h)	3.2
KT7	1:4	600 °C (3h)	3.2
KT8	1:4	625 °C (3h)	3.2
KT9	1:4	550 °C (3h)	3.2
KT10	1:4	575 °C (3h)	3.2
KT11	1:4	600 °C (3h)	3.2
KT12	1:4	625 °C (3h)	3.2
KT13	1:4	550 °C (3h)	2.8
KT14	1:4	575 °C (3h)	2.8
KT15	1:4	600 °C (3h)	2.8
KT16	1:4	625 °C (3h)	2.8
KT17	1:4	550 °C (3h)	2.7
KT18	1:4	575 °C (3h)	2.7
KT19	1:4	600 °C (3h)	2.7
KT20	1:4	625 °C (3h)	2.8
KT21	1:4	550 °C (3h)	3.0
KT22	1:4	575 °C (3h)	2.8
KT23	1:4	600 °C (3h)	2.5
KT24	1:4	625 °C (3h)	3.0
KT21A	1:6	550 °C (3h)	3.2
KT22A	1:6	575 °C (3h)	3.2
KT23A	1:6	600 °C (3h)	3.2
KT24A	1:6	625 °C (3h)	3.2

The lower band gap for the photocatalyst calcined at 600 °C (KS5) and for the photocatalysts calcined at low heating profiles (from KT13 bis KT24) can explain why these sulfur doped TiO₂ photocatalysts are more active than the others especially in the visible light region (e.g. by KS5 see DCA-degradation by pH-stat system at $\lambda \geq 420$ nm section 7.2.2.). These results are in good agreement with those founded in the literature.²⁵ Liu et al.²⁵ also synthesized sulfur doped TiO₂ photocatalysts, with titanium (IV) tetrachloride as a titanium precursor and with thiourea as a sulfur source, for the degradation of phenol by visible light illumination. This research suggested the formation of a second absorption edge in the visible region (from 400 nm to 470 nm), showing that more photons can be used by photocatalyst excitation. It is concluded that the first and the second edges are related to the band gap of the original TiO₂ and the sulfur doped sample, respectively. The new absorption edge showed that a new energy band was formed.

For that reason it was necessary to study further some physical parameters, such as calcination temperature, calcination rate and molar ratio of titanium (IV) isopropoxide to thiourea. No significant shift into the visible region could be observed by the study of different molar ratios of titanium (IV) isopropoxide to thiourea (data not shown). However, wider absorption edges were observed by the study of different heating profiles in the region of 10 °C/h to 100°C/h.

Fig. 21 shows diffuse reflectance spectra for the sulfur doped TiO₂ photocatalysts calcined at 550 °C, 575 °C, 600 °C and 625°C with calcination profiles 10 °C/h, 50°C/h and 100°C/h.



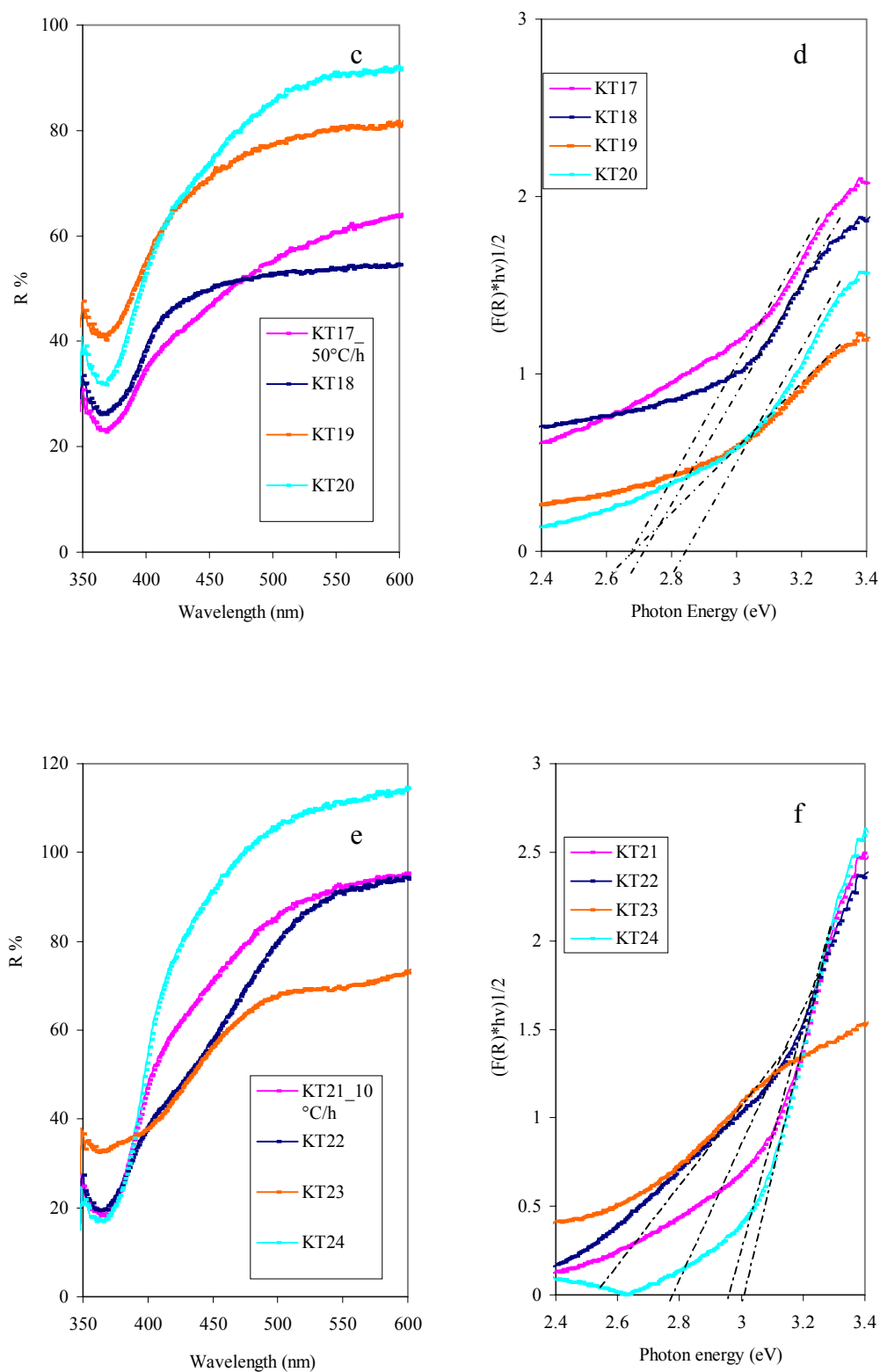


Fig. 21. Plot of the Reflectance spectra (a, c and e) and transformed Kubelka Munk function (b, c, f) of sulfur doped TiO_2 prepared with a molar ratio 1:4, calcinated for 3 hours at different temperatures 550 °C, 575 °C, 600 °C and 625 °C and temperature ramps 10 °C/h, 50 °C/h and 100 °C/h, respectively.

From the reflectance spectra, a shift into the visible light region was observed from the temperature ramps 10 °C/h to 100 °C/h. The experimental reflection measurements obtained confirm the important role of low heating profiles for the preparation of new materials, which are active in the visible light region. All the photocatalysts (KT13- KT24), which were calcined with temperature ramps from 10 °C/h to 100 °C/h, showed wide absorption edges, shifting to longer wavelengths and extending their absorbance into the visible light region (wavelength values from 400 nm to 470 nm). The crystalline size of anatase for the sulfur doped TiO₂ photocatalysts calcined at 550 °C, 575 °C, 600 °C and 625 °C with corresponding heating profiles of 10 °C/h and 100 °C/h, was estimated by XRD. The values are in the range of 14- 28 nm (corresponding to a heating profile of 10 °C/h) and 19.5- 28.5 nm (100°C/h as heating profile).

7.1.3 Lanthanum-doped TiO₂

Lanthanum doped TiO₂ photocatalysts were synthesized by the sol-gel process starting from titanium butoxide (IV) and lanthanum nitrate. For the photoactivity study of lanthanum doped TiO₂ the dependency on lanthanum concentration (0.4 % and 0.9 %) and calcination temperature (400°C, 500°C, 600°C and 700°C) has been studied (see section 7.3.) under indoor visible light illumination. The characterization of these photocatalysts by means of diffuse reflectance spectra and elemental analysis is shown below in Table 11 and Table 12.

Table 11. Elemental analysis of the lanthanum doped TiO₂ photocatalysts showing a range of lanthanum concentrations and different calcination temperatures.

<i>Name</i>	<i>La-Conc. solution (%)</i>	<i>Calc. T (°C)</i>	<i>Ti %</i>	<i>La %</i>	<i>C %</i>
KL1	0.4 %	400 °C (3h)	59	0.11	0.22
KL2	0.4 %	500 °C (3h)	59	0.12	0.16
KL3	0.4 %	600 °C (3h)	59	0.12	0.06
KL4	0.4 %	700 °C (3h)	59	0.13	0.03
KL5	0.9 %	400 °C (3h)	59	0.32	0.04
KL6	0.9 %	500 °C (3h)	59	0.33	0.02
KL7	0.9 %	600 °C (3h)	59	0.25	0.02
KL8	0.9 %	700 °C (3h)	59	0.26	0.03

It can be concluded that with a lanthanum concentration in solution of 0.4 %, the higher the calcination temperature is, the lower the carbon concentration. However, Lanthanum concentration did not change. In the case of a higher Lanthanum concentration, with the theoretical value of 0.9 % in solution, the carbon concentration decreases drastically.

Table 12. Experimental band gap values calculated by Kubelka Munk function from diffuse reflectance spectra. Section 6.3.4. explains how it is possible to calculate the experimental band gap values. The samples were measured as powders and BaSO₄ was taken as the background reflectance spectrum.

<i>Name</i>	<i>La-Conc. (%)</i>	<i>Calc. T (°C)</i>	<i>Eg (eV)</i>
KL1	0.4 %	400 °C (3h)	3.2
KL2	0.4 %	500 °C (3h)	3.2
KL3	0.4 %	600 °C (3h)	3.2
KL4	0.4 %	700 °C (3h)	3.2
KL5	0.9 %	400 °C (3h)	3.2
KL6	0.9 %	500 °C (3h)	3.2
KL7	0.9 %	600 °C (3h)	3.2
KL8	0.9 %	700 °C (3h)	3.2

There is no shift into the visible region for the lanthanum doped TiO₂ catalysts. Therefore, the data from the diffuse reflection spectra are not included. The values of the experimental band gaps are similar to commercial UV- photocatalysts such as Hombikat UV 100. This could explain the low activity of these photocatalysts under indoor solar illumination conditions. Liqiang et al.⁶⁴ also did not find any shift to longer wavelengths, suggesting that La³⁺ was uniformly dispersed onto the TiO₂ surface in the form of La₂O₃ clusters with small particle size. They concluded that La³⁺ did not enter into the TiO₂ crystal lattice to substitute for Ti⁴⁺, because the radius of La³⁺ (1.15 Å) is much bigger than that of Ti⁴⁺ (0.64 Å).

7.2 Photocatalytic activity study of sulfur doped TiO₂

7.2.1 Study of undoped samples under UV (A)- illumination

The catalysts, the photocatalytic activities of which have been measured, were Hombikat UV 100 and the undoped samples prepared only from titanium (IV) isopropoxide or titanium (IV) butoxide, as titania precursors. The preparation of the catalysts was identical to that used for the sulfur- and lanthanum- doped catalysts but without the addition of these atoms. The samples were calcined at different temperatures 500, 600 and 700 °C, respectively for three hours. The illumination for the photocatalytic test was carried out using Philips R-UV A 100 W lamps with an emission maximum of 351 nm and an intensity of 1.55 mW/cm² at the upper reactor windows. (Experimental procedure is described in detail in section 6.4.1.1).

The undoped TiO₂ photocatalysts which have been tested under UV(A)- illumination conditions are listed in Table 2. The commercial photocatalyst Hombikat UV 100 has also been measured and taken as a standard.

In Fig. 22 the photoactivity of the undoped TiO₂ photocatalysts in comparison with the standard Hombikat UV 100 has been studied for the degradation of DCA by TOC- content under UV (A)-illumination conditions.

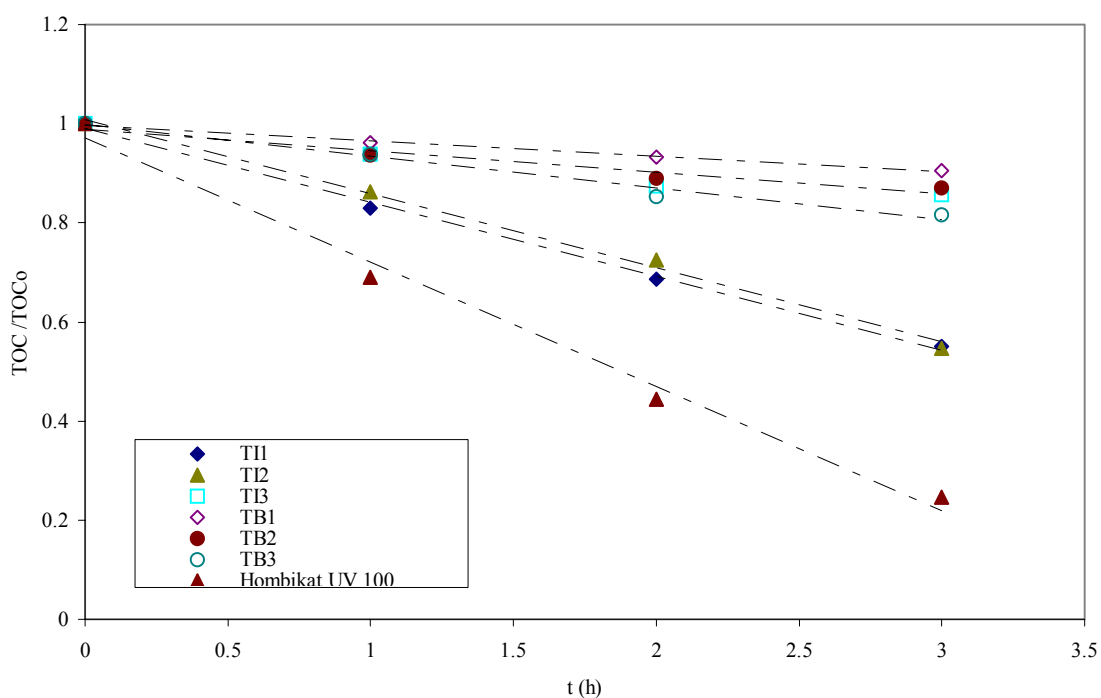


Fig. 22. Plot of TOC-concentration as a function of the illumination time (h) by DCA-degradation. *Experimental conditions:* 1mM DCA dissolved in 200 mL distilled water, KNO₃ (10 mM) under pH = 3 and 0.5 g/L catalyst (titania precursors: titanium (IV) isopropoxide and titanium (IV) butoxide calcined at different temperatures 500 °C, 600 °C and 700 °C, respectively) illuminated for 3 hours, under UV- illumination conditions (light intensity UV (A) 15.5 W/m²).

The degradation of DCA in the presence of TiO₂ and molecular oxygen detected by TOC-measurements follows zero-order kinetics (see Fig. 22). This assumption also corroborates the work done before by Hufschmidt et al.⁴⁷ and Martin Lindner⁴⁸ for the DCA- degradation study. From the slopes the kinetic degradation rates are calculated and used for the determination of the photonic efficiencies (calculation process is explained in section 6.3.5.).

Table 13. Photonic efficiencies and initial DCA- degradation rates calculated for the undoped samples and for the commercial catalysts Hombikat UV 100.

Photocatalyst	Rate DCA*1E-09	
	(M*s ⁻¹)	P.E.(%) C _{DCA}
TiI1	40.7 (R ² = 0.98)	2.0
TiI2	38.2 (R ² = 0.99)	1.9
TiI3	15.6 (R ² = 0.99)	0.8
TiB1	9.5 (R ² = 0.99)	0.5
TiB2	16.0 (R ² = 0.94)	0.8
TiB3	17.8 (R ² = 0.99)	0.9
Hombikat UV 100	79.9 (R ² = 0.98)	3.9

Experimental conditions: 1mM DCA dissolved in 200 mL distilled water, KNO₃ (10 mM) and 0.5 g/L catalyst illuminated for 3 hours, light intensity UV (A) 15.5 W/m².

It is noticeable that the catalysts prepared from titanium (IV) isopropoxide are much more active under UV (A)- illumination and also more sensitive, (in the case of temperature profiles study) than those prepared from titanium (IV) butoxide. The obtained photonic efficiencies of titanium isopropoxide (IV), calcined at 500°C (TI1) and 600°C (TI2), are in the same range as Hombikat UV 100 (commercial UV- TiO₂ photocatalyst). Photonic efficiencies of titanium (IV) isopropoxide calcined at 700°C (TI3) are much lower, due to the transformation to rutile, decreasing the photocatalytic properties of the catalyst.

Hufschmidt et al.⁴⁷ achieved photonic efficiency values for the standard catalyst Hombikat UV 100 (light intensity value of 23 W/m² (16 UV (A)-light tubes 40 W) of $\zeta = 6.8\%$ at pH = 3 and $\zeta = 3.13\%$ at pH = 9. This could be explained by the different experimental conditions such as higher catalyst concentration (1 g/L) and pollutant concentration (DCA 5 mM). As shown in Fig. 8 b, (the dependence of photonic efficiency on DCA-concentration) a solution with 5 mM DCA concentration corresponds to a photonic efficiency value of 12 %, whereas 1 mM DCA concentration has an efficiency of about only 6 %.

7.2.2 Degradation of DCA by pH-Stat titration system

To measure the different catalysts under the same reproducible experimental conditions at different wavelengths ($\lambda \geq 320$ nm, $\lambda \geq 420$ nm, $\lambda \geq 495$ nm), the so-called pH-stat titration technique has been used (explained in detail in section 6.4.1.2.). The corresponding experimental set-up is shown in Fig. 12.

The sulfur doped TiO₂ powder was calcined at several different temperatures (500 °C, 600 °C, 700 °C) for three hours, and yellow powders were obtained. The intensity of the yellow color depends on the calcination temperature (see Fig. 19). The commercial photocatalysts Hombikat UV 100 and Kronos VLP 7001 and the sulfur doped catalysts KS2, KS5 and KS8 have also been tested. The commercial catalysts have been studied as standards.

During the blank experiments (e.g., in the absence of any photocatalyst or in the presence of the photocatalyst but without any illumination), no photoactivity was found.

In Fig. 23 the TOC- removal of the catalysts which were calcined at 500 °C (KS2), 600 °C (KS5) and 700 °C (KS8), measured at a wavelength ≥ 320 nm by DCA- degradation study is shown.

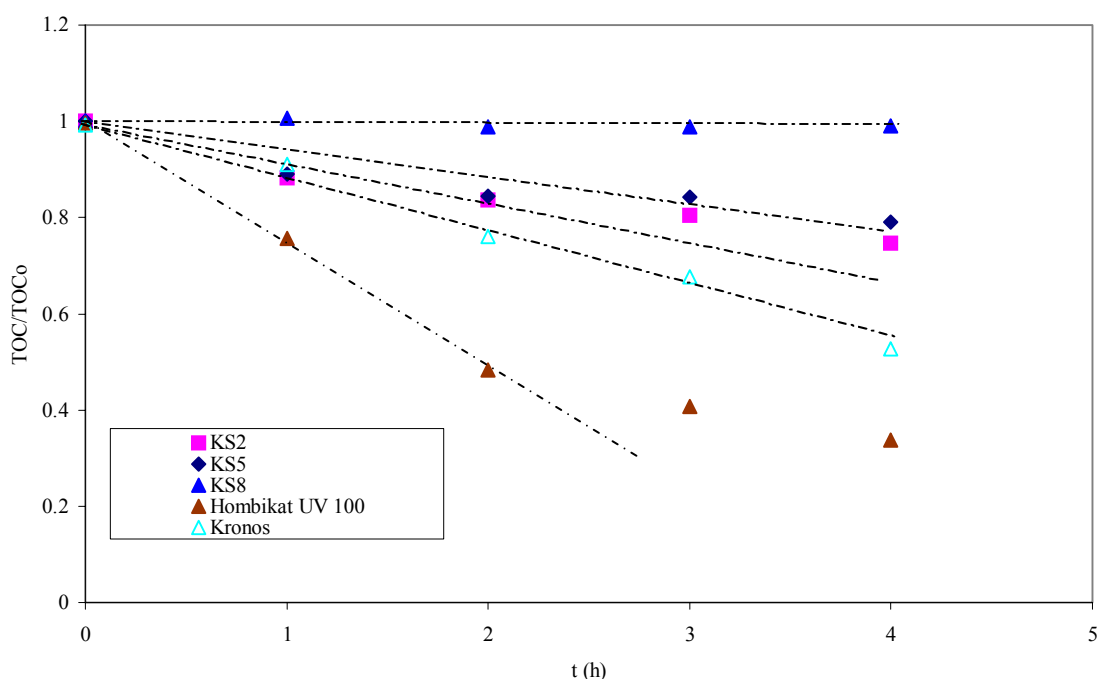


Fig. 23. Plot of TOC-concentration versus irradiation time (h). *Experimental conditions:* Degradation of DCA (1 mM) in an aqueous solution of KNO₃ (200 mL) at pH= 3.0, 0.5 g/L of photocatalyst (commercial photocatalysts and the sulfur doped TiO₂ calcined at 500 °C (KS2), 600 °C (KS5) and 700 °C (KS8) for three hours), $\lambda_{\text{ex}} \geq 320$ nm, $I_{\text{UV(A)}} = 190$ W/m².

The activity measurements of the powders excited by UV (A) - light shows, first of all, that a limit of the calcination temperature seems to exist for the sulfur doped material. At calcination temperatures higher than or equal to 700 °C, no photoactivity was found for the degradation of DCA. This is probably due to the transformation into rutile and also with increasing calcination temperatures of titania powder, the specific surface area decreases. This can negatively influence the photoactivity.⁷¹

When excited with UV (A) -light the powders, calcined at 500 °C (KS2) and 600 °C (KS5), exhibit very similar photocatalytic behaviour. After 4 hours the degree of degradation achieved for both of them (KS2 and KS5) was approximately 20%, compared to about 60 % degradation achieved with Hombikat UV 100.

Both commercial catalysts are more active than the sulfur doped TiO₂ under identical operational conditions, especially Hombikat UV 100 which achieves more than 50 % degradation of DCA within 4 hours of illumination. Meanwhile, with a light intensity of 15.5 W/m² (as shown Fig. 22) Hombikat UV 100 achieved 80 % DCA-degradation in only 3 hours.

The initial photonic efficiencies and initial reaction rates following zero order kinetics have been calculated and are presented in Table 14.

Table 14. Photonic efficiencies and DCA- rates calculated for the commercial and sulfur doped TiO₂ catalysts with a wavelength ≥ 320 nm and a light intensity UV (A) value of 190 W/m².

<i>Photocatalyst</i>	<i>Rate DCA *1E-09 (M*s⁻¹)</i>	<i>P.E. (%)</i>
KS2	22.4 (R ² = 0.95)	0.50
KS5	21.9 (R ² = 0.94)	0.49
KS8	1.67 (R ² = 0.94)	0.04
Hombikat UV 100	73.7 (R ² = 0.99)	1.64
Kronos	33.4 (R ² = 0.97)	0.74

Experimental conditions: Degradation of DCA (1 mM) in an aqueous solution of KNO₃ (200 mL) at pH= 3.0, 0.5 g/L of photocatalyst (commercial photocatalysts and the sulfur doped TiO₂ calcined at 500 °C (KS2) and 600 °C (KS5) for three hours), $\lambda_{ex} \geq 320$ nm, $I_{UV(A)} = 190$ W/m².

Fig. 24 shows the TOC- decrease of the powders employing the 420 nm cut-off filter.

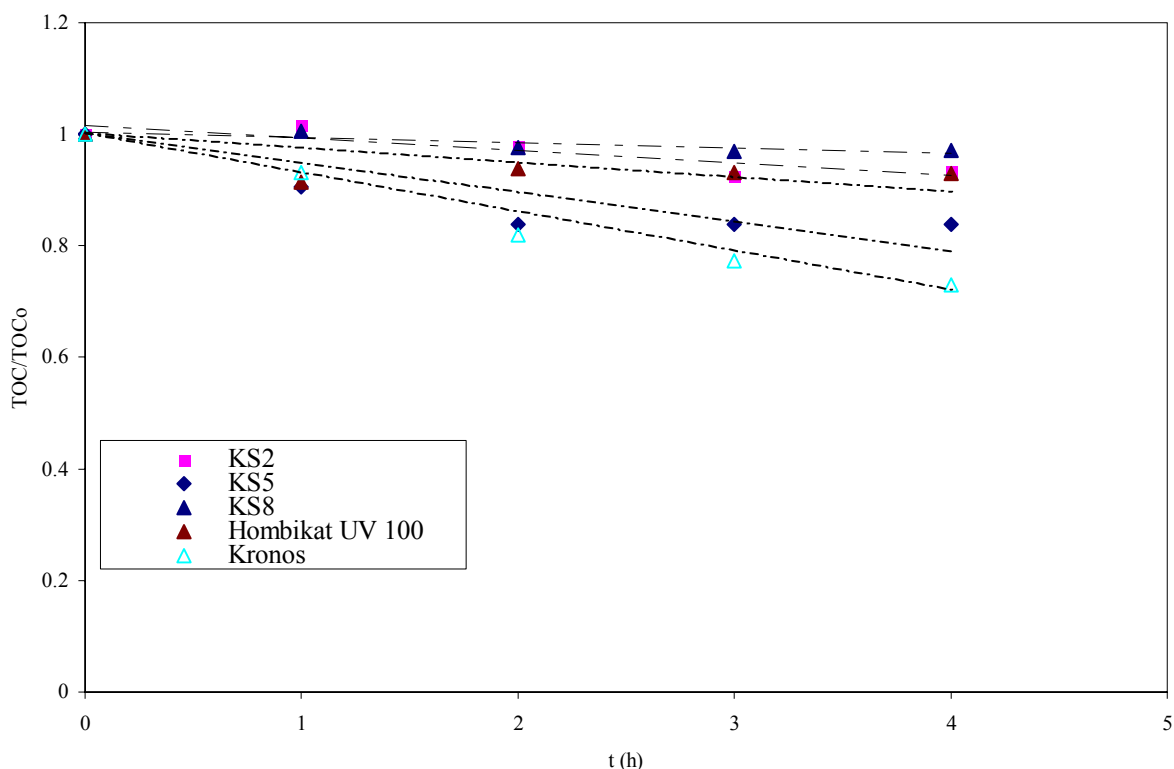


Fig. 24. Plot of TOC- reduction versus irradiation time (h). *Experimental conditions:* Degradation of DCA (1 mM) in an aqueous solution of KNO_3 (200 mL) at pH= 3.0, 0.5 g/L of photocatalyst (commercial photocatalysts and the sulfur doped TiO_2 calcined at 500 °C (KS2), 600 °C (KS5) and 700 °C (KS8) for three hours), $\lambda_{\text{ex}} \geq 420$ nm, $I_{\text{UV (A)}} = 3.7 \text{ W/m}^2$.

It should be noted (see data in Table 16) that the material KS5 exhibits almost the same activity as the commercial product from Kronos. The powder, calcined at 600 °C (KS5), exhibits photoactivity when illuminated at wavelengths higher than 420 nm, while the powders calcined at 500 °C (KS2) and 700 °C (KS8) no longer show any degradation of DCA.

The same experiment was repeated with illumination wavelengths exceeding 495 nm (this procedure was also repeated with the commercial catalysts Hombikat UV 100 and Kronos). As shown in Fig. 25, no photoactivity (under these synthesized conditions) was observed at the wavelength ≥ 495 nm. This fact was confirmed by the TOC-measurements. This could be probably explained due to the absorbed photons which do not have enough energy to induce the transfer of electrons from the valence band to the conduction band at these longer wavelengths.

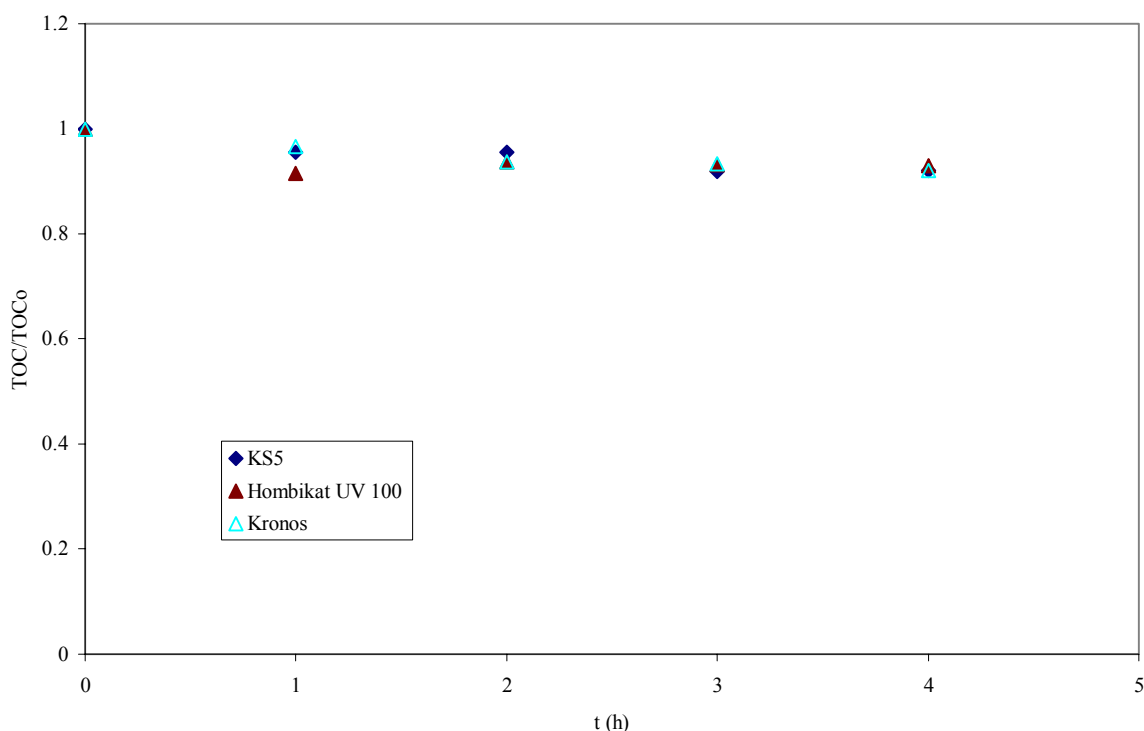


Fig. 25. Reduction of TOC- concentration versus experimental time (h). *Experimental conditions:* Degradation of DCA (1 mM) in an aqueous solution of KNO₃ (200 mL) at pH= 3.0, 0.5 g/L of photocatalyst (commercial photocatalysts and the sulfur doped TiO₂ calcined at 600 °C (KS5) for three hours), $\lambda_{\text{ex}} \geq 495$ nm.

Table 15. Initial DCA- rates calculated for the commercial and self made catalysts with a wavelength value of 420 nm (the photonic efficiencies were calculated with a corresponding light intensity $I_{\text{UV(A)}} = 3.7 \text{ W/m}^2$) and 495 nm.

<i>Photocatalyst</i>	<i>Lambda ≥ 420 nm</i>		<i>Lambda ≥ 495 nm</i>
	<i>Rate DCA *1E-09 (M*s⁻¹)</i>	<i>P.E. (%)</i>	<i>Rate DCA *1E-09 (M*s⁻¹)</i>
KS2	22.4 (R ² = 0.99)	26.1	n.d.
KS5	23.3 (R ² = 0.98)	27.1	6.48 (R ² = 0.99)
KS8	3.18 (R ² = 0.98)	3.7	n.d.
Hombikat UV 100	8.74 (R ² = 0.99)	10.2	1.67 (R ² = 0.99)
Kronos	25.4 (R ² = 0.99)	29.5	8.68 (R ² = 0.99)

Experimental conditions: Degradation of DCA (1 mM) in an aqueous solution of KNO₃ (200 mL) at pH= 3.0, 0.5 g/L of photocatalyst (commercial photocatalysts and the sulfur doped TiO₂ calcined at 500 °C (KS2) and 600 °C (KS5) for three hours), $\lambda_{\text{ex}} \geq 420$ nm $I_{\text{UV(A)}} = 3.7 \text{ W/m}^2$ and $\lambda_{\text{ex}} \geq 495$ nm, respectively.

As mentioned before for longer wavelengths ($\lambda_{\text{ex}} \geq 420$ nm) the photoactivity of Kronos and KS5 remained in the same range, whereas the photocatalytic activity of our standard UV-photocatalyst (Hombikat UV 100) decreased drastically eight times lower in comparison to results obtained at wavelengths $\lambda_{\text{ex}} \geq 320$ nm (see Table 14). It is also interesting to note, that Martin Lindner⁴⁸ obtained a photonic efficiency of 7.5 % for Hombikat UV 100 under the same illumination conditions ($\lambda_{\text{ex}} \geq 320$ nm) by DCA- degradation (1 mM), in comparison to our value 1.07 % (presented in Table 14). One of the main reasons could be the catalyst concentration: Lindner added ten times higher catalyst concentration (5 g/L) than for our DCA- degradation study (0.5 g/L). From Fig. 8 a (Lindner) it is possible to extrapolate the corresponding value of 1.2 (%) photonic efficiency for a catalyst loading of 0.5 g/L. This result is in very good agreement with our obtained value of 1.64 %. In comparison with the values in Table 13 the photonic efficiency for Hombikat UV 100 was 4.99 % for a light intensity of 15.5 W/m^2 , this result verifies the tendency explained by Lindner's studies (Fig. 8 d); the photonic efficiency increases with the decrease of light intensity. The photonic efficiencies at wavelengths $\lambda_{\text{ex}} \geq 420$ nm for the catalysts KS2, KS5 and Kronos are much higher than Hombikat UV 100. That could be explained due to the contribution of absorbed photons corresponding to longer wavelengths which increase the photocatalytic activity of the new catalysts into the visible region.

7.2.3 Degradation of DCA under outdoor solar illumination

A Duran glass reactor (see Fig. 14) was put outside for 4 hours with 1mM DCA dissolved in 200 mL distilled water containing KNO_3 (10 mM). The concentration of the catalyst was 0.5 g/L and every hour a sample was assayed to measure its TOC- content. Neither stirring nor bubbling of oxygen was carried out during these experiments, the reactors were closed with screw caps to prevent evaporation during the whole experiment. The light intensity was measured with a UV (A)- light meter instrument every hour and the value was 9.9 W/m^2 .

In order to find out the most suitable temperature conditions, the sulfur doped powder was calcined at different temperatures: 300 °C (KS1), 500 °C (KS2), 550 °C (KS3), 575 °C (KS4), 600 °C (KS5), 625 °C (KS6), 650 °C (KS7), 700 °C (KS8), 750 °C (KS9) for three hours, and yellow powders were obtained.

The results obtained in this experimental series for the different sulfur doped TiO_2 photocatalysts are plotted in Fig. 26.

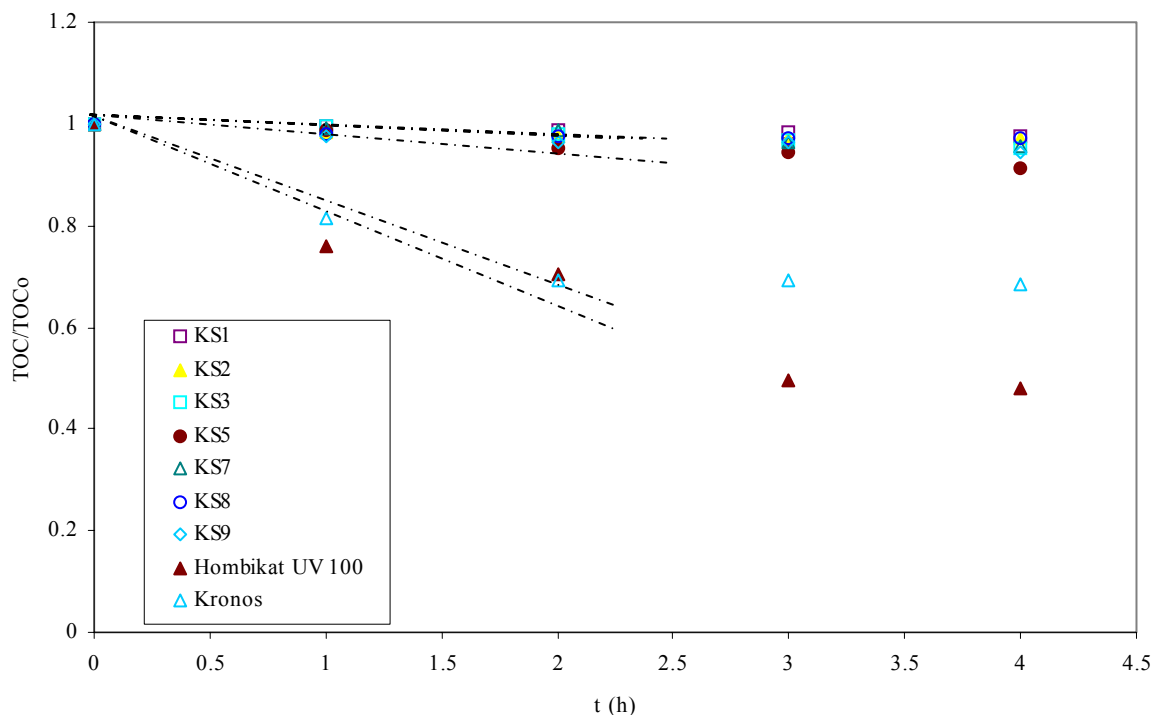


Fig. 26. Plot of TOC-reduction versus experimental time (h). *Experimental conditions:* 1mM DCA dissolved in 200 mL distilled water KNO_3 (10 mM) and 0.5 g/L (the commercial Hombikat UV 100 and Kronos and the sulfur doped TiO_2 catalysts calcined at different temperatures 300 °C (KS1), 500 °C (KS2), 550 °C (KS3), 575 °C (KS4), 600 °C (KS5), 625 °C (KS6), 650 °C (KS7), 700 °C (KS8), 750 °C (KS9) for three hours) during 4 hours under solar illumination $I_{\text{UV(A)}} = 9.9 \text{ W/m}^2$.

Table 16. The initial DCA-rates for the different photocatalysts have been determined following a kinetic of zero order. The relative rates have been calculated for each photocatalysts in relation with the initial DCA-rate of Hombikat UV 100, which was taken as standard.

	<i>Rate DCA * 1E-09</i> (<i>M*s-1</i>)	<i>Relative Rate</i> <i>Rate_{DCA}/Rate_{Hombikat}</i>	<i>P.E.(%)</i>
<i>KS1</i>	1.56 ($R^2 = 0.99$)	0.04	0.24
<i>KS2</i>	3.65 ($R^2 = 0.99$)	0.09	0.57
<i>KS3</i>	2.6 ($R^2 = 0.99$)	0.06	0.41
<i>KS5</i>	7.35 ($R^2 = 0.99$)	0.18	1.15
<i>KS7</i>	1.56 ($R^2 = 0.99$)	0.04	0.24
<i>KS8</i>	3.07 ($R^2 = 0.99$)	0.07	0.48
<i>KS9</i>	4.69 ($R^2 = 0.99$)	0.11	0.73
<i>Hombikat UV 100</i>	41.0 ($R^2 = 0.90$)	1.00	6.42
<i>Kronos</i>	42.5 ($R^2 = 0.99$)	1.04	6.66

Experimental conditions: 1mM DCA dissolved in 200 mL distilled water KNO_3 (10 mM) and 0.5 g/L catalyst during 4 hours under solar illumination $I_{\text{UV(A)}} = 9.9 \text{ W/m}^2$.

Under these illumination conditions, Hombikat UV 100 and Kronos are the only catalysts exhibiting any significant activity. The Kronos catalyst is a commercial catalyst which is expected to be active under visible light. However, its activity is in the same range as for the UV (A) active photocatalyst Hombikat UV 100.

In comparison with the data given in Table 14, the DCA-degradation rates of Hombikat UV 100 ($4.1\text{E-}08$) under solar illumination are lower (about two times) than obtained at the wavelengths $\lambda_{\text{ex}} \geq 320$ nm with the value of $7.37\text{E-}08 \text{ M*s}^{-1}$. On the other hand, Kronos shows similar DCA-rates under solar illumination ($4.2\text{E-}08 \text{ M*s}^{-1}$) and at the wavelengths $\lambda_{\text{ex}} \geq 320$ nm ($3.3\text{E-}08 \text{ M*s}^{-1}$). These differences can be explained due to the different light intensity in both systems and the distribution of the light. However, the DCA-degradation rate of the sulfur-modified TiO_2 photocatalysts decreases three times under solar illumination conditions in comparison to the values obtained at the wavelength of $\lambda_{\text{ex}} \geq 320$ nm e.g., the DCA-degradation rate for the photocatalyst KS5 (calcined at 600°C , for three hours) is $2.19\text{E-}08 \text{ M*s}^{-1}$. Hombikat UV 100 at wavelengths $\lambda_{\text{ex}} \geq 320$ nm is 44 % more active than KS5 (see Fig. 23) but at longer wavelengths ($\lambda_{\text{ex}} \geq 420$ nm) its activity is less than 13 % in comparison to KS5, due to the decrease of UV (A) -photons. Under solar illumination Hombikat shows 20 % better activity than KS5, indicating that only UV (A) photons are responsible for the photocatalytic DCA-degradation.

It would appear that the light conditions and particularly the experimental conditions such as reaction time and stirring rate during these experiments were not adequate for our purposes, also the UV (A) light intensity was probably too high. Therefore, it was decided to perform a second set of experiments under indoor illumination conditions with constant stirring and taking samples for TOC-measurement every 24 hours for 5 days.

7.2.3.1 Indoor solar illumination photoactivity test by DCA-degradation

The photocatalytic activity of the sulfur doped TiO_2 catalysts (calcined at different temperatures from 500°C to 750°C (corresponding to the notation: KS2- KS9) for three hours) for DCA-degradation was studied under indoor conditions (Hannover, from May to June'07). Every week a couple of experiments were carried out under the same experimental conditions except for the type of catalyst used in order to compare at least this pair to one another. The light intensity (mW/cm^2) was measured once every day at 14:00 pm with a UV (A)- Light Meter instrument and at the same time a sample was taken for TOC-determination.

The results obtained in this experimental series are plotted in Fig. 27, Fig. 28, Fig. 29, in Appendix Fig. 51 and Fig. 52 for the sulfur doped TiO_2 photocatalysts studied.

In order to compare these photocatalysts with the commercial ones, the same experiment was carried out for Hombikat UV 100 and Kronos (see Fig. 27).

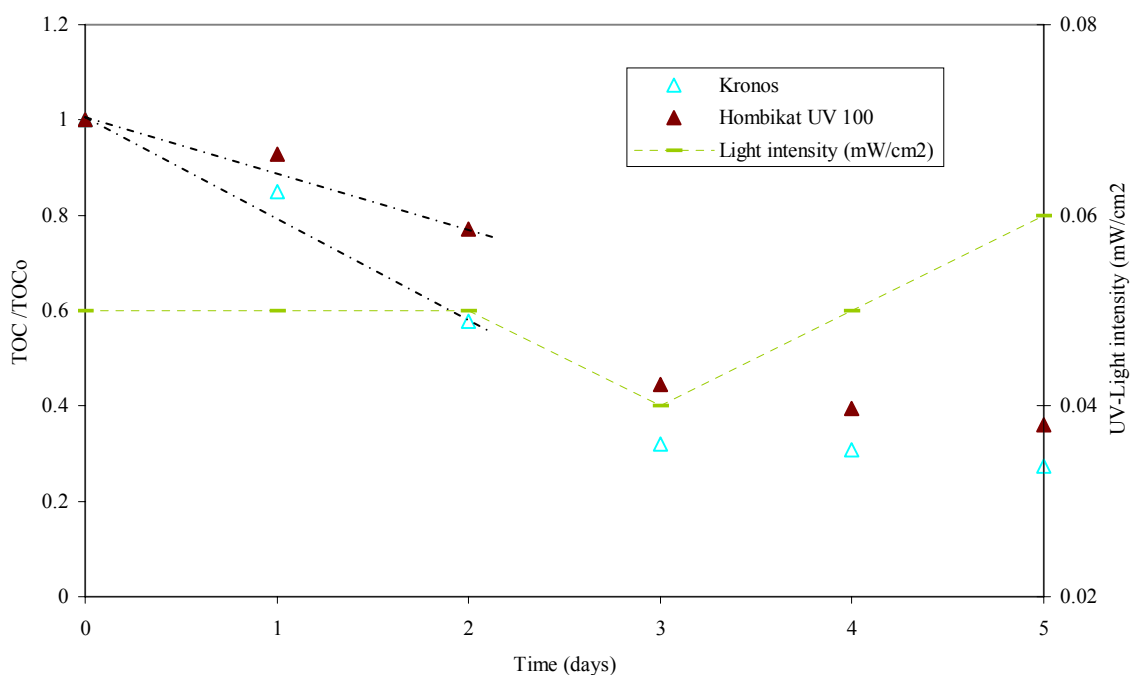


Fig. 27. Plot of TOC-reduction versus experimental time (days). *Experimental conditions:* 1mM DCA dissolved in 200 mL distilled water, KNO_3 (10 mM) and 0.5 g/L commercial photocatalyst Hombikat UV 100 and Kronos, reaction time of 5 days, under indoor illumination conditions mean value $I_{\text{UV}(\text{A})} = 0.5 \text{ W/m}^2$.

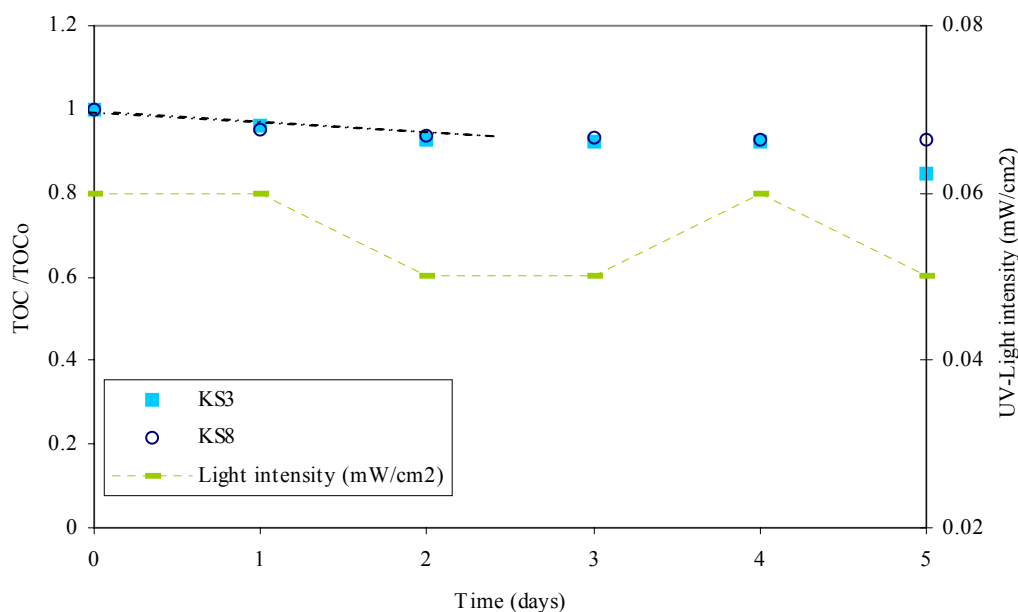


Fig. 28. Plot of TOC-reduction versus experimental time (days). *Experimental conditions:* 1mM DCA dissolved in 200 mL distilled water, KNO_3 (10 mM) and 0.5 g/L photocatalyst (sulfur doped TiO_2 photocatalysts calcined at 500 °C (KS3) and 750 °C (KS8), respectively) reaction time 5 days, under indoor illumination conditions mean value $I_{\text{UV}(\text{A})} = 0.5 \text{ W/m}^2$.

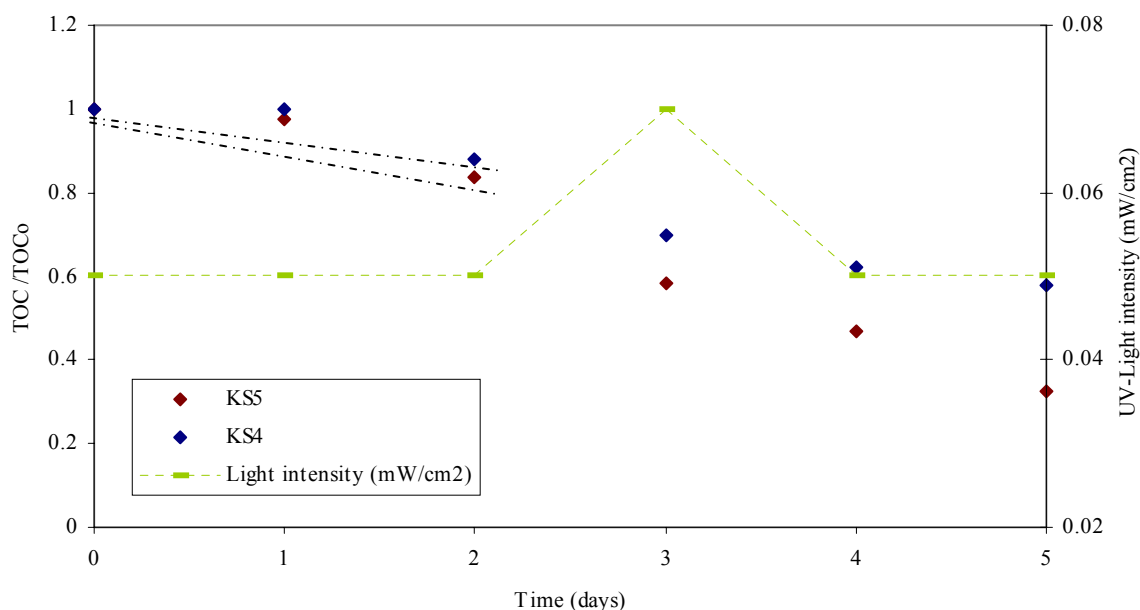


Fig. 29. Plot of TOC-reduction versus experimental time (days). *Experimental conditions:* 1mM DCA dissolved in 200 mL distilled water, KNO₃ (10 mM) and 0.5 g/L photocatalyst (sulfur doped TiO₂ calcined at 600 °C (KS5) and 575 °C (KS4), respectively) reaction time 5 days, under indoor illumination conditions mean value $I_{UV(A)} = 0.5 \text{ W/m}^2$.

Table 17. The initial DCA- rates of the sulfur doped TiO₂ photocatalysts are shown, following a kinetic of zero order. The relative rates have been calculated for each photocatalysts in relation with the DCA-rate of Hombikat UV 100, which was taken as standard. For the calculation of photonic efficiencies it is assumed that every day has only 14 hours solar illumination $I_{UV(A)} = 0.5 \text{ W/m}^2$.

<i>Photocatalyst</i>	<i>Rate DCA * 1E-09</i>	<i>Relative Rate</i>	
	<i>(M*s-1)</i>	<i>RateCat/RateHombikat</i>	<i>P.E. (%)</i>
<i>KS2</i>	0.64 ($R^2 = 0.98$)	0.28	1.99
<i>KS3</i>	1.15 ($R^2 = 0.90$)	0.50	3.55
<i>KS4</i>	1.19 ($R^2 = 0.81$)	0.52	3.69
<i>KS5</i>	1.62 ($R^2 = 0.80$)	0.71	5.02
<i>KS6</i>	2.81 ($R^2 = 0.91$)	1.23	8.70
<i>KS7</i>	1.89 ($R^2 = 0.90$)	0.83	5.85
<i>KS8</i>	0.65 ($R^2 = 0.92$)	0.29	2.01
<i>KS9</i>	0.96 ($R^2 = 0.93$)	0.42	2.97
<i>Hombikat UV 100</i>	2.27 ($R^2 = 0.91$)	1.00	7.05
<i>Kronos</i>	4.19 ($R^2 = 0.98$)	1.84	12.99

Experimental conditions: 1mM DCA dissolved in 200 mL distilled water, KNO₃ (10 mM) and 0.5 g/L photocatalyst (sulfur doped TiO₂ calcined in the range from 500 °C to 750 °C) with a reaction time of 5 days.

Under these experimental conditions, Hombikat UV 100, Kronos VLP 7001 and the sulfur doped TiO₂ catalysts calcined at 575 °C (KS4), 600 °C (KS5) and 625 °C (KS6) for 3 hours, are the most active photocatalysts. 70 % of TOC removal was observed for Kronos (see Fig. 27), following by KS5 with 68 % TOC removal, meanwhile TOC mineralization for KS4 was 40 % (see Fig. 29) and 58 % for the photocatalyst KS6 (see Fig. 52 in Appendix).

As shown in Fig. 51 and Fig. 28 for calcination temperatures from 500°C - 550°C to 700°C - 750°C no significant photoactivity was found for the sulfur modified TiO₂ photocatalysts under indoor illumination conditions. This fact was also confirmed under other illumination conditions such as by using a Xe-lamp with 320 nm and 420 nm cut-off filters (section 7.2.2.) and solar illumination (section 7.2.3.). A possible reason could be that at lower calcination temperatures, the physical properties of the photocatalysts such as crystallinity, BET- surface and particle size, do not achieve an optimal value, reducing its photoactivity. The same occurs at higher calcination temperatures (from 700 °C) and also the presence of rutile will be increased.

It was possible to achieve an optimal calcination temperature range from 575°C to 650°C for the sulfur doped TiO₂ photocatalysts as shown in Fig. 27 and Fig. 29. It is observed in Table 17, that DCA-rate increases with calcination temperature corresponding to this interval, e.g. for the sulfur doped TiO₂ photocatalyst calcined at 575°C (KS4), the calculated DCA-rate is 1.19E-09 M*s⁻¹, for KS5 the corresponding rate is 1.62E-09 M*s⁻¹, meanwhile the maximal DCA-rate value is for KS6 (sulfur doped TiO₂ photocatalyst calcined at 625°C) with a value of 2.81E-09 M*s⁻¹. In comparison with the data in Table 16 (under solar illumination conditions) the photonic efficiency of Hombikat UV 100 is in the same range from 6.42 % to 7.05 %. However, for Kronos it is two times lower 6.66 % (under solar illumination) and for KS5 almost five times 1.15 %. It is obviously the additional contribution of photons corresponding to the visible light region ($\lambda \geq 400$ nm).

The sulfur modified photocatalyst calcined at 600°C (KS5) for three hours has the best photocatalytic properties for DCA-degradation (under indoor solar illumination conditions) getting a TOC-removal of 68%. That corroborates the published results by Prof. Ohno et al.²⁷ They explained this fact due to the extension of the photocatalytic properties of this photocatalyst at longer wavelengths ($\lambda \geq 400$ nm) determined by diffuse reflectance spectroscopy (DRS). The sulfur doped TiO₂ photocatalyst calcined at 600°C (KS5) showed also the best photoactivity for 4-Chlorophenol degradation with a yield of 23 % after 180 min. (Data obtained in the PhD work of Janczarek, who also followed Prof. Ohno's recipe to synthesize the photocatalysts, see section 6.1.2.). The difference of the Janczarek experimental time is due to the selection of model compound. Phenolic compounds such as 4-Chlorophenol (4- CP) significantly absorb visible light at wavelengths $\lambda > 400$ nm, following another kinetic mechanism (see indirect photocatalysis in section 5.3.2.).

DCA-photodegradation has been improved under these experimental conditions e.g. longer experimental time, constant stirring rate and indoor illumination conditions. It is now necessary to study, in detail, how to develop the properties of our sulfur modified TiO₂ photocatalysts e.g., with different calcination temperatures in the range from 575°C to 675°C, different sulfur concentrations (7.2.3.3.) and heating profiles (7.2.3.4.).

7.2.3.2 Dependence on the relative position of the reactor

The photocatalytic activity of sulfur doped TiO_2 and commercial photocatalysts for the degradation of DCA was studied under indoor solar conditions to test the effect of indoor sunlight. Six reactors were placed near the window for 5 days containing 1 mM DCA dissolved in 200 mL distilled water in the presence of KNO_3 (10 mM). At the beginning of the experiment a value of $\text{pH}=3$ was achieved for each reactor. During the first three days a polycarbonate box was put over the six reactors to avoid any UV (A)-light and after that time the experiments were carried out for two days more without the box.

Hombikat UV 100 and the sulfur doped TiO_2 photocatalysts, calcined at $500\text{ }^\circ\text{C}$, were each tested three times, (as shown in Fig. 30) in order to see if there is some influence on the photocatalytic activity of the catalyst depending upon the reactor's position in the system.

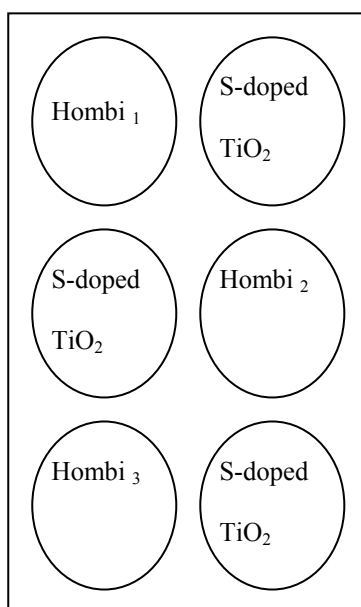


Fig. 30. Layout of catalysts position

Fig. 14 shows the set-up used for the activity tests of the photocatalysts. The obtained results are plotted in Fig. 31.

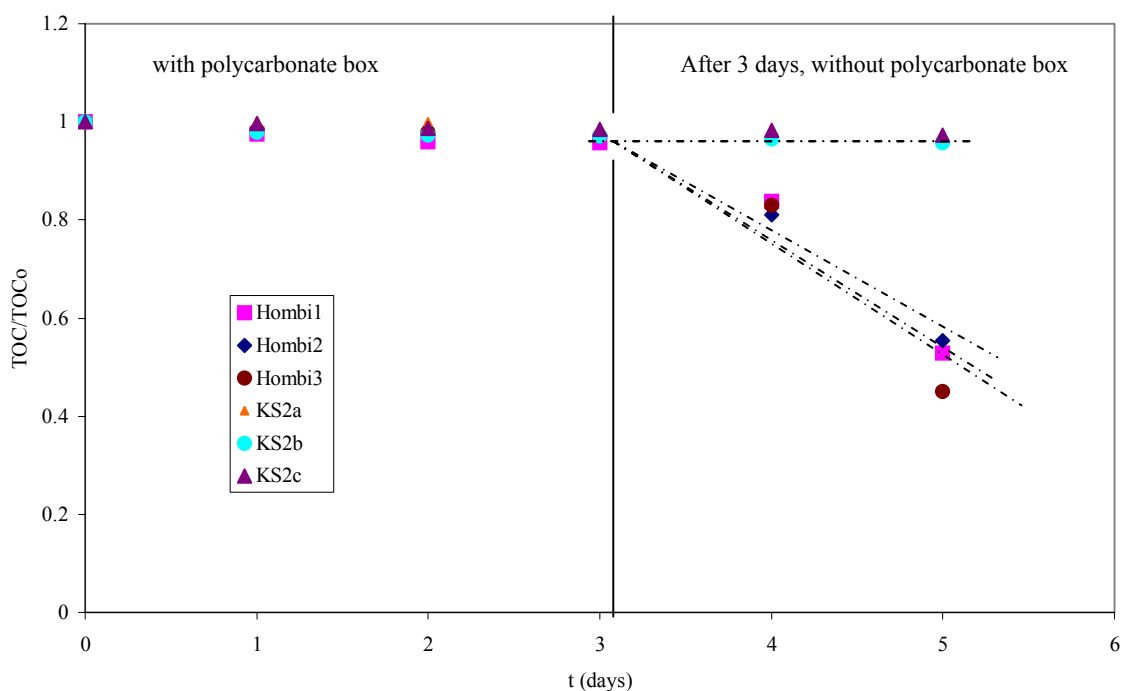


Fig. 31. Plot of TOC-reduction versus experimental time (h). *Experimental conditions:* 1mM DCA dissolved in 200 mL distilled water, KNO_3 (10 mM) and 0.5 g/L catalyst (with a molar ratio of 1:4) with a reaction time of 5 days, under indoor illumination conditions.

Table 18. The calculated photonic efficiencies and DCA-rates for Hombikat UV 100 and sulfur doped TiO_2 catalyst (KS2) (during the last two days of the illumination experiments without the polycarbonate box, taking into account that one day has only 14 hours solar illumination).

		<i>Rate DCA*1E-09</i>	
		<i>(M*s-1)</i>	<i>P.E. (%) C_{DCA}</i>
Hombikat UV 100	<i>1</i>	3.71	14.37
	<i>2</i>	3.78	14.65
	<i>3</i>	4.96	19.18
KS2	<i>1</i>	0.045	0.18
	<i>2</i>	0.15	0.58
	<i>3</i>	0.091	0.35

Experimental conditions: 1mM DCA dissolved in 200 mL distilled water, KNO_3 (10 mM) and 0.5 g/L catalyst with an experimental time of 5 days.

The reactors' position in the system does not have any important effect on the calculated photocatalytic activity (see Fig. 31). It is very important to confirm this, as a meaningful comparison between each photocatalyst is only possible if the relative position in which the experiment has been carried out does not play any role.

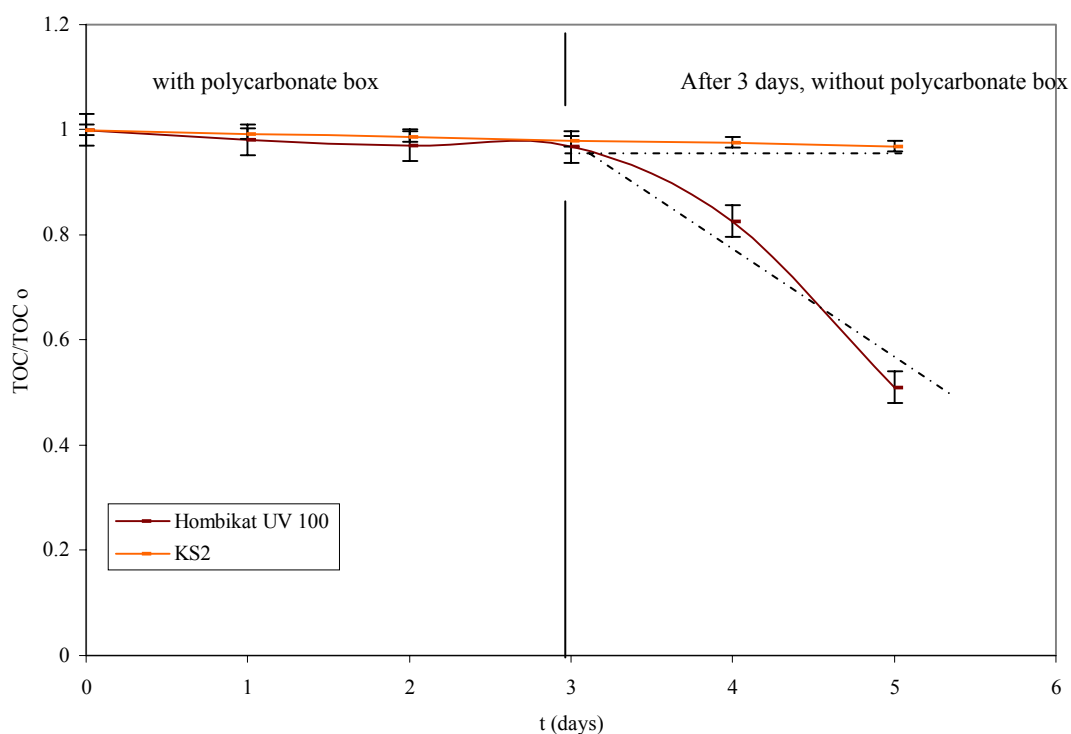


Fig. 32. Normalized TOC-values versus illumination time (hours) Mean values and standard deviation calculated for Hombikat UV 100 (2.03) and the sulfur doped TiO₂ catalyst (0.16) calcined at 500 °C (KS2) for 3 hours, for the degradation of DCA under indoor illumination conditions: 1mM DCA dissolved in 200 mL distilled water, KNO₃ (10 mM) and 0.5 g/L catalyst, reaction time 5 days, $I_{UV(A)} = 0.4 \text{ W/m}^2$.

Table 19. Photonic efficiencies calculated (during the last two days without the polycarbonate box) from the mean values of Hombikat UV 100 and the sulfur doped TiO₂ catalyst (KS2): 1mM DCA dissolved in 200 mL distilled water, KNO₃ (10 mM) and 0.5 g/L catalyst, with a reaction time of 5 days, $I = 0.4 \text{ W/m}^2$.

	<i>Rate DCA *1E-09</i>	
	<i>(M*s-1)</i>	<i>P.E. (%) C_{DCA}</i>
Hombikat UV 100	4.15	16.07
KS2	0.10	0.37

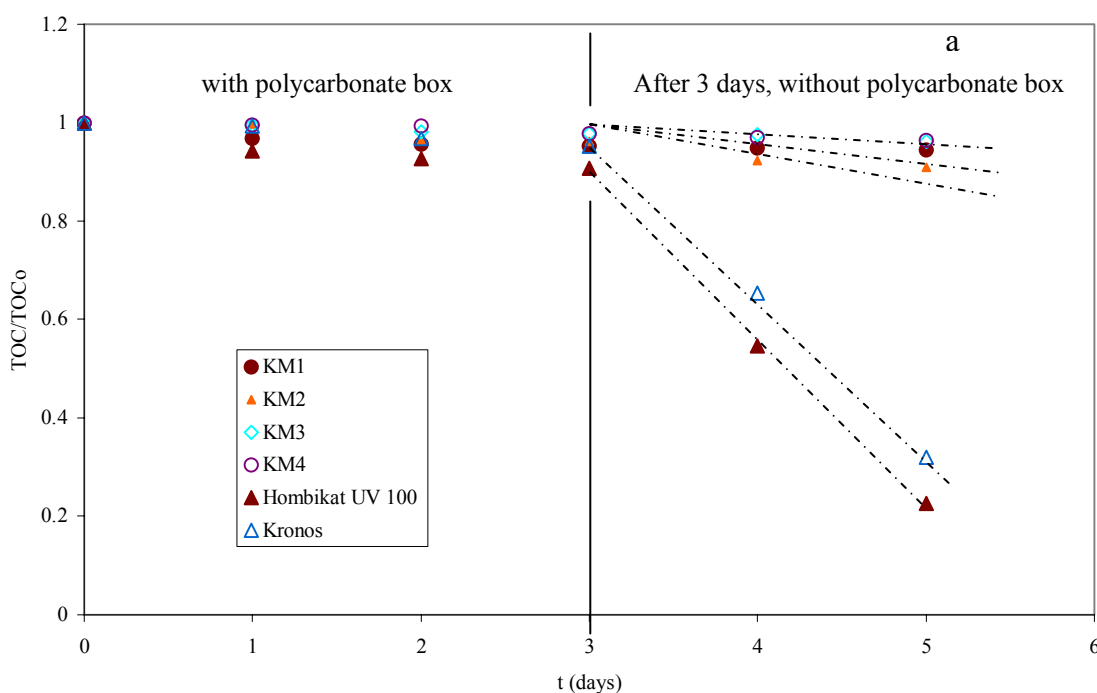
Experimental conditions: 1mM DCA dissolved in 200 mL distilled water, KNO₃ (10 mM) and 0.5 g/L catalyst with an experimental time of 5 days.

During the last two days without the polycarbonate box, the degradation of DCA in the presence of TiO_2 and oxygen can be assumed to follow a kinetic of zero order (see Fig. 32, the explanation for photonic efficiency calculations are given in section 6.3.4.).

7.2.3.3 Study of sulfur-concentration and calcination temperature

To study the effect of different sulfur contents other molar ratios of titanium (IV) isopropoxide to thiourea were chosen: 1:2 and 1:6. The new sulfur- modified TiO_2 photocatalysts were calcined at several different temperatures: 500°C; 600°C; 650°C; and 750°C for 3 hours and 7 hours, each. Six photocatalysts were tested at the same time (see photoactivity test Fig. 13) under indoor illumination conditions for five days. For the first three days the polycarbonate box was put over the reactors in order to have only visible light irradiation, the last two days were without the box. Every day a sample was taken and TOC-removal was measured.

Fig. 33 shows the influence of the different calcination temperatures (3 or 7 hours) on the photoactivity of the sulfur doped catalysts.



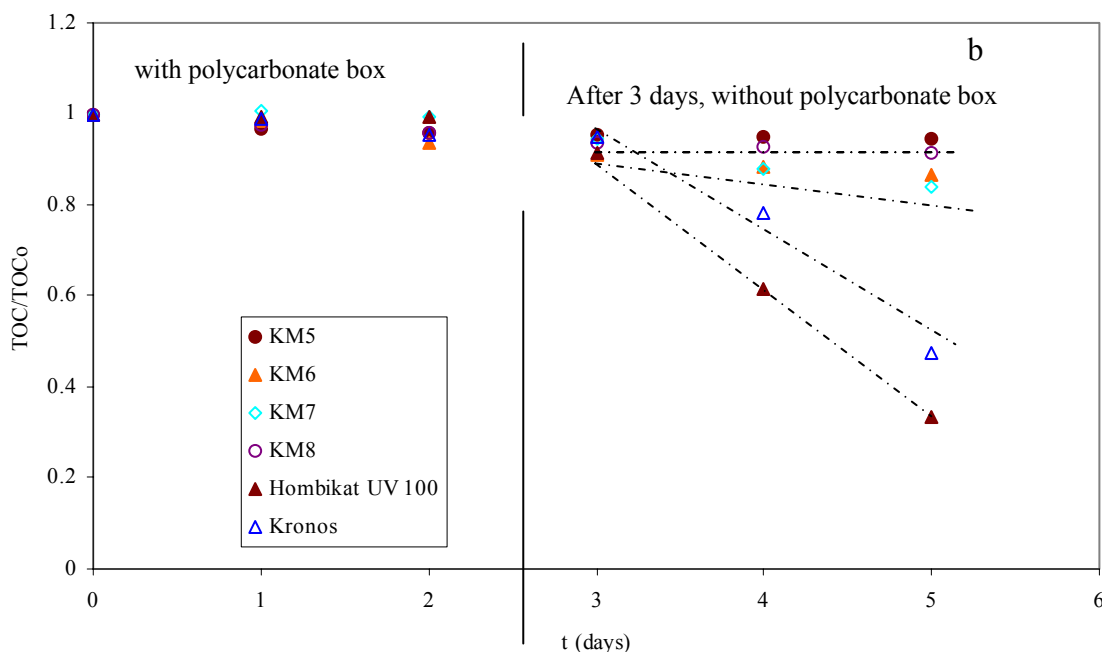


Fig. 33. TOC- removal for the DCA-degradation versus experimental time (days). *Experimental conditions:* 1mM DCA dissolved in 200 mL distilled water, KNO_3 (10 mM) and 0.5 g/L photocatalyst (a) synthesized with a molar ratio of titanium (IV) isopropoxide and thiourea 1:6, calcined for 3 h. b) calcined for 7 h with a reaction time of 5 days under indoor illumination conditions.

Table 20. Photonic efficiencies calculated during the last two days without the polycarbonate box, taking into account that every day has only 14 hours illumination ($I_{\text{UV}(A)} = 0.4 \text{ W/m}^2$) for Hombikat UV 100, Kronos and the sulfur doped TiO_2 catalyst (calcined in the range from 500 °C to 750 °C), with a molar ratio of 1:6 (titanium (IV) isopropoxide to thiourea).

<i>Photocatalyst</i>	<i>Rate DCA *1E-09</i>	
	<i>(M*s-1)</i>	<i>P.E. (%)</i>
<i>KM1</i>	0.55 ($R^2 = 0.99$)	2.14
<i>KM2</i>	0.91 ($R^2 = 0.93$)	3.51
<i>KM3</i>	0.38 ($R^2 = 0.86$)	1.47
<i>KM4</i>	0.35 ($R^2 = 0.97$)	1.36
<i>Hombikat UV 100</i>	7.68 ($R^2 = 0.99$)	29.71
<i>Kronos</i>	6.74 ($R^2 = 0.99$)	26.08
<i>KM5</i>	0.55 ($R^2 = 0.99$)	2.14
<i>KM6</i>	1.33 ($R^2 = 0.99$)	5.13
<i>KM7</i>	1.60 ($R^2 = 0.98$)	6.19
<i>KM8</i>	0.83 ($R^2 = 0.99$)	3.22
<i>Hombikat UV 100</i>	6.62 ($R^2 = 0.99$)	25.62
<i>Kronos</i>	5.20 ($R^2 = 0.99$)	20.12

Experimental conditions: 1mM DCA dissolved in 200 mL distilled water, KNO_3 (10 mM) and 0.5 g/L catalyst with an experimental time of 5 days.

All the powders have been tested and it appears that the obtained TOC removal is much lower than with molar ratio titanium (IV) isopropoxide to thiourea 1:4 (see Table 17), this was also confirmed by reflectance measurements. No shift into the visible region was observed for other molar ratios, (except for 1:4). Therefore, it could be concluded that the optimal molar ratio is 1:4 (titanium (IV) isopropoxide to thiourea), supporting the work of Prof. Ohno et al.²⁷ and Periyat et al.³⁰. Periyat et al. have tested various molar ratios 1:1, 1:2, 1:4, 1:8 and 1:16, obtaining 1:4 as the optimal one. The catalysts with a higher sulfur concentration, e.g. with a molar ratio of 1:6, do not show any noticeable photoactivity. Also the increase of thiourea concentration during the synthesis did not cause higher carbon content of the photocatalysts (see Table 9).

In fact, only Hombikat UV 100 and Kronos VLP 7001 showed remarkable activity for the degradation of DCA of 80 % and 60 % after two days of reaction time, respectively. No photocatalytic activity was observed for any photocatalysts during the three days within the polycarbonate box.

7.2.3.4 Study of the dependence of different heating rates

So far, the most active sulfur doped photocatalysts have been calcined at 600 °C for three hours (with a molar ratio of 1:4 for titanium isopropoxide and thiourea in ethanol). For this reason, a fine-tuning of the synthetic method was carried out. The oven was set to study the dependency of different temperature profiles (10 °C, 50 °C, 100 °C, 200 °C, 300 °C and 400 °C per hour) and the photocatalysts were calcined within the range of 600 °C: at 550, 575, 600 and 625°C for three hours, in each case. Six photocatalysts have been tested at the same time under indoor illumination conditions for five days. For the first three days the polycarbonate box was put over the reactors in order to avoid the presence of UV-light irradiation, the last two days were without the polycarbonate cover. Every day a sample was taken for TOC-measurements.

Fig. 34 and in Appendix Fig. 53, Fig. 54, Fig. 55, Fig. 56 and Fig. 57 show the results obtained for the degradation of DCA under indoor solar illumination conditions.

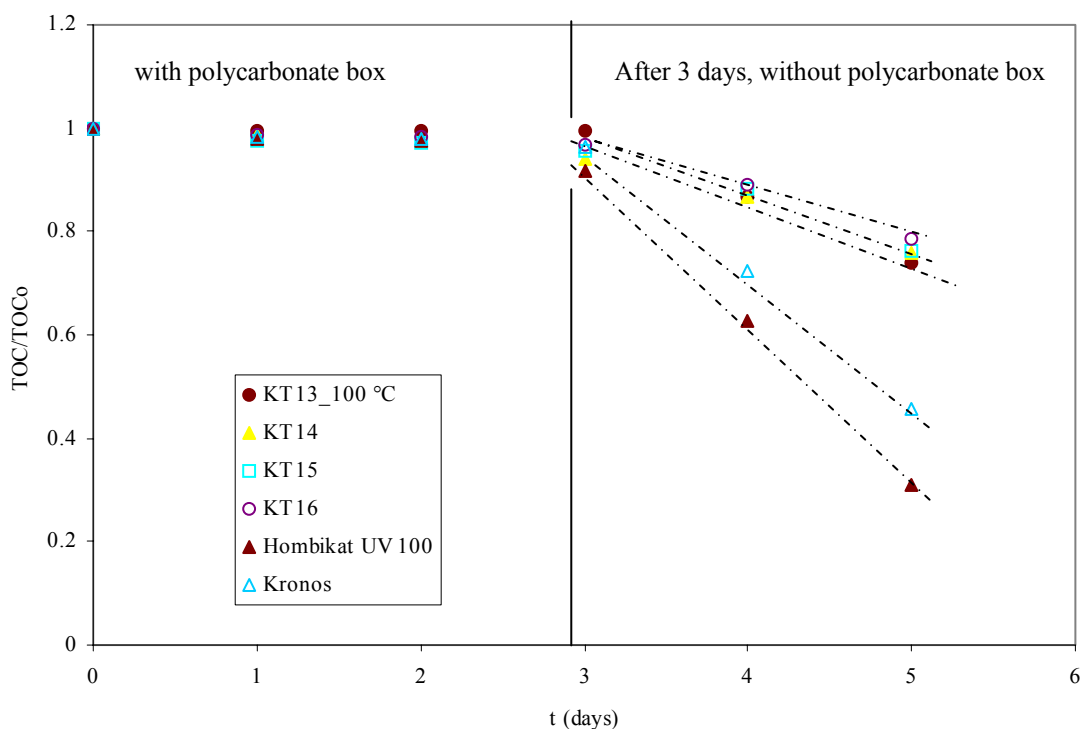


Fig. 34. TOC-mineralization of DCA for the photocatalysts: Hombikat UV 100, Kronos and sulfur doped TiO_2 , which were calcined at $550\text{ }^\circ\text{C}$ (KT13), $575\text{ }^\circ\text{C}$ (KT14), $600\text{ }^\circ\text{C}$ (KT15) and $625\text{ }^\circ\text{C}$ (KT16) for three hours with $100\text{ }^\circ\text{C/h}$ as calcinations program versus experimental time (5 days), $I_{\text{UV(A)}} = 0.4\text{ W/m}^2$.

Table 21. DCA- degradation rates of the sulfur doped TiO_2 catalysts which were calcined for three hours at different temperatures: $550\text{ }^\circ\text{C}$, $575\text{ }^\circ\text{C}$, $600\text{ }^\circ\text{C}$ and $625\text{ }^\circ\text{C}$, and with different temperature profiles $10\text{ }^\circ\text{C/h}$, $50\text{ }^\circ\text{C/h}$, $100\text{ }^\circ\text{C/h}$, $200\text{ }^\circ\text{C/h}$, $300\text{ }^\circ\text{C/h}$ and $400\text{ }^\circ\text{C/h}$. The DCA- degradation rates for the commercial catalysts (Hombikat UV 100 and Kronos VLP 7001) are also included.

<i>DCA- degradation rates for commercial catalysts * 1E-09 (M*s⁻¹)</i>			<i>DCA- rates for sulfur doped TiO₂ catalysts * 1E-09 (M*s⁻¹)</i>			
<i>Hombikat UV 100</i>	<i>Kronos</i>	<i>T. prof. (°C/h)</i>	<i>550 °C</i>	<i>575 °C</i>	<i>600 °C</i>	<i>625 °C</i>
6.71	6.33	10	3.05	2.82	1.5	0.73
4.17	3.58	50	0.53	1.27	0.88	0.62
6.85	5.38	100	2.6	2.39	2.37	2.12
4.71	3.4	200	0.78	1.52	2.05	1.15
5.96	3.9	300	0.52	1.09	0.92	0.73
5.47	3.47	400	0.99	0.42	0.52	0.82

Experimental conditions: 1mM DCA dissolved in 200 mL distilled water, KNO_3 (10 mM) and 0.5 g/L photocatalyst with a reaction time of 5 days.

Table 22. Photonic efficiencies of the sulfur doped TiO₂ catalysts which were calcined for three hours at different temperatures: 550 °C, 575 °C, 600 °C and 625 °C, and with different temperature profiles 10 °C/h, 50 °C/h, 100 °C/h, 200 °C/h, 300 °C/h and 400 °C/h.

<i>Photonic efficiencies for commercial catalysts (%)</i>			<i>Photonic efficiencies for sulfur doped TiO₂ catalysts (%)</i>			
<i>Hombikat UV 100</i>	<i>Kronos</i>	<i>T. prof. (°C/h)</i>	<i>550 °C</i>	<i>575 °C</i>	<i>600 °C</i>	<i>625 °C</i>
25.97	24.50	10	11.80	10.91	5.81	2.83
16.14	13.85	50	2.05	4.91	3.41	2.40
26.51	20.82	100	10.06	9.25	9.17	8.20
18.23	13.16	200	3.02	5.88	7.93	4.45
23.07	15.09	300	2.01	4.22	3.56	2.83
21.17	13.43	400	3.83	1.63	2.01	3.17

Experimental conditions: 1mM DCA dissolved in 200 mL distilled water, KNO₃ (10 mM) and 0.5 g/L photocatalyst with a reaction time of 5 days, $I_{UV(A)} = 0.4 \text{ W/m}^2$.

The DCA-degradation rates have been determined assuming a kinetic of order zero from the corresponding slopes of the respective studied catalysts taking into account the reaction time without the polycarbonate box only.

The DCA-degradation rates were normalized in relation to our standard photocatalyst (Hombikat UV 100) and plotted in Fig. 35, in order to compare the temperature profile dependency. In Fig. 35 the values corresponding to 150 °C/h as temperature profile were taken from Table 17 (under solar illumination conditions $I_{UV(A)} = 0.5 \text{ W/m}^2$).

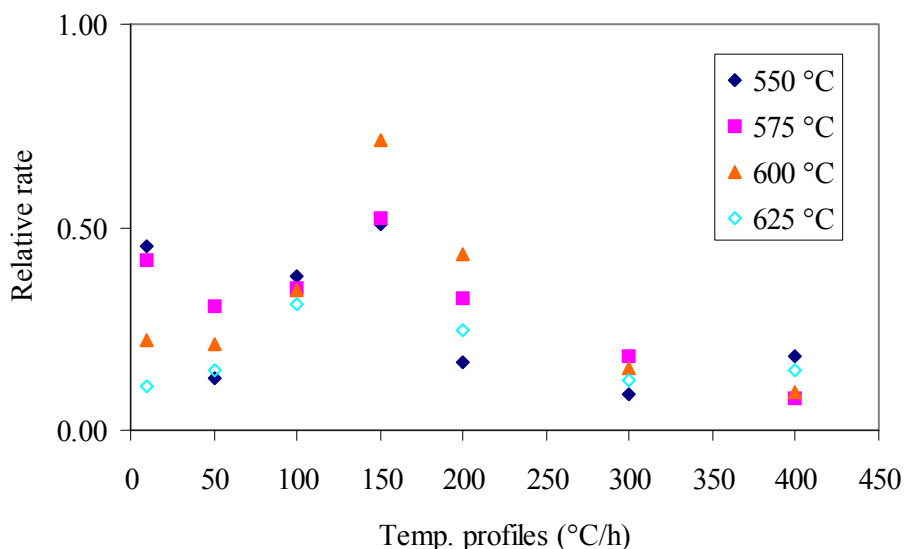


Fig. 35. Plot of relative rates versus temperature profiles for the sulfur doped TiO₂ photocatalysts calcined at 550 °C, 575 °C, 600 °C and 625 °C, respectively under different temperature profiles 10 °C/h, 50 °C/h, 100 °C/h, 150 °C/h, 200 °C/h, 300 °C/h and 400 °C/h.

Faster temperature profiles showed no improvement to the photocatalytic properties of the catalysts and verified the importance of heating profiles for the synthesis of new materials. These results confirmed the experimental reflection spectra measurements data shown in Fig. 21. The reflection spectra of lower temperature profiles from 10 °C/h to 100 °C/h show a wider shoulder at longer wavelengths $\lambda \geq 400$ nm, extending the photoactivity of the catalysts into the visible light region.

The commercial photocatalysts Hombikat UV 100 and Kronos were always the most active photocatalysts. The modified sulfur doped TiO₂ photocatalysts showed an enhancement of the photocatalytic properties by reducing the temperature profiles e.g., for 10 °C/h the catalysts calcined at 550 °C (KT21) and 575 °C (KT22) showed a decrease of 30 % DCA degradation, however for 100 °C/h the obtained results were in the same range. As shown in Fig. 35 lower temperature profiles enhance the physical properties of the photocatalysts increasing the degradation rates and favouring a gradient of temperature, in contrast higher temperature profiles exhibit lower degradation rates. The indoor illumination conditions depend on the weather, so at this point it was decided to design a new chamber with artificial visible light illumination in order to get reproducible illumination conditions.

7.2.4 Degradation of DCA under artificial visible illumination

7.2.4.1 Study of standard catalyst

To study the dependence on the photoactivity of different heating profiles such as 10 °C/h and 100 °C/h, a new illumination chamber was used (as shown Fig. 16). The new system has six lamps (type of lamp: ibv L18W742 Coolwhite 18 W) for artificial illumination experiments in order to achieve more reproducible experimental conditions. The commercial catalysts such as Hombikat UV 100, Kronos, Degussa P25 and Toho have been tested under the same experimental conditions in order to compare them with the sulfur doped TiO₂ photocatalysts.

Fig. 36 shows the change in TOC values for DCA degradation during illumination of the commercial catalysts Hombikat UV 100, Kronos (VLP 7001- commercial photocatalyst), Degussa P 25 and Toho (commercial sulfur doped TiO₂ photocatalyst), with a UV (A)-light intensity of 0.3 W/m² at a distance of 60 cm (lamps-reactors).

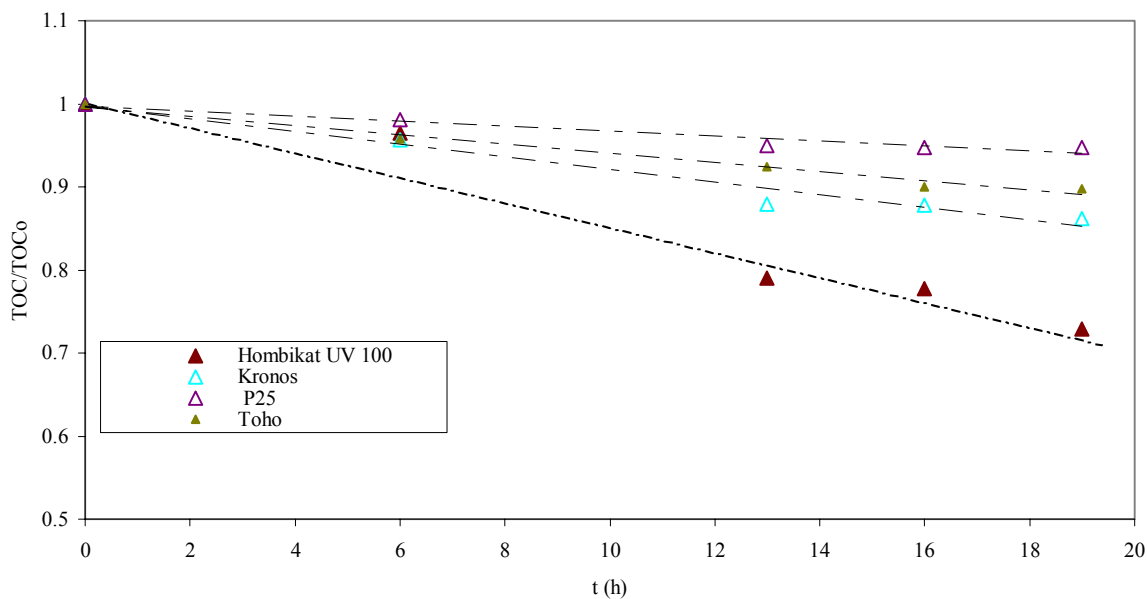


Fig. 36. Plot of TOC- decrement for DCA- degradation study versus illumination time (h) under artificial illumination conditions: 1mM DCA dissolved in 200 mL distilled water, KNO_3 (10 mM) and 0.5 g/L commercial catalyst illuminated for 19 hours ($I_{\text{UV(A)}} = 0.3 \text{ W/m}^2$).

Despite the low UV (A) light intensity, Hombikat UV 100 remained as the most active photocatalyst with a TOC degradation of about 25 %, following by Kronos with 17 % and Toho with 10 %. Surprisingly, Degussa P25, which contains anatase, rutile and amorphous phase in the ratio of 78:14:8, respectively showed very low photoactivity properties for DCA degradation under these work conditions. It was reported by Ohtani et al.⁷² that the composition of Degussa P25 is not very homogeneous and it could be possible to get different compositions in the same batch. Due to this effect it might be that the quantity taken for Degussa P25 contained less rutile, reducing the photoactivity of Degussa P25 at longer wavelengths. Nevertheless, the degradation rate of Hombikat UV 100 was higher than expected, this could be explained by a photon limit effect, decreasing the recombination of holes and electrons and enhancing the photoreactivity of Hombikat UV 100.

7.2.4.2 Study of heating- profiles dependency

The sulfur doped catalysts which have been tested were calcined at different calcination temperatures in the range from 550 °C to 625°C and with heating profiles 10 °C/h (KT21- KT24) and 100°C/h (KT13- KT16).

Fig. 37 and Fig. 38 show the change of TOC values for DCA degradation during illumination of the sulfur doped TiO₂ catalyst calcined at 550°C, 575°C, 600°C and 625°C for three hours (10°C/h and 100 °C/h as calcination ramp), with a UV (A) light intensity of 0.3 W/m².

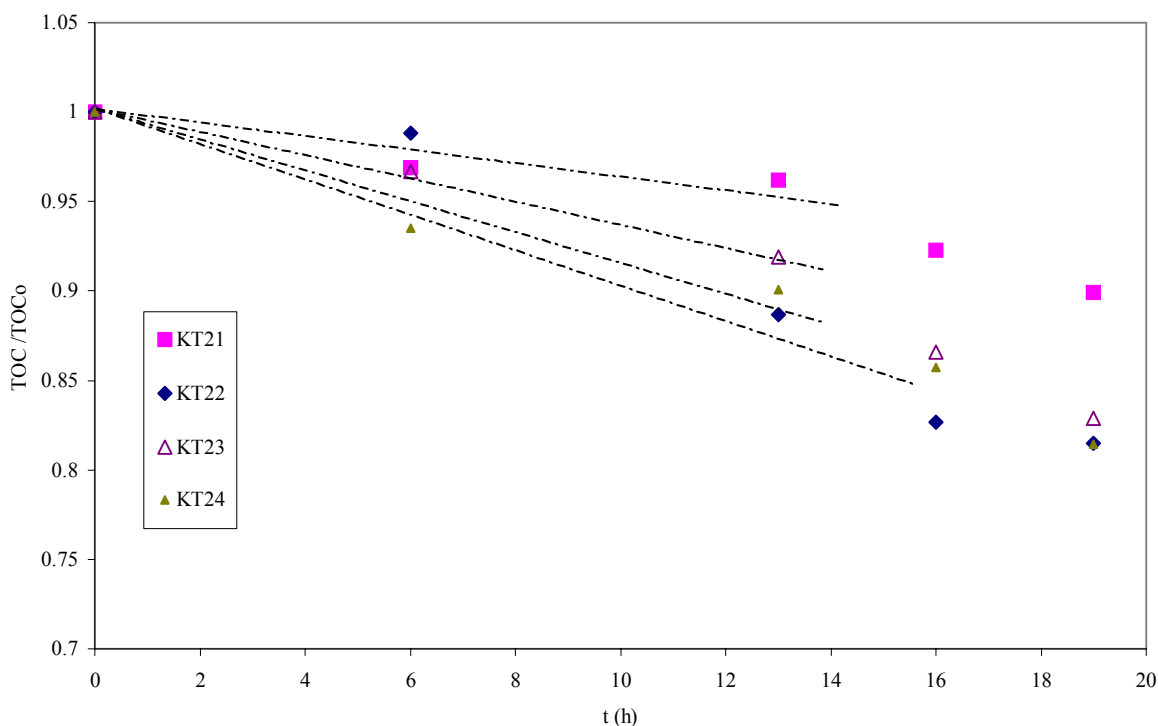


Fig. 37. Decrease of TOC- values versus illumination time (h) for the sulfur doped TiO₂ photocatalysts calcined at 550°C (KT21), 575°C (KT22), 600°C (KT23) und 625°C (KT24) for three hours (10°C/h as calcination ramp), with an UV (A) light intensity of 0.3 W/m².

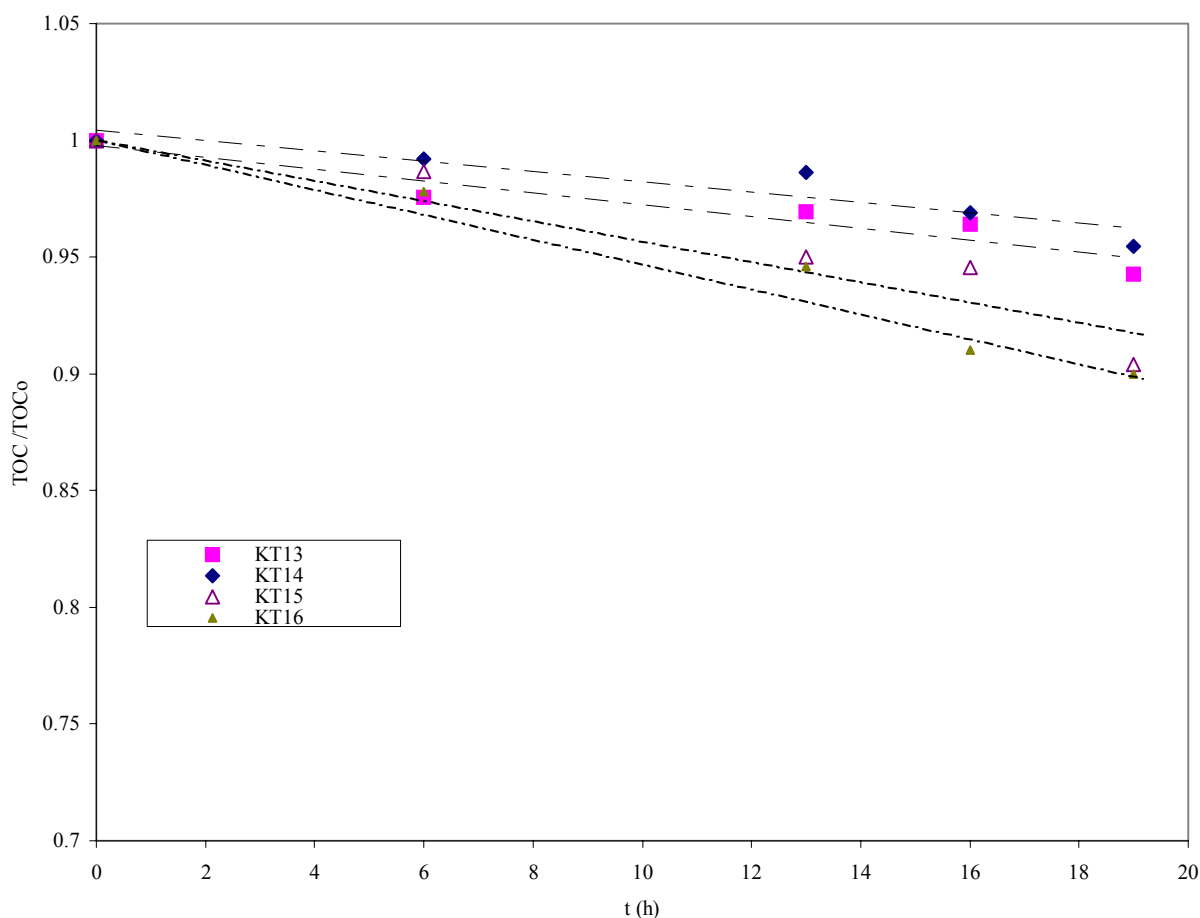


Fig. 38. TOC-mineralization versus illumination time (h) under artificial illumination conditions. *Experimental conditions:* 1mM DCA dissolved in 200 mL distilled water, KNO_3 (10 mM) and 0.5 g/L catalyst (sulfur doped TiO_2 photocatalysts with a molar ratio of 1:4 and $100\text{ }^\circ\text{C/h}$ as heating profile for different calcination temperatures $550\text{ }^\circ\text{C}$ (KT13), $575\text{ }^\circ\text{C}$ (KT14), $600\text{ }^\circ\text{C}$ (KT15) and $625\text{ }^\circ\text{C}$ (KT16)) illuminated for 19 hours, UV (A) light intensity value of 0.3 mW/m^2 and the distance from the lamps to the reactors 60 cm.

It can be observed that the modified sulfur doped TiO_2 catalysts calcined at $575\text{ }^\circ\text{C}$ (KT22), $600\text{ }^\circ\text{C}$ (KT23) and $625\text{ }^\circ\text{C}$ (KT24) with a calcination ramp of $10\text{ }^\circ\text{C/h}$ are as active as the commercial photocatalyst Kronos with a UV(A) light intensity of 0.3 W/m^2 , followed by the commercial catalyst Toho (see Fig. 36). On the other hand, KT13, KT14, KT15 and KT16, which have been calcined at the same temperatures but with a different heating profile of $100\text{ }^\circ\text{C/h}$, are less active. It can be concluded that the calcination temperature profile plays a very important role in the photoactivity of the catalyst. Obviously, a slower heating rate of $10\text{ }^\circ\text{C/h}$ in comparison to $100\text{ }^\circ\text{C/h}$ enhances the photocatalytic properties of the catalysts.

7.2.4.3 Dependence on sulfur molar ratio

The sulfur doped TiO₂ catalysts which have been measured under artificial illumination experiments in order to study the dependence on higher sulfur molar ratio: KT21A, KT22A, KT23A, KT24A.

Fig. 39 shows the change in TOC- concentration for DCA degradation during illumination of sulfur- doped TiO₂ calcined at 550°C (KT21A), 575°C (KT22A), 600°C (KT23A) and 625°C (KT24A) for three hours (with a calcination profile of 10 °C/h), containing a higher molar ratio of 1:6 titanium (IV) isopropoxide to thiourea and with a UV(A) light intensity of 0.3 W/m² and distance from the lamps to the reactors of 60 cm.

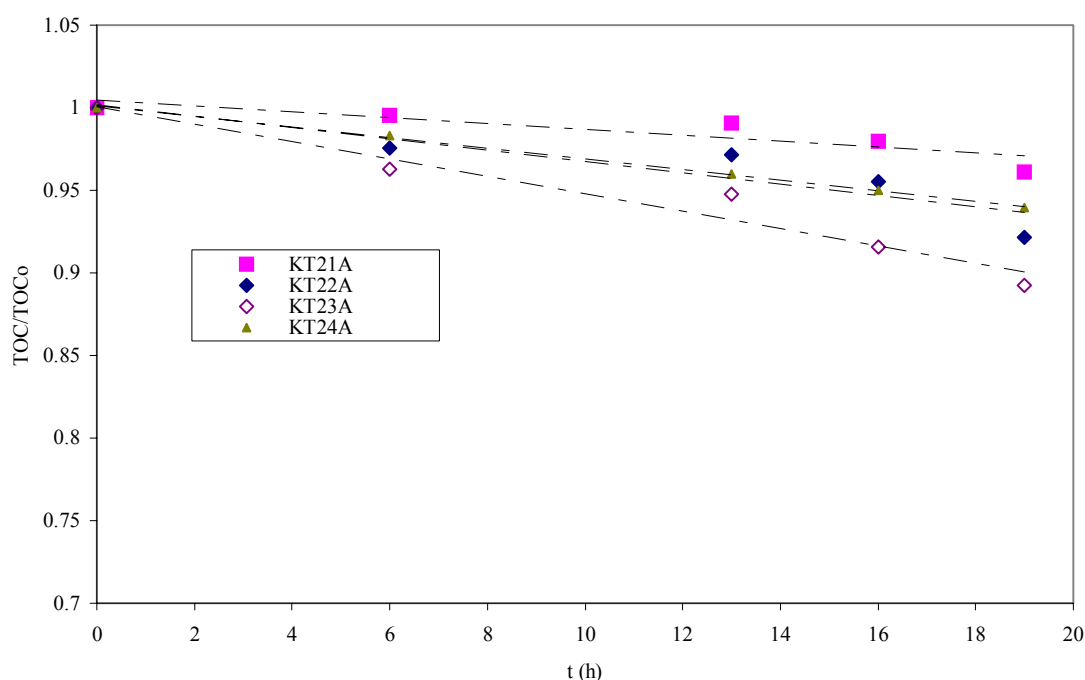


Fig. 39. Plot of TOC-removal for DCA- degradation study versus experimental time (h) under artificial illumination conditions: 1mM DCA dissolved in 200 mL distilled water, KNO₃ (10 mM) and 0.5 g/L catalyst (with a molar ratio of 1:6) illuminated for 19 hours, UV(A) light intensity value of 0.3 W/m² and distance of 60 cm (reactor-lamp).

The increase of the sulfur content does not especially improve the photocatalytic properties of the self made catalysts, however under these experimental conditions: calcination ramp (10 °C/h), calcination temperatures (550°C, 575°C, 600°C and 625°C); it is possible to determine some photocatalytical activity. However, experiments which had been carried out before by faster calcination ramp did not show any significant photoactivity, see Fig. 33).

Table 23. The DCA-rates, DCA- relative rates and photonic efficiencies for the commercial catalysts and for the sulfur doped TiO₂ catalysts which were calcined for three hours at different temperatures 550°C, 575°C, 600°C and 625°C, calcination profiles (10°C/h and 100°C/h) and sulfur molar ratios (1:4 and 1:6 in relation to titanium (IV) isopropoxide and thiourea). The relative rates have been calculated in relation to the DCA- degradation rate of Hombikat UV 100.

<i>Photocatalyst</i>	<i>DCA-rate *1E-09</i>		
	<i>(M*s-1)</i>	<i>Relative rate</i>	<i>P.E. (%)</i>
<i>KT13</i>	0.65 (R ² = 0.90)	0.14	3.36
<i>KT14</i>	0.29 (R ² = 0.86)	0.06	1.52
<i>KT15</i>	1.07 (R ² = 0.95)	0.24	5.51
<i>KT16</i>	1.15 (R ² = 0.95)	0.26	5.97
<i>KT21</i>	0.81 (R ² = 0.90)	0.18	4.18
<i>KT22</i>	2.41 (R ² = 0.86)	0.54	12.45
<i>KT23</i>	1.74 (R ² = 0.99)	0.39	8.96
<i>KT24</i>	2.13 (R ² = 0.95)	0.47	10.98
<i>KT21A</i>	0.21 (R ² = 0.99)	0.05	1.06
<i>KT22A</i>	0.61 (R ² = 0.82)	0.14	3.12
<i>KT23A</i>	1.12 (R ² = 0.92)	0.25	5.79
<i>KT24A</i>	0.86 (R ² = 0.99)	0.19	4.46
<i>Hombikat UV 100</i>	4.49 (R ² = 0.90)	1.00	23.19
<i>Kronos</i>	2.58 (R ² = 0.98)	0.57	13.32
<i>Degussa P25</i>	1.06 (R ² = 0.99)	0.24	5.48
<i>Toho</i>	1.62 (R ² = 0.98)	0.36	8.34

The photonic efficiency values for the commercial catalysts Hombikat UV 100 (23.19 %) and Kronos (13.32 %) are lower than for indoor illumination conditions with the corresponding values of 25.97 % and 24.50 % (data from Table 22). There is not a big difference in values in relation to Hombikat UV 100 but there is a considerable difference for Kronos. These differences could be explained due to the light intensity and the reaction time (about 42 hours under indoor illumination conditions for 3 days without the polycarbonate box in comparison to 19 hours for artificial light conditions). The photonic efficiencies have been calculated in relation to the rate of UV (A) light and are shown in Fig. 40.

Fig. 40 shows the dependence of photonic efficiency on a) molar ratio (1:4 (KT21- KT24) and 1:6 (KT21A- KT24A) titanium (IV) isopropoxide to thiourea) and b) heating profiles 10 °C/h (KT21- KT24) and 100 °C/h (KT13- KT16), respectively for the sulfur doped TiO₂ catalysts.

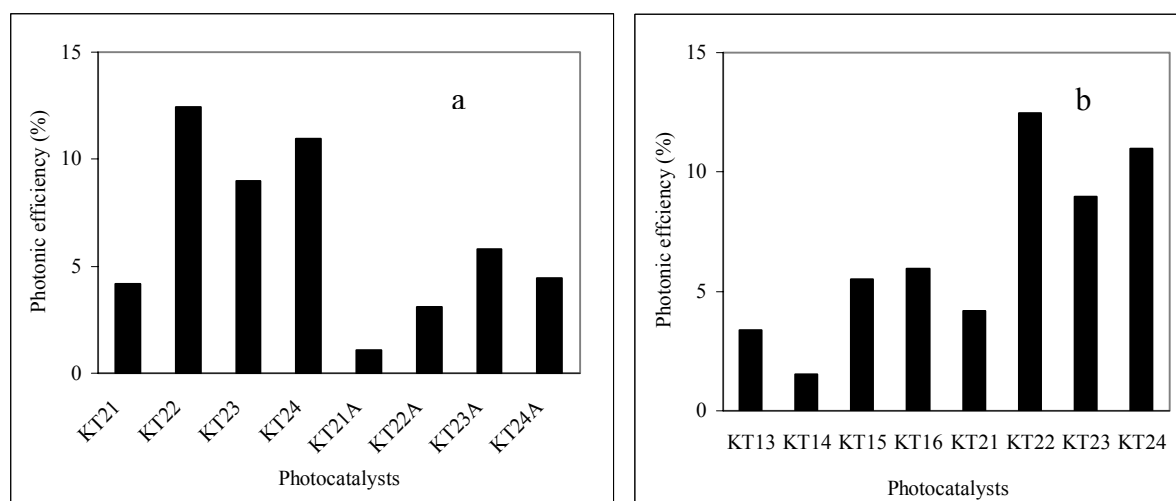


Fig. 40. Plot of photonic efficiency values as function of the different sulfur doped TiO₂ catalysts a) molar ratio 1:4 (Photocatalysts KT21- KT24) and 1:6 (Photocatalysts KT21A- KT24A) b) heating profile 10 °C/h (KT21- KT24) and 100 °C/h (KT13- KT16).

As was concluded under indoor illumination conditions, lower heating profiles enhance the physical properties of the photocatalysts (section 7.2.4.2.). This fact is also in good agreement with the data shown in Fig. 40 b). The photonic efficiency values of the catalysts prepared with a heating profile value of 100 °C/h are in the range of 5 %, meanwhile with a heating profile value of 10 °C/h the photonic efficiency values increase about two fold. This difference was not so pronounced under indoor illumination conditions, but the difference of light intensity and reaction time must be considered. The optimal molar ratio is again confirmed as 1:4 (titanium (IV) isopropoxide to thiourea) (as shown in Fig. 40). Molar ratios lower than 1:4, e.g. 1:2, have lower photonic efficiency values (see Table 20) than 1:4 and 1:6.

This study confirms the important role of the heating profile for the synthesis of new materials, e.g. (see Fig. 40) the sulfur modified TiO₂ photocatalyst (KT14) calcined at 575°C with a calcination profile of 100°C/h has a photonic efficiency value of 1.52 %. For the same catalyst with a lower calcination profile of 10 °C/h (KT22), the photonic efficiency increases about eight fold than for KT14 with a value of 12.45 %. However, for the same catalyst but with a different sulfur molar ratio of 1:6 (titanium (IV) isopropoxide to thiourea), KT22 A, the photonic efficiency decreases to 3.12 %.

7.3 Photocatalytic activity study of lanthanum-doped TiO₂

Two different lanthanum contents have been tested (0.4 % and 0.9 %). Fig. 41 shows the decrease of TOC values from DCA-degradation under indoor solar illumination conditions (see section 6.4.1.4.) for the catalysts: lanthanum doped TiO₂ with a lanthanum content of 0.4 %, calcined for three hours at different temperatures (400 °C (KL1), 500 °C (KL2), 600 °C (KL3), 700°C (KL4)), in comparison to Hombikat UV 100 and the blank sample without any lanthanum.

Table 24. List of the lanthanum doped TiO₂ catalysts which have been tested.

<i>Name</i>	<i>La-Conc. (%)</i>	<i>Calc. T (°C)</i>
KL1	0.4 %	400 °C (3h)
KL2	0.4 %	500 °C (3h)
KL3	0.4 %	600 °C (3h)
KL4	0.4 %	700 °C (3h)
KL5	0.9 %	400 °C (3h)
KL6	0.9 %	500 °C (3h)
KL7	0.9 %	600 °C (3h)
KL8	0.9 %	700 °C (3h)

Fig. 41 shows the change in TOC values for DCA degradation during indoor illumination conditions of the lanthanum doped catalysts, commercial catalysts Hombikat UV 100 and undoped TiO₂ (Blank), with a UV (A)-light intensity of 0.4 W/m².

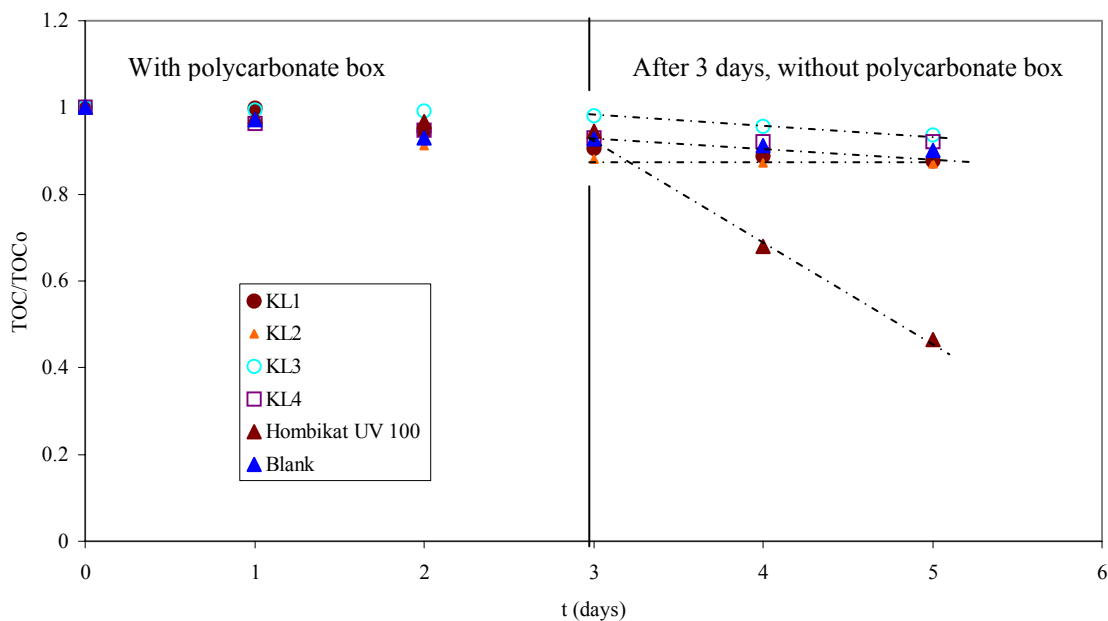


Fig. 41. Plot of TOC-removal for DCA- degradation study under indoor illumination conditions versus experimental time (days): 1mM DCA dissolved in 200 mL distilled water, KNO_3 (10 mM) and 0.5 g/L lanthanum-doped TiO_2 photocatalyst (calcined at 400 °C (KL1), 500°C (KL2), 600°C (KL3) and 700°C (KL4), with 0.4 % Lanthanum content) illuminated for 5 days with a UV (A)-light intensity of 0.4 W/m^2 .

Less than 10 % mineralization of DCA could be determined by TOC removal measurements. The new photocatalysts did not show any significant activity under indoor illumination conditions. Lanthanum addition did not significantly improve, under these preparation conditions, the photocatalytic properties of the photocatalysts. Within the scope of measuring accuracy no DCA- degradation was observed during the first three days with the polycarbonate box for any material.

Fig. 42 shows the decrease of TOC values from DCA-degradation for the photocatalysts: lanthanum doped TiO_2 with a lanthanum content of 0.9 %, calcined for three hours at different temperatures (400 °C (KL5), 500 °C (KL6), 600 °C (KL7), 700°C (KL8), in comparison to Hombikat UV 100 and Kronos.

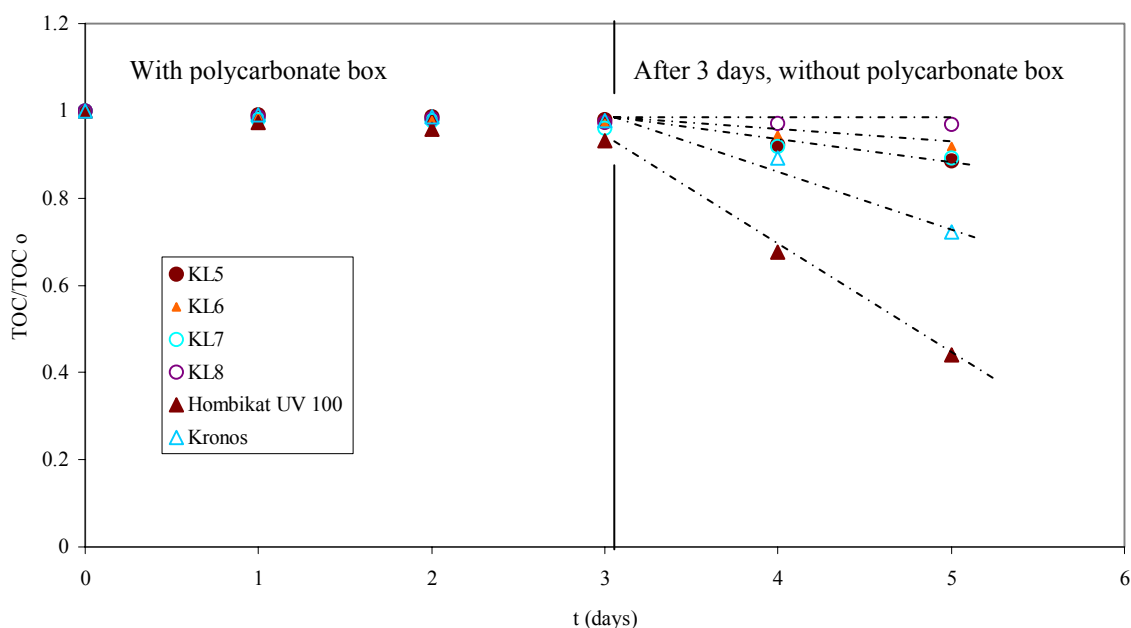


Fig. 42. Plot of TOC- decrement for DCA- degradation study under indoor illumination conditions versus experimental time (days): 1mM DCA dissolved in 200 mL distilled water, KNO_3 (10 mM) and 0.5 g/L lanthanum doped TiO_2 catalyst (calcined at 400°C (KL5), 500 °C (KL6), 600 °C (KL7) and 700 °C (KL8), with 0.9 % lanthanum content) illuminated during 5 days with a UV (A)-light intensity of 0.4 W/m^2 .

Table 25. DCA-rates, relative rates and photonic efficiencies for the lanthanum doped TiO_2 photocatalysts in dependence of the lanthanum concentration. The relative rates were calculated in relation to the Hombikat UV 100 rate corresponding to each run.

<i>Photocatalyst</i>	<i>DCA-rate * 1E-09</i>		
	<i>(M*s⁻¹)</i>	<i>Relative rate</i>	<i>P.E. (%)</i>
<i>KL1</i>	1.22 ($R^2 = 0.99$)	0.23	4.72
<i>KL2</i>	1.29 ($R^2 = 0.99$)	0.24	5.01
<i>KL3</i>	1.29 ($R^2 = 0.99$)	0.24	5.01
<i>KL4</i>	0.79 ($R^2 = 0.99$)	0.15	3.07
<i>Hombikat UV 100</i>	5.31 ($R^2 = 0.99$)	1.00	20.54
<i>TiB2</i>	0.99 ($R^2 = 0.99$)	0.19	3.84
<i>KL5</i>	1.14 ($R^2 = 0.99$)	0.21	4.4
<i>KL6</i>	0.81 ($R^2 = 0.99$)	0.15	3.12
<i>KL7</i>	1.08 ($R^2 = 0.99$)	0.19	4.19
<i>KL8</i>	0.32 ($R^2 = 0.99$)	0.06	1.23
<i>Hombikat UV 100</i>	5.54 ($R^2 = 0.99$)	1.00	21.45
<i>Kronos</i>	2.75 ($R^2 = 0.99$)	0.50	10.64

Under these experimental conditions the DCA-degradation rates were not very high, only 10 % TOC removal was observed. The photocatalysts were not very active but also Kronos did not show high efficiency, this might be attributed to the decrease of effective visible light absorption. For a Lanthanum concentration of 0.4 % (KL1- KL3) is observed in the range of temperatures from 400 °C to 600 °C (an improvement of the photonic efficiency values of the materials in comparison to the undoped catalyst TiB2). For higher concentrations of lanthanum 0.9 %, the difference was not so significant. In the case of both lanthanum concentrations, especially for 0.9 %, the photonic efficiencies for the catalysts calcined at 700 °C (KL4 and KL8) decreased dramatically. This is probably due to the transformation into rutile at this temperature. The photonic efficiency values of lanthanum TiO₂ catalysts are in the same range as the results obtained for sulfur doped TiO₂ catalysts at 400 °C/h. (see Table 21). These results agree with the work of Liqiang et al.⁶⁴ They studied lanthanum doped TiO₂ photocatalysts for phenol photodegradation under UV (A) light ($\lambda \geq 365$ nm), obtaining a decrease of 23 % phenol from the initial concentration (surface complexation, see section 5.1.3.2.). They also found no shift into the visible region by DRS measurements and suggested that La³⁺ was uniformly dispersed onto TiO₂ surface in the form of small clusters of La₂O₃.

7.4 Photocatalytic disinfection of E. coli and microbiological analysis concerning the amount of microorganisms (C.F.U.)

7.4.1 Study of different UV-irradiation sources

The experiments have been carried out (see section 6.4.3.) using a membrane pump to recirculate at a rate of 18 L/h, with suspensions containing *E. coli* and TiO₂ (5 g/L) in 5 L of a physiological salt solution (0.9 g/L NaCl, pH= 7.3). The experimental set-up (see Fig. 18). consists of an annular immersion lamp reactor (1200 mL) and a reservoir (5 L), both are vigorously stirred. UV- irradiation was performed by employing either a Heraeus mercury high-pressure lamp TQ718, which emits illumination in the UV (B) region ($280 \text{ nm} \leq \lambda \leq 315 \text{ nm}$) and in the UV (C) region ($100 \text{ nm} \leq \lambda \leq 280 \text{ nm}$), or a Heraeus mercury high-pressure lamp TQ 718Z4, which emits predominantly in the UV (A) region ($315 \text{ nm} \leq \lambda \leq 380 \text{ nm}$), in both cases the lamps were sheathed by a Jena quartz glass tube.

A series of experiments have been performed to study the bacterial survival in the system under different conditions, as shown in Fig. 43.

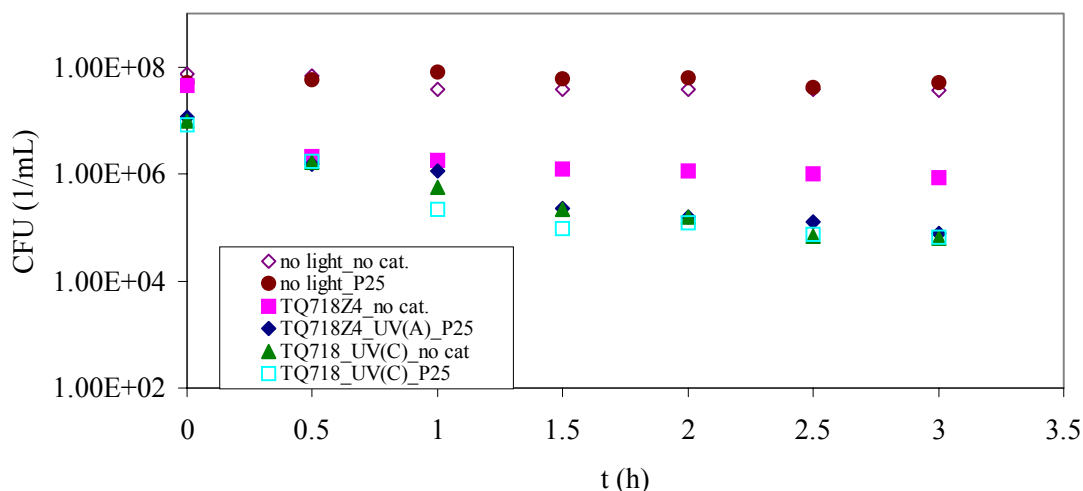


Fig. 43. Disinfection achieved by phototreatment of a model bacteria suspension (*Escherichia coli*) with an ampicillin concentration of 75 mg/L dissolved in 5 L of a physiological salt solution for a total period of 3 hours.

It can be seen that no disinfection occurs in the absence of light. As shown in Fig. 43 no significant difference can be determined between presence and absence of TiO_2 , employing the two lamps. The lamp TQ 718 was a little bit more effective after 3 hours than the lamp TQ 718 Z4. This fact is readily explained by differences in the intensity and, in particular, in the wavelength distribution of the light. The time required for the two-log inactivation of *E. coli* was about 90 min. either with or without catalyst. This value is shorter than that obtained by Watts et al.⁷³, who find a two-log disinfection time of 150 min. Meanwhile Herrera et al.⁷⁴ got two-log inactivation of total coliforms in 60 min. Wei et al.⁵³ achieved higher inactivation rates with almost complete bacterial deactivation in 30 min. Inactivation rate constants were calculated based on first order kinetics (see Table 26) in which $-\ln(C.F.U.t/C.F.U.o)$ was plotted as a function of time (where $C.F.U.t$ is the number of CFU/mL at a time t and $C.F.U.o$ is the number of CFU/mL at time zero). The slope of the line was k , the first order inactivation rate constant⁷³ (see Fig. 44).

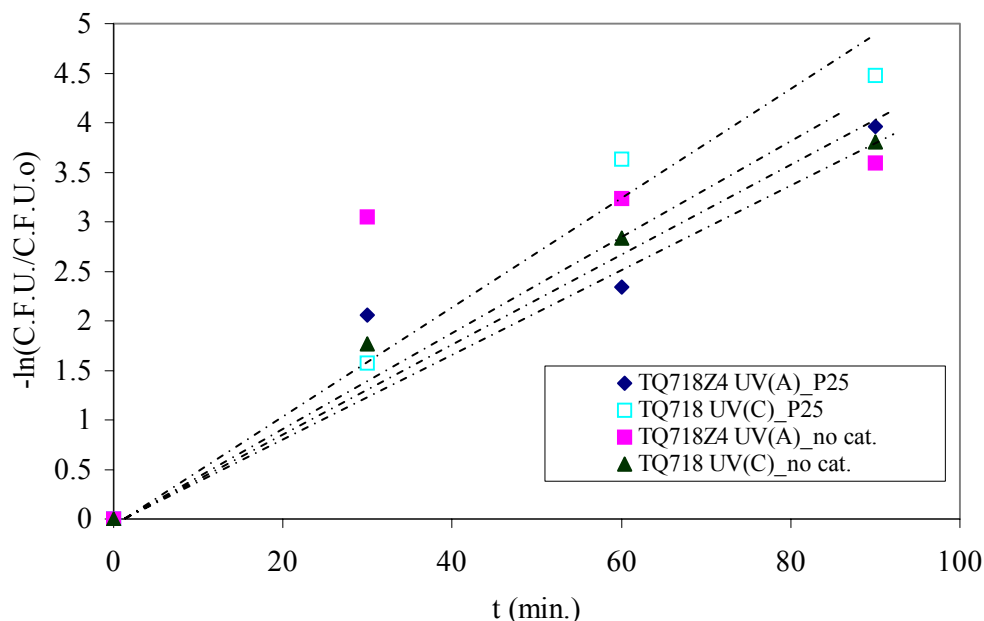


Fig. 44. Plot of first order kinetics of *E. Coli* disinfection using ampicillin concentration of 75 mg/L dissolved in 5 L of a physiological salt solution for a total period of 3 hours.

Table 26. Comparison of initial rate constants for *E. Coli* inactivation with R^2 values greater than 0.90, (except for the measurement without TiO_2 catalyst) and using the lamp TQ718Z4 UV (A), obtained from exponential regression.

Lamp	TiO_2 (5 g/L)	TiO_2 (0 g/L)	$K_{rateo}(min^{-1})$
TQ718 UV(C)	0.04 ($R^2=0.97$)	0.04 ($R^2=0.97$)	
TQ718Z4 UV(A)	0.05 ($R^2=0.92$)	0.04 ($R^2=0.61$)	

The experiments which were carried out in the dark, but in presence of catalyst, do not show any disinfection rate. That means that TiO_2 itself can not produce a detrimental effect on *E. coli*. The experiments in the presence of light, and either catalyst or absence of catalyst, present very similar initial rate constants. This indicates that no remarkable photocatalytic effect was found as yet. It was thus necessary to optimize the experimental conditions. The low disinfection rate of the lamp TQ 718 (UV (C)) in the absence of catalyst is unusual, but could be explained by the interruption of illumination caused by the reservoir- the bacteria have time to recover.

This study were reported by Rincón et al.⁵⁵ and they suggested that the synthesis of catalase enzyme constitutes one of the major defense mechanism of *E. coli* against oxidation stress. This enzyme reduces the intracellular concentration of hydrogen peroxide by causing its decomposition to water and oxygen. However, The $\cdot\text{OH}$ concentration in solution increases with illumination time due to its production by photooxidation of adsorbed water on the surface of TiO_2 . Probably the ratio between irradiation and dark times, as well as the extent of each period itself, determines not only the $\cdot\text{OH}$ production but also the efficiency of the bacterial recovery.

7.4.2 Study of flow rate dependency

In order to improve the recirculation of our system, the flow rate of the pump was increased to 70 L/h. As shown Fig. 45, the obtained results do not show any improvement in the disinfection of *E. Coli*. This effect was tested only for the lamp TQ 718, which emits in the UV (C) region. The notation Vs and Vb correspond to the flow rates values of 18 L/h and 70 L/h, respectively.

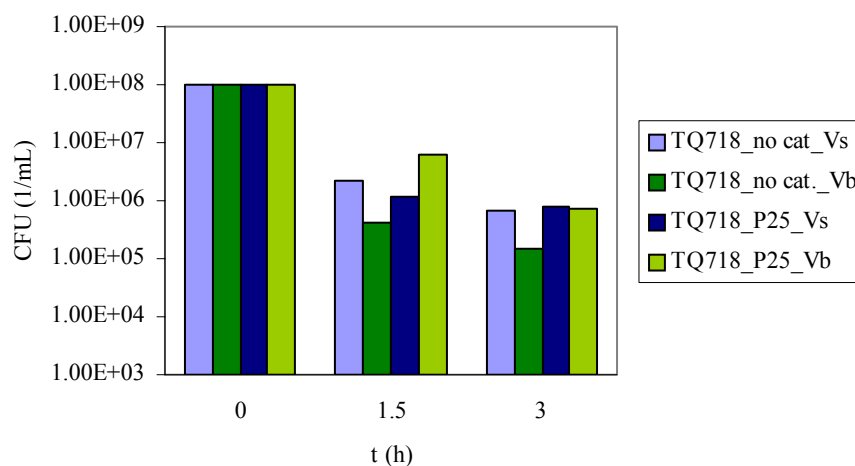


Fig. 45. Plot of the change of CFU versus time, experimental conditions: aliquot of *E. Coli* with a concentration of ampicillin 75 mg/L dissolved in 5 L of a physiological salt solution, illumination performed with the lamp TQ718 for a total period of 3 hours.

The inactivation of *E. Coli* increases more noticeable in the case of the blank with a faster flow rate. This fact might be explained due to an additional stress on the cells, not only due to the effect of the light but also the more rapid recirculation (the bacteria does not have enough time to recover). However, the same experiment, but in presence of catalyst, dramatically inhibits the disinfection of *E. Coli*, specially after 90 min. It could be caused by TiO_2 particles, which shade the cells, so that light in the TiO_2 - cell slurry became limiting.

The total disinfection rate constants were calculated and plotted in Fig. 46 and Table 27.

The notation V_s and V_b correspond to the flow rates values of 18 L/h and 70 L/h, respectively.

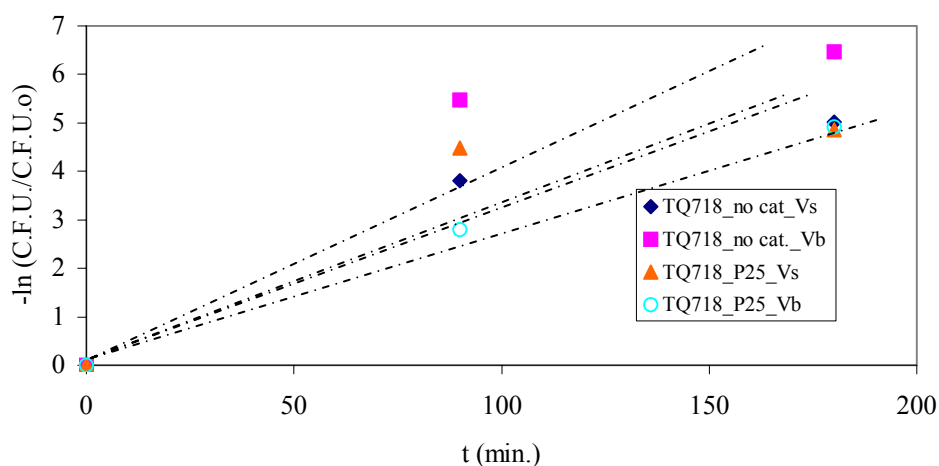


Fig. 46. Plot of first order kinetics of *E. coli* disinfection using ampicillin concentration of 75 mg/L dissolved in 5 L of a physiological salt solution for a total period of 3 hours.

Table 27. Total rate constants for *E. Coli* inactivation with R^2 values obtained from exponential regression.

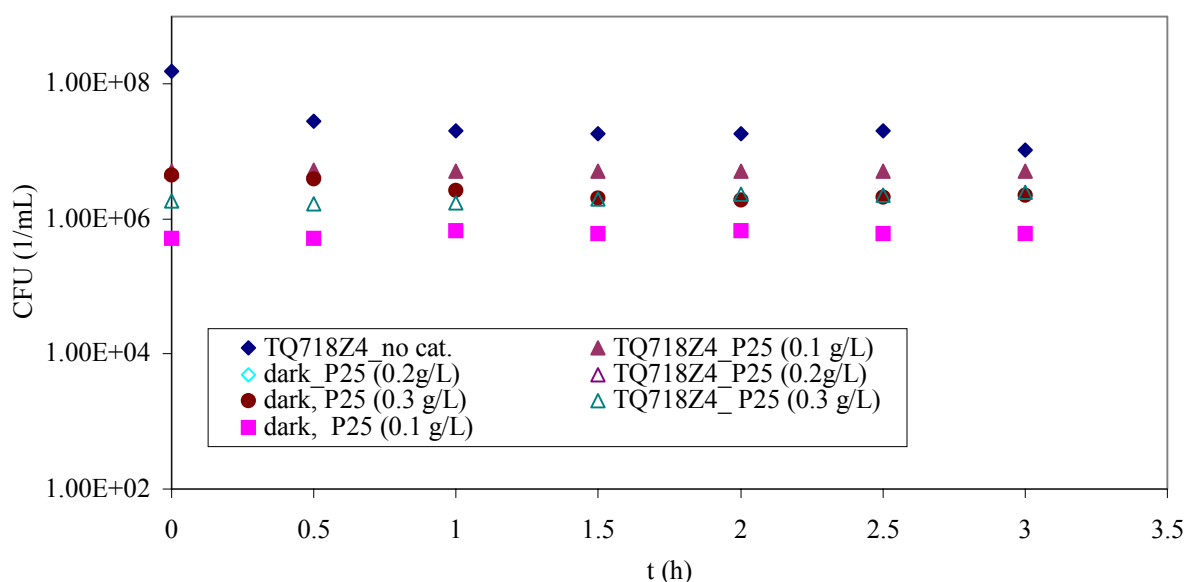
<i>TQ718 UV(C)</i>			
	TiO_2 (5 g/L)	TiO_2 (0 g/L)	
$V_s = 18 \text{ L/h}$	0.027 ($R^2=0.77$)	0.028 ($R^2=0.90$)	$K_{rate} (\text{min}^{-1})$
$V_b = 70 \text{ L/h}$	0.027 ($R^2=0.99$)	0.036 ($R^2=0.83$)	$K_{rate} (\text{min}^{-1})$

Comparing both blank experiments, it can be seen that UV radiation produced by the lamp TQ718 has a bactericidal effect on *E. coli*, and the additional stress of higher flow rate leads to an acceleration of the rate of *E. coli* inactivation. A shielding effect of the TiO₂ photocatalyst could be the reason for the low disinfection rate obtained in the experiment in the presence of light and catalyst (higher flow rate) preventing the direct interaction between the UV (C)-light and the microorganisms.

7.4.3 Study of different catalyst loadings

The next experiments were carried out using the lamp TQ 718 Z4, which emits mainly in the UV (A) region and also has some emission in the UV (C) region. Our plan was to only work in the UV (A) region, so a new reactor was equipped with a Duran glass filter in order to avoid the effects of UV (C) light in the system. The experiments have been carried out using a membrane pump to recirculate at a rate of 18 L/h, with suspensions containing *E. coli* and different concentrations of a TiO₂ standard catalyst (Degussa P25; 0.1, 0.2, 0.3, 0.5, 1 and 2 g/L, respectively) in 5 L of a physiological salt solution (0.9 g/L NaCl, pH = 7.3).

A series of experiments have been performed to study the bacterial survival in the system under mainly UV (A) light. To determine the optimal dose of catalyst for certain cell concentrations, photocatalytic reactions were performed with TiO₂ concentrations ranging from 0.1 to 2 g/L, as shown in Fig. 47.



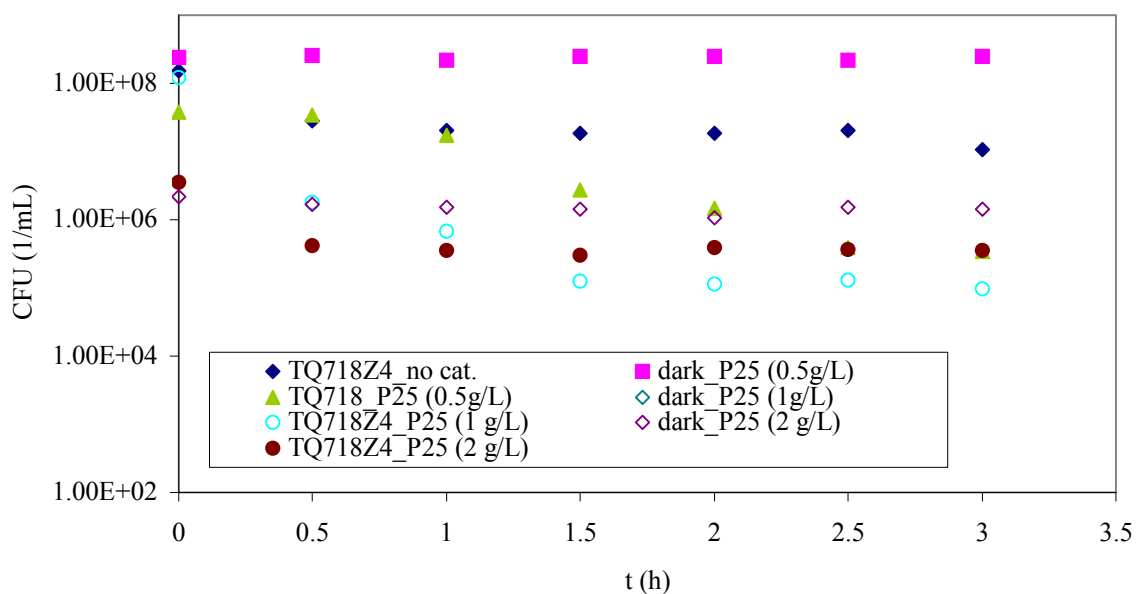


Fig. 47. Disinfection achieved by photocatalytic treatment of a model bacteria suspension (*Escherichia Coli*). Experimental conditions: aliquot of *E. coli* with a concentration of ampicillin 75 mg/L and a concentration of catalyst Degussa P25 ranging from 0.1 to 2 g/L, dissolved in 5 L of a physiological salt solution, illumination performed with the lamp TQ718Z4 for 3 hours.

As shown in Fig. 47, in the presence of UV (A) light a noteworthy reduction of the bacterial count can be observed. Another parameter which plays a very important role is the catalyst concentration, a decrease of approximately three orders of magnitude of the CFU was found when a concentration of 1 g/L of Degussa P25 was chosen. No degradation was observed with catalyst concentrations ranging from 0.1 to 0.3 g/L. With 0.5 g/L concentration of catalyst, the decline of the bacterial count was still appreciable.

It is interesting to note that the photocatalytic antibacterial effect of UV (A) light without photocatalyst is more pronounced than that observed in the presence of photocatalyst concentrations between 0.1 to 0.3 g/L. This can be explained by a shielding effect of the TiO_2 at this low loading inhibiting the direct interaction between the UV (A) light and the *E. coli*.

Fig. 48 summarizes the dependency of C.F.U. rate on catalyst (Degussa P25) concentration in the range from 0 to 2 g/L measuring with the lamp TQ718Z4.

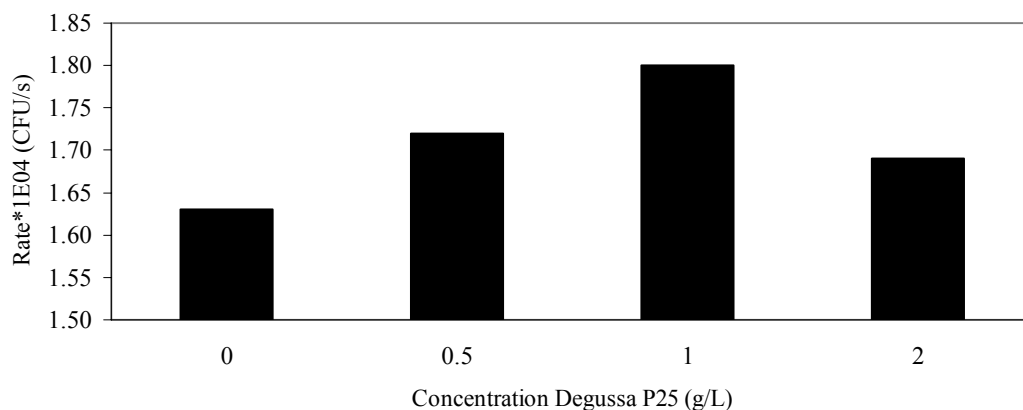


Fig. 48. Plot of C.F.U. rates versus Catalyst Degussa P25 concentration (g/L). Experimental conditions: aliquot of *E. coli* with a concentration of ampicillin 75 mg/L and a concentration of catalyst Degussa P25 ranging from 0.1 to 2 g/L, dissolved in 5 L of a physiological salt solution, illumination performed with the lamp TQ718Z4 for 3 hours.

The highest activity was found employing a catalyst concentration of 1 g/L resulting in a reduction of the *E. Coli* content (CFU) by 3 orders of magnitude within the first 90 minutes of illumination as compared with a reduction of less than one order of magnitude in the absence of any photocatalyst. As can be seen in Fig. 48 degradation rates depend on the concentration of the catalyst, following the order $R(1\text{g/L}) > R(0.5\text{ g/L}) > R(2\text{ g/L})$, thus it is in good agreement with the work performed by Maness et al.⁵⁹

8 Conclusions and Outlook

In the first part of the work, the synthesis of several sulfur doped photocatalysts by a sol-gel process is described and their photoactivity properties examined by DCA- degradation under different illumination conditions are reported. The results obtained are summarized as follows:

- A shift into the visible light region could be observed due to the new shoulder absorption edge of the synthesized sulfur doped TiO₂ (from 400 to 470 nm).
- Calcination rates play a very important role in the enhancement of the photocatalytic properties of the new materials, especially in the range of 10 °C/h – 100 °C/h. This is the first in detail study of the dependence on heating profiles for synthesis of new photocatalyst, no data having reported in the literature before.
- The crystalline size of anatase was estimated from XRD- data, according to the Scherrer formula, to be in the range of 14 – 28 nm and 19.5-28.5 nm for the sulfur doped TiO₂ photocatalysts calcined at 550 °C, 575 °C, 600 °C and 625 °C, with 10 °C/h and 100 °C/h heating profiles. There were no major differences between these values, showing a complex compromise of different physical parameters for the photocatalytic properties between small crystalline size, large surface area and small particle size, concentration of the dopant, etc.
- The most active photocatalyst was prepared with a molar ratio of 1:4 (titanium (IV) isopropoxide to thiourea), calcined at 600 °C for 3 hours and with a 10 °C/h calcination rate.
- For very low UV (A)- light intensity and in the presence of longer wavelengths ($\lambda = 440$ nm, artificial light illumination conditions) the self made sulfur doped TiO₂ photocatalysts calcined at 575 °C (KT22), 600 °C (KT23) and 625 °C (KT24) with 10 °C/h heating profile showed higher photocatalytic properties than Toho (commercial sulfur doped TiO₂ photocatalyst) and similar photoactivity to Kronos (commercial photocatalyst). Hombikat UV 100 was always the most active photocatalyst in all UV (A) light conditions (see Fig. 49).

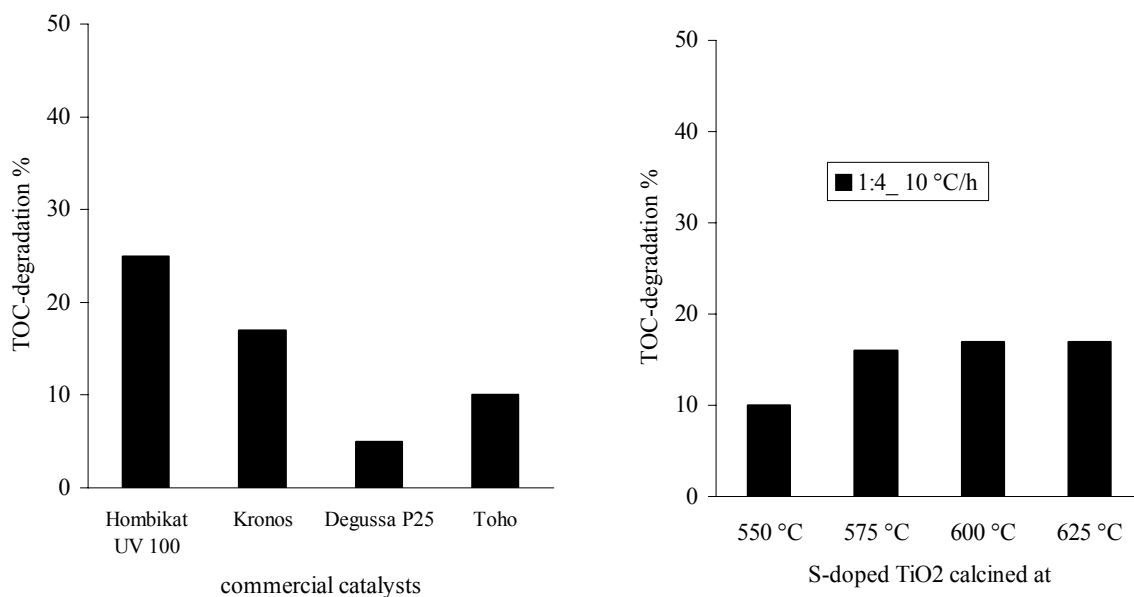


Fig. 49. Study of TOC-degradation (%) determined by TOC (%) - measurements for commercial catalysts Sachtleben Hombikat UV 100, Kronos, Degussa P25 and Toho and for the sulfur doped TiO₂ catalysts calcined at 550 °C, 575 °C, 600 °C and 625 °C with 10 °C/h calcination ramp under artificial light illumination conditions.

In the course of this PhD-work different experimental illumination conditions (cut off filter 320 nm and 420 nm, sun-light, indoor without cover, indoor with cover and artificial light) have been tested in order to study the activity of the commercial and the sulfur doped TiO₂ photocatalysts, making possible a comparison between them as shown in Fig. 50.

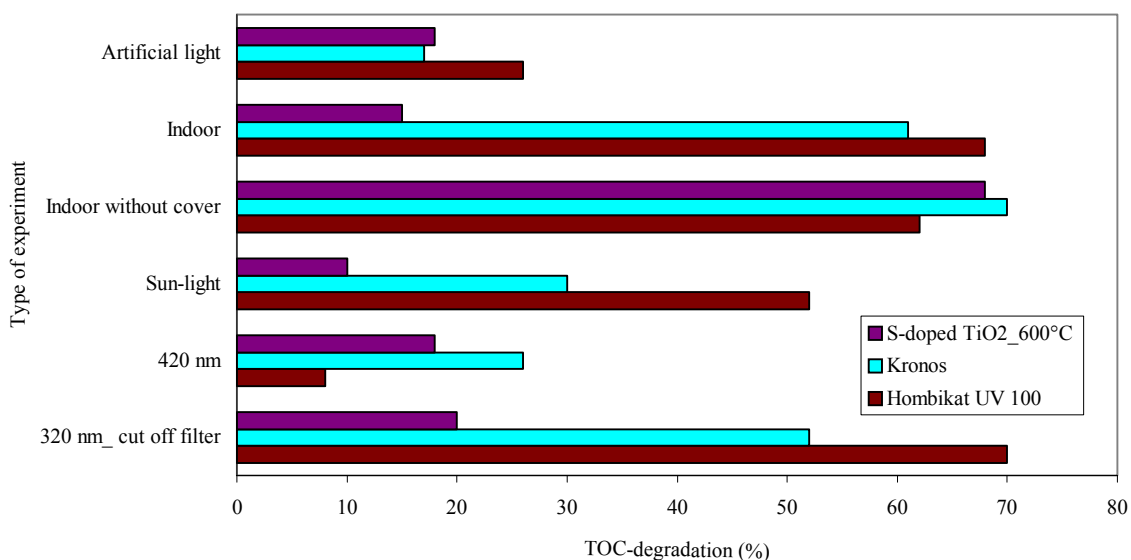


Fig. 50. Study of TOC-degradation (%) in comparison to different experimental illumination conditions and different photocatalysts such as Kronos, Hombikat UV 100 and the sulfur doped TiO₂ calcined at 600 °C.

The commercial photocatalyst Sachtleben Hombikat UV 100 shows higher activity for the degradation of DCA under any kind of UV-light as mentioned before e.g. Xe-lamp with a cut off filter of 320 nm, indoor with and without cover, and sun light. However, for sun light the DCA-degradation is lower than expected. This might be explained by the dependence on the illumination time as well as no stirring having been carried out during this kind of experiment, reducing the photocatalysts efficiency.

Kronos is the more powerful photocatalyst for longer wavelengths, e.g. indoor with and without cover, and is the same as our self made sulfur doped TiO₂ photocatalyst. Meanwhile, the sulfur doped TiO₂ photocatalyst is not very active under UV-light illumination conditions. The photocatalytic activity of the sulfur doped TiO₂ photocatalyst improves with longer illumination times under sun-light illumination conditions as seen by comparison between e.g. sun light (5 h illumination time, 10 % DCA- degradation), indoor without cover (5 days, 68 % DCA-degradation), indoor with cover (total 5 days but only 2 days without cover, 15 % DCA-degradation) and artificial visible light illumination (5 days, 18 % DCA-degradation).

Recent literature reports indicate that sulfur could either add to the TiO₂ matrix as a cation or an anion depending upon the sulfur source employed. Umebayashi et al.³⁵ prepared sulfur-doped TiO₂ by oxidation annealing of titanium disulfide (TiS₂) and reported that sulfur is doped as an anion in titania. Ohno et al.²⁷ found that S⁴⁺ replaces some of the lattice Ti⁴⁺, leading to visible light activity. Previous studies reported that if thiourea was used, the substitution of Ti⁴⁺ by S⁶⁺ would be more favourable than replacing O²⁻ with S²⁻. Periyat et al.³⁰ synthesized sulfur-doped TiO₂ photocatalysts but with sulfuric acid as the sulfur source, concluding also that the substitution of Ti⁴⁺ by S⁶⁺ would be chemically more favourable: the bond strength of the Ti-S bond (418 kJ/mol) is less than the already existing Ti-O bond (672 kJ/mol), meanwhile anionic sulfur doping is difficult because the ionic radius of the S²⁻ (1.7 Å) ion is larger than that of O²⁻ (1.22 Å)⁷⁵. Nevertheless, it is more than probable that the band gap narrowing is due to the anionic S doping originating from mixing the S 3p states with the valence band, leading to an increase in the valence band width.

In the case of lanthanum doped TiO₂ samples, no shift into the visible light region was observed. The optimal concentration of lanthanum was also 0.4 %.

The photoactivity of the new photocatalysts was very low for DCA degradation under indoor illumination conditions, confirming the studies by Liquiang et al.⁶⁴ They reported that La³⁺ was present in the TiO₂ crystal lattice, due to the difference in the ionic radius: the radius of La³⁺ is 1.15 Å while that of Ti⁴⁺ is 0.64 Å. They suggested that La³⁺ was uniformly dispersed onto the TiO₂ surface in the form of small clusters of La₂O₃. This synthetic method modifies TiO₂ at the surface, leading to some advantages:

- Increase in the concentration of surface oxygen, vacancies and defects.
- Inhibition on TiO₂ phase transformation.

A very important contribution of this work has been the choice of our aliphatic pollutant dichloroacetic acid (DCA), eviting the absorption of light under visible light region e.g. dyes and catalyst surface complexes e.g. phenolic compounds. Prof. Ohno^{76, 77} showed that methylene blue, as well as, presumably, other kinds of organic dyes, are inadequate as a model compound for testing visible light induced photocatalytic activity. One of the principal problems is that the dye molecules can absorb photons, especially in the visible light range, and thus photoexcited electrons could be injected into the photocatalyst particles. The self-dye degradation takes place due to the presence of molecular oxygen and can not be applied to photocatalytic detoxification.

In the second part of this work, a new method was designed and developed to study *E. coli* disinfection using UV light. *E. coli* has been used as biological indicator of disinfection efficiency in drinking water disinfection systems. The optimum conditions for *E. coli* inactivation such as flow rate, type of light (UV A (315 nm- 400 nm), B (280 nm- 315 nm) and C (100 nm- 280 nm)) and different TiO₂ concentrations were examined. The results are as follow:

- Bacterial inactivation by UV-light occurs in both the absence or presence of a catalyst. UV (C)-light is a well -established powerful germicide. However the system UV (A) /TiO₂ has shown a photocatalytic enhancement of the *E. coli* inactivation by the optimized experimental conditions.
- An increase of flow rate slowed the disinfection of microorganisms. Due to the rapid recirculation, the activation of TiO₂ particles by light is limiting.
- Catalyst loading plays a very important role. Different experiments were carried out with concentrations in the range from 0.1 g/L to 2 g/L, showing 1 g/L catalyst as the optimal concentration. At lower loadings much of the light was transmitted through the slurry solution in the reactor, while at higher loadings all the incident photons were absorbed by the slurry.
- The disinfection reaction follows first order kinetics, with some exceptions due to temperature fluctuations of the system (from 25 °C to 42 °C).

The work described in this thesis contributes to deeper knowledge in the search for new materials which might be active under visible light illumination conditions. The important influence of heating profiles and calcination temperatures on the catalysts properties has been studied in detail. Recent literature^{8, 39} shows a new synthesis trend with co- doped compounds using the properties of non-metals, such as sulfur and nitrogen, giving a narrower band gap due to the mix of p states of N or S with O2p from oxygen and the rare earth elements such as lanthanum contributing with their special electronic structure (f states), improving the conversion efficiency of TiO₂.

It will be a very interesting challenge to continue work into the field of photocatalytic disinfection, getting an application into longer wavelengths. In this respect, there are possible future of sulfur doped TiO_2 photocatalysts.⁷⁵ Nevertheless, it will first be necessary to do studies of catalyst toxicity to determine limiting parameters such as catalyst loading, allowed content of sulfur, etc.

Finally, it will be interesting to apply all this new knowledge about sewage treatment to real industrial wastewater detoxification.

9 Literature

1. Blanco, J.; Malato, S.; Estrada, C.; Bandala, E.; Gelover, S.; Leal, T., *Purificación de aguas por fotocatalisis heterogénea: estado del arte* In. ed.; Red Cyted VIII-G: Argentina, 2001; Cap. 3, p 51.
2. Liu, G.; Wu, T.; Zhao, J.; Hidaka, H.; Serpone, N., *Photoassisted degradation of dye pollutants. Irreversible degradation of alizarin red under visible light radiation in air-equilibrated aqueous TiO₂ dispersions*. Environm. Sci. Technol. 2007, 33, 2081-2087.
3. Kaneko, M., *Photocatalysis: Science and technology*; Springer: Tokyo, 2002; p 365.
4. Fujishima, A.; Hashimoto, K.; Watanabe, T., *TiO₂ Photocatalysis, fundamentals and applications*; BKc, Tokyo, 1999; p 176.
5. Fujishima, A.; Tata, N.; Rao, D., *Titanium dioxide photocatalysis*. J. of photochemistry and photobiology C: Photochemistry Reviews 2000, 1, 1-21.
6. Hoffmann, M. R.; Martin, S. T.; Choi, W.; Bahnemann, D., *Environmental applications of semiconductor photocatalysis*. J. Chem. Rev. 1995, 95, 69-96.
7. Gärtner, M. *Semiconductor-Support interaction in photocatalysis*. PhD- thesis at the Friedrich-Alexander-Universität, Erlangen-Nürnberg, 2005.
8. Wei, H.; Wu, Y.; Lun, N.; Zhao, F., *Preparation and photocatalysis of TiO₂ nanoparticles co-doped with nitrogen and lanthanum*. J. materials science 2004, 39, 1305-1308.
9. Wu, T.; Liu, G.; Zhao, J.; Hidaka, H.; Serpone, N., *Evidence for H₂O₂ generation during the TiO₂ assisted photodegradation of dyes in aqueous dispersions under visible light illumination*. J. Phys. Chem. B 1999, 103, 4862 - 4867.

10. Kisch, H.; Macyk, W., *Visible light photocatalysis by modified titania*. ChemPhysChem 2002, 3, 399-400.
11. Kim, S.; Choi, W., *Visible-light induced photocatalytic degradation of 4-chlorophenol and phenolic compounds in aqueous suspension of pure titania: demonstrating the existence of a surface-complex-mediated path*. J. Phys. Chem. B 2005, 109, 5143-5149.
12. Bhatkhande, D.; Pangarkar, V. G.; Beenackers, A., *Photocatalytic degradation for environmental applications- a review*. Chem. Technol. Biotechnol. 2001, 77, 102-116.
13. Herrmann, J. M., *Heterogeneous photocatalysis: fundamentals and applications to the removal of various types of aqueous pollutants*. Catalysis Today 1999, 53, 115-129.
14. Kamble, S. P.; Sawant, S. B.; Pangarkar, V. G., *Novel solar based photocatalytic reactor for degradation of refractory pollutants*. AIChE Journal 2004, 50, (7), 1647-1650.
15. Rockett, A., *The materials science of semiconductors*; Springer: New York, 2007; p 622.
16. Bahnemann, D.; Bockelmann, D.; Goslich, R., *Mechanistic studies of water detoxification in illuminated TiO₂ suspensions*. Solar Energy Materials 1991, 24, 564-583.
17. Choi, W.; Termin, A.; Hoffmann, M. R., *The role of metal ion dopants in quantum size TiO₂: Correlation between photoreactivity and charge carrier recombination dynamics*. J Phys. Chem. 1994, 98, 13669 - 13679.
18. Yu, J. C.; Yu, J. C.; Ho, W.; Jiang, Z.; Zhang, L., *Effects of F- doping on the photocatalytic activity and microstructures of nanocrystalline TiO₂ powders*. J. Chem. Mater. 2002, 14, 3808- 3816.
19. Choi, Y.; Umebayashi, T.; Yoshikawa, M., *Fabrication and characterization of C-doped anatase TiO₂ photocatalysts*. J. Mater. Sci. 2004, 39, 1837-1839.
20. Gómez; López; Ortiz-Islas; Navarrete; Sánchez; Tzompanztzi; Bokhimi, *Effect of sulfonation on the photoactivity of TiO₂ sol-gel derived catalysts*. J. Molecular Catalysis A: Chemical 2003, 193, 217-226.

21. Ho, W.; Yu, J. C.; Lee, S., *Low-temperature hydrothermal synthesis of S-doped TiO₂ with visible light photocatalytic activity*. J. Solid State Chemistry 2006, 179, 1171-1176.
22. Irie, H.; Watanabe, Y.; Hashimoto, K., *Carbon-doped anatase TiO₂ powders as a visible light sensitive photocatalyst*. J. Chem. Lett. 2003, 32, (8), 772.
23. Janczarek, M. *Modification of titanium dioxide towards photocatalytic activity in visible light*. PhD- thesis at the University Erlangen-Nürnberg, Erlangen-Nürnberg, 2005.
24. Kobakayawa, K.; Murakami, Y.; Sato, Y., *Visible light active N-doped TiO₂ prepared by heating of titanium hydroxide and urea*. J. Photochemistry and photobiology A: Chemistry 2005, 170, 177-179.
25. Liu, S.; Chen, X., *A visible light response TiO₂ photocatalyst realized by cationic S-doping and its application for phenol degradation*. J. Hazardous Materials 2008, 152, 48-55.
26. Moon, J.; Yun, C. Y.; Chung, K.; Kang, M.; Yi, J., *Photocatalytic activation of TiO₂ under visible light using Acid red 44*. J. Catal. Today 2003, 87, 77-86.
27. Ohno, T.; Akiyoshi, M.; Umebayashi, T.; Asai, K.; Mitsui, T.; Matsumura, M., *Preparation of S-doped TiO₂ photocatalysts and their photocatalytic activities under visible light*. Applied Catalysis A: General 2004, 265, 115-121.
28. Ohno, T., *Preparation of visible light active S-doped TiO₂ photocatalysts and their photocatalytic activities*. Water Science and Technology 2004, 49, (4), 159-163.
29. Ohno, T.; Mitsui, T.; Matsumura, *Photocatalytic Activity of S-doped TiO₂ Photocatalyst under Visible Light*. Chemistry Letters 2003, 32, (4), 364.
30. Periyat; Pillai; McCormack; Colreavy; Hinder, *Improved high temperature stability and sun-light driven photocatalytic activity of sulfur doped anatase*. J. Phys. Chem. C 2008, 112, 7644-7652.

31. Sakthivel, S.; Kisch, H., *Daylight photocatalysis by carbon modified titanium dioxide*. *Angew. Chem. Int. Ed.* 2003, 42, 4908-4911.
32. Tang, X.; Li, D., *Sulfur-doped highly ordered TiO₂ nanotubular arrays with visible light response*. *J. Phys. Chem. C* 2008, 112, 5405-5409.
33. Umebayashi, T.; Yamaki, T.; Tanaka, S.; Asai, K., *Visible light induced degradation of methylene blue on S-doped TiO₂*. *J. Chem. Lett.* 2003, 32, (4), 330-331.
34. Umebayashi, T.; Yamaki, T.; Itoh, H.; Asai, K., *Band gap narrowing of titanium dioxide by sulfur doping*. *Appl. Phys. Lett.* 2002, 81, (3), 454-456.
35. Umebayashi, T.; Yamaki, T.; Yamamoto, S.; Miyashita, A.; Tanaka, S.; Sumita, S.; Asai, K., *Sulfur doping of rutile titanium dioxide by ion implantation: photocurrent spectroscopy and first principles band calculation studies*. *Appl. Phys.* 2003, 93, (9), 5156-5160.
36. Wang, J.; Yu, S.; Komatsu, M.; Zhang, Q.; Saito, F.; Sato, T., *Preparation and characterization of nitrogen doped SrTiO₃ photocatalyst*. *Photochem. and Photob. A: Chemistry* 2004, 165, 149-156.
37. Wang, Z.; Cai, W.; Homg, X.; Zhao, X.; Xu, F.; Cai, C., *Photocatalytic degradation of phenol in aqueous nitrogen doped TiO₂ suspensions with various light sources*. *App. Cat. B: Env.* 2005, 57, 223-231.
38. Wang, H.; Lewis, J. P., *Second generation photocatalytic materials: anion doped TiO₂*. *J. Phys. Condens. Matter* 2006, 18, 421-434.
39. Xia, H.; Zhuang, H.; Xiao, D.; Zhang, T., *Photocatalytic activity of La³⁺/S/TiO₂ photocatalyst under visible light*. *J. Alloys and compounds* 2007, 465, (1-2), 328- 332.
40. Xie, Y.; Zhao, Q.; Zhao, X.; Li, Y., *Low temperature preparation and characterization of N-doped and N-S-doped codoped TiO₂ by sol-gel route*. *Catal. Lett.* 2007, 188, 231-237.

-
41. Yang, S.; Gao, L., *New method to prepare nitrogen doped titanium dioxide and its photocatalytic activities irradiated by visible light*. J. Am. Ceram. Soc. 2004, 87, 1803-1805.
 42. Pruden, A.; Ollis, D., *Photoassisted heterogeneous catalysis: the degradation of trichloroethylene in water*. J. catal. 1983, 82, 404-417.
 43. Bahnemann, D.; Bockelmann, D.; Goslich, R.; Hilgendorff, M.; Weichgrebe, D., *Photocatalytic detoxification: Novel catalysts, mechanisms and solar applications*. Ollis D.F., Al-Ekabi H.; Elsevier Science Publishers: Amsterdam, 1993; p 301 - 319.
 44. Bahnemann, D.; Bockelmann, D.; Goslich, R.; Hilgendorff, M., *Photocatalytic detoxification of polluted aquifers: Novel catalysts and solar applications*. Helz G.R., Zepp R.G., Crosby D.G.; Lewis Publishers: 1994; p 349 - 367.
 45. Bahnemann, D.; Cunningham, J.; Fox, M. A.; Pelizzetti, E.; Pichat, P.; Serpone, N., *Photocatalytic treatment of waters. Aquatic and surface photochemistry*. Helz G.R., Zepp R.G. and Crosby D.G.; Lewis Publishers: 1994; Chapter 21.
 46. Zalazar, C.; Romero, R.; Martin, C.; Cassano, A., *Photocatalytic intrinsic reaction kinetics I: mineralization of dichloroacetic acid*. J. Chem. Engineering Science 2005, 60, 5240-5254.
 47. Hufschmidt, D.; Bahneman, D.; Tesa, J.; Emilio, C.; Litter, M., *Enhancement of the photocatalytic activity of various TiO₂ materials by platinisation*. J. of Photochemistry and Photobiology A: Chemistry 2002, 148, 223-231.
 48. Lindner, M. *Optimierung der photokatalytischen Wasserreinigung mit Titandioxid: Festkörper- und Oberflächenstruktur des Photokatalysators*. Doktorarbeit an der Universität Hannover, Hannover 1997.
 49. Blanco, J.; Malato, S. *Solar photocatalytic mineralization of real hazardous waste water at the pre-industrial level*, ASME International solar energy conference, San Francisco, California, 1994; p 27-30.

-
50. Blanco, J.; Malato, S. *Effective industrial waste water treatment by solar photocatalysis; Application to fine chemicals spanish company*, 7th International symposium on solar thermal concentrating technologies, Moscow, Russia, 1994; Moscow, Russia, 1994; p 26-30.
51. Matsunaga, T.; Tomoda, R.; Nakajima, T.; Nakamura, N.; Komine, T., *Continuous-sterilization system that uses photoconductor powders*. Appl. Environ. Microbiol. 1988, 54, 1330- 1333.
52. Ireland, J., *Microbiological issues related to drinking water disinfection chemistry: Opportunities for further TiO₂ research*; Photocatalytic purification and treatment of water and air. Ollis D.F, Al-Ekabi H.; Elsevier Science Publishers: 1993.
53. Wei, C.; Lin, W.; Zainal, Z.; Williams, N.; Zhu, K.; Kruzic, A.; Smith, R.; Rajeshwar, K., *Bactericidal activity of TiO₂ photocatalyst in aqueous media: toward a solar assisted water disinfection system*. Environ. Sci. Technol. 1994, 28, 934-938.
54. Ibáñez, J. A.; Litter, M.; Pizarro, R. A., *Photocatalytic bactericidal effect of TiO₂ on Enterobacter cloacae. Comparative study with other Gram (-) bacteria*. J. Photochemistry and photobiology A: Chemistry 2003, 157, 81-85.
55. Rincón, A. G.; Pulgarin, C., *Photocatalytical inactivation of E. coli: effect of (continuous-intermittent) light intensity and of (suspended-fixed) TiO₂ concentration*. Applied Catalysis B: Environmental 2003, 44, 263 - 284.
56. Coleman, H. M.; Marquis, C. P.; Scott, J. A.; Chin, S.; Amal, R., *Bactericidal effects of titanium dioxide-based photocatalysts*. Chemical Engineering J. 2005, 113, 55-63.
57. Dillert, R.; Siemon, U.; Bahnemann, D. W., *Photocatalytic disinfection of municipal wastewater*. Chem. Eng. Technol 1998, 21, 4.
58. Organisation, W. H., *Guidelines for drinking water quality*; Geneva, Switzerland, 2004.

-
59. Maness Pin Ching; Sharon, S., *Bactericidal activity of photocatalytic TiO₂ reaction: toward an understanding of its killing mechanism*. Appl. and Env. Microb 1999, 65, (9), 4094-4098.
60. Armon, R.; Laot, N.; Narkis, N.; Neeman, I. *Photocatalytic inactivation of different bacteria and bacteriophages in drinking water at different TiO₂ concentrations and with or without exposure to O₂*, The second international conference on TiO₂ photocatalytic purification and treatment of water and air, Cincinnati, USA, 1996.
61. Broca, *Biología de los microorganismos*. 8 ° edición revisada; Prentice may: 2000.
62. Edward, I., *Fundamentals of microbiology*; The Benjamin/Cummings Publishing Company, 1994.
63. Singleton, P., *Bacteria in Biology*. Biotechnology and Medicine, 6 Edn.; Wiley: Hoboken, NJ, 2004; p 559.
64. Liqiang; Xiaojun; Baifu; Baiqi; Weimin; Honggang, *The preparation and characterization of La doped TiO₂ nanoparticles and their photocatalytic activity*. Solid State Chemistry 2004, 177, (10), 3375-3382.
65. Kortüm; Schreyer, *Über die Gewinnung "typischer Farbkurven" von Pulvern aus Reflexionsmessungen*. Angew. Chem 1955, 67, (22), 694- 698.
66. Kortüm; Braun; Herzog, *Prinzip und Meßmethodik der diffusen Reflexionsspektroskopie*. Angew. Chem. 1963, 75, (14), 653-657.
67. Han; Wu; Hsieh, *Science technol. B* 2007, 25, (2), 430-435.
68. Barton; Wilson; Soled; Iglesia, *Structure and electronic properties of solid acids based on tungsten oxide nanostructures*. J Phys. Chem. B 1999, 103, (4), 630-640.

-
69. Lindner, M.; Bahnemann, D. W.; Hirthe, B.; Griebler, W.-D., *Neue Katalysatoren zur photokatalytischen Abwasserreinigung*. wlb Wasser, Luft und Boden 1994, 11-12, 38-34.
70. Eckhard, B., *Microbiologische Methoden: eine Einführung in grundlegende Arbeitstechniken*. 2. Auflage; Spektrum Akademischer Verlag GmbH: Heidelberg, 2001; p 429.
71. Zhang, L.; Yu, J. C.; Yip, H.; Li, Q.; Kwong, K.; Xu, A.; Wong, P., *Ambient light reduction strategy to synthesize silver nanoparticles and silver coated TiO₂ with enhanced photocatalytic and bactericidal activities*. Langmuir 2003, 19, 10372-10380.
72. Ohtani, B., *What is Degussa P25? Crystal composition analysis, reconstruction from isolated pure particles, and photocatalytic activity test*, 17th. International Conference on photochemical conversion and storage of solar energy, Sydney, 2008.
73. Watts, R. J.; Kong, S.; Orr, M.; Miller, G.; Henry, B., *Photocatalytic inactivation of coliform bacteria and viruses in secondary wastewater effluent*. Wat. Res. 1995, 29, (1), 95-100.
74. Herrera, J. A.; Rodríguez, J. M.; Viera, A.; Tello, E.; Valdés, C.; Arana, J.; Pérez, J., *The photocatalytic disinfection of urban waste waters*. Chemosphere 2000, 41, 323-327.
75. Yu, J. C.; Ho, W.; Yu, J. C.; Yip, H.; Wong, P. K.; Zhao, J., *Efficient visible light induced photocatalytic disinfection on sulfur doped nanocrystalline titania*. Environ. Sci. Technol. 2005, 39, 1175- 1179.
76. Yan, X.; Ohno, T.; Nishijima, K.; Abe, R.; Ohtani, B., *Is methylene blue an appropriate substrate for a photocatalytic activity test? A study with visible-light responsive titania*. Chem. Phys. Lett. 2006, 429, (4-6), 606-610.
77. Ohtani, B., *Preparing articles on photocatalysis-beyond the illusions, misconceptions and speculation*. J. Chem. Lett. 2008, 37, (3), 217-229.

10 List of Abbreviations and Symbols

Abbreviations

A	Acceptor
CB	Conduction band
D	Donor
DCA	Dichloroacetic acid
E. coli	Escherichia coli
E _g	Band gap (eV)
IR	Infrared
KM	Kubelka Munk
NHE	Normal Hydrogen Electrode
P.E.	Photonic efficiency
R	Diffuse reflectance
RDS	Reflection measurements
TOC	Total Organic Carbon
n.d.	No determined
UV	Ultraviolet region von 100 nm bis 380 nm
UV (A)	Ultraviolet region $315 \text{ nm} \leq \lambda \leq 380 \text{ nm}$
UV (B)	Ultraviolet region $280 \text{ nm} \leq \lambda \leq 315 \text{ nm}$
UV (C)	Ultraviolet region $100 \text{ nm} \leq \lambda \leq 280 \text{ nm}$
VB	Valence band
XRD	X-ray diffraction

Symbols

A	Anatase
A	Area (m ²)
C	concentration (M)
C ₀	initial concentration
c	speed of light 3E+08 (m*s ⁻¹)
C.F.U.	Colony formed units (1/mL)
e ⁻	Electron
h ⁺	Positively charged hole
h	Plank constant 6.63E-34 (J*s)
I	Intensity of the light (W*m ⁻²)
I _{hν}	Incident UV(A) photon flux (mol*m ⁻² *s ⁻¹)
I _{hν(vol)}	Incident UV(A) (mol*I*s ⁻¹), related to reactor volume
N	Avogadro number 6.02E+23 (mol ⁻¹)
R	Rutile
rpm	revolutions per minute
V	Volume (L)
λ	Lambda value (nm)
ξ	Photonic efficiency (%)

Empirical formula

O_2^-	Superoxide anion
O_2H^\cdot	Hydrogen superoxide radical
H_2O_2	Hydrogen peroxide
OH^\cdot	Hydroxyl radical
CHCl_2COOH	Dichloroacetic acid
$\text{CHCl}_2\text{COO}^\cdot$	Dichloroacetate radical
$\text{HCl}_2\text{C}^\cdot$	Dichloromethyl radical
$\text{CHCl}_2\text{OO}^\cdot$	Dichloromethylperoxyl radical
TiO_2	Titanium dioxide
$\text{Ti}(\text{OCH}(\text{CH}_3)_2)_4$	Titanium (IV) isopropoxide
$\text{Ti}(\text{OBu})_4$	Titanium (IV) isopropoxide
KNO_3	Potassium nitrate
NaOH	Sodium hydroxide
HCO_3^-	Hydrogen carbonate
CO_3^{2-}	Carbonate
CO_2	Carbon dioxide

11 Appendix

11.1 Additional data

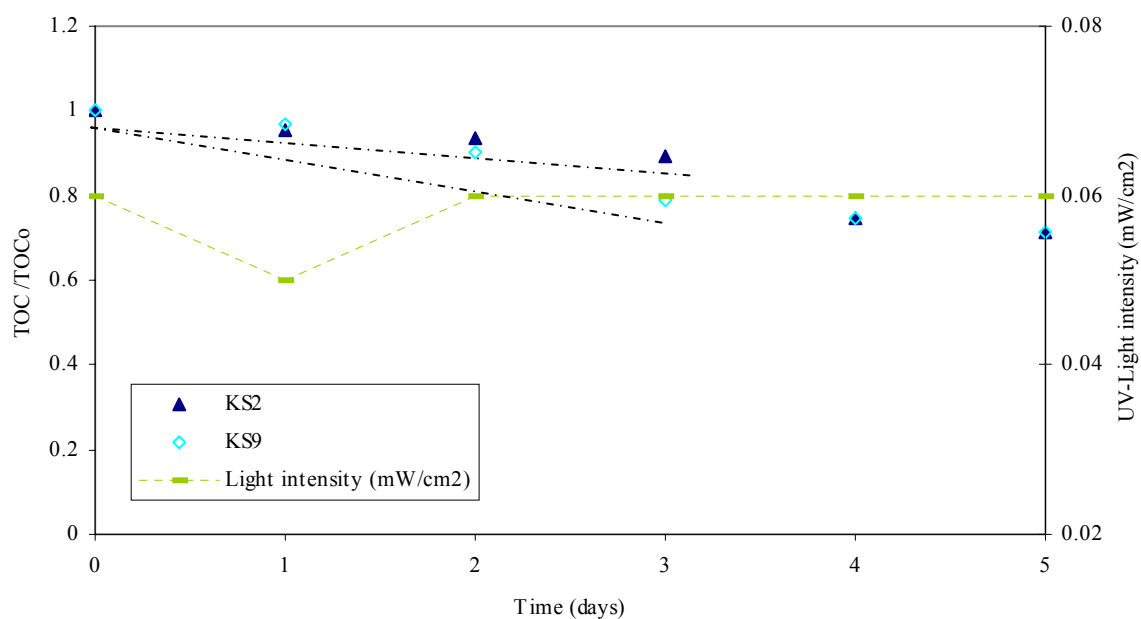


Fig. 51. Plot of TOC-reduction versus experimental time (days). *Experimental conditions:* 1mM DCA dissolved in 200 mL distilled water, KNO₃ (10 mM) and 0.5 g/L photocatalyst (sulfur doped photocatalysts calcined at 550°C (KS2) and 700 °C (KS9), respectively) reaction time 5 days, under indoor illumination conditions.

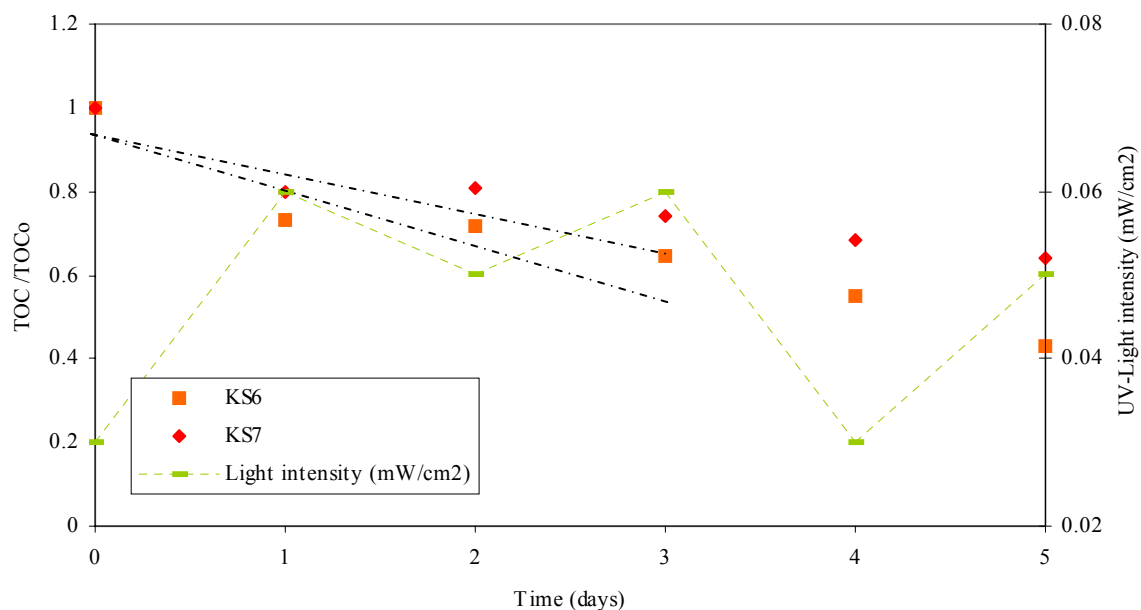


Fig. 52. Plot of TOC-reduction versus experimental time (days). *Experimental conditions:* 1mM DCA dissolved in 200 mL distilled water, KNO_3 (10 mM) and 0.5 g/L photocatalyst (sulfur doped TiO_2 calcined at 625 °C(KS6) and 650 °C (KS7), respectively) reaction time 5 days, under indoor illumination conditions.

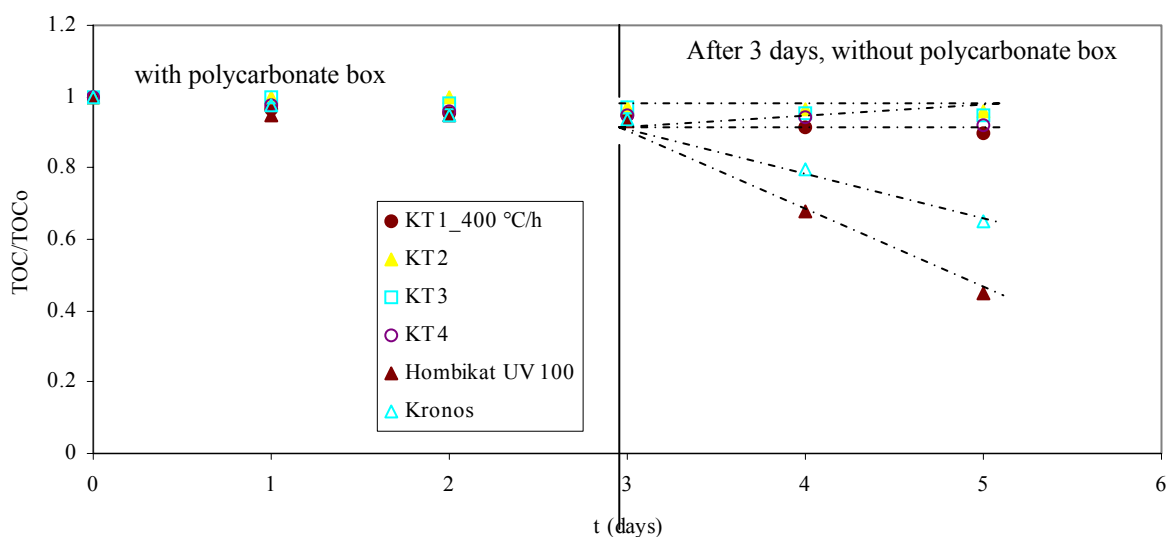


Fig. 53. Plot of TOC removal for the catalysts Hombikat UV 100, Kronos and sulfur doped TiO_2 , which were calcined at 550 °C (KT1), 575 °C (KT2), 600 °C (KT3) and 625 °C (KT4) for three hours, 400 °C/h as calcination profile versus experimental time (days). *Experimental conditions:* 1mM DCA dissolved in 200 mL distilled water, KNO_3 (10 mM) and 0.5 g/L photocatalyst (synthesized with a molar ratio of titanium (IV) isopropoxide and thiourea) with a reaction time of 5 days.

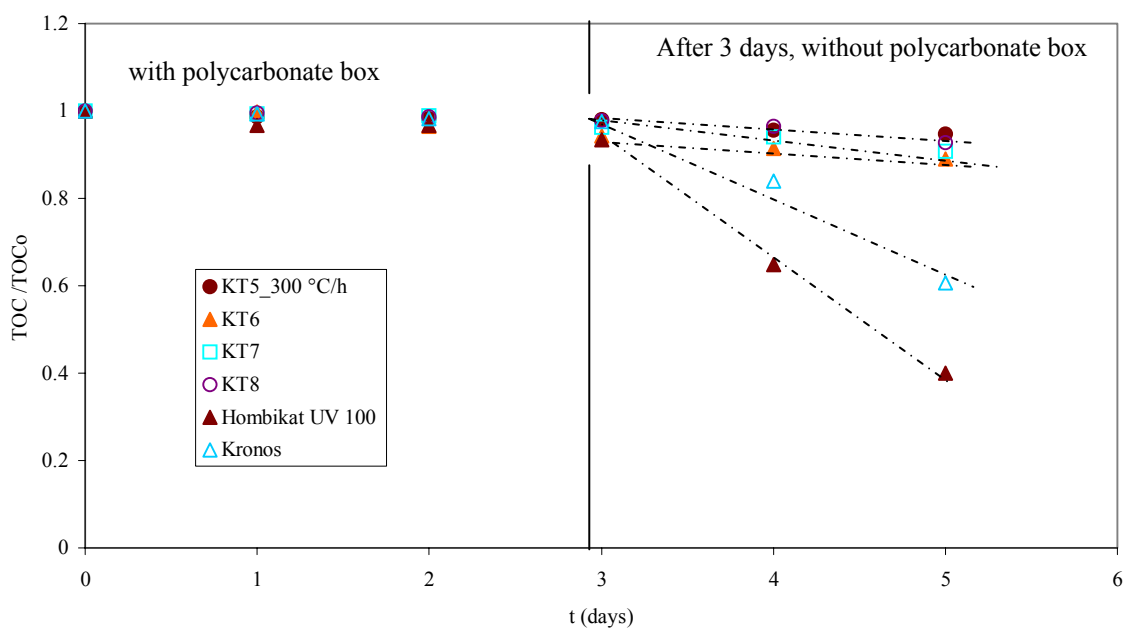


Fig. 54. Plot of TOC removal for the catalysts Hombikat UV 100, Kronos and sulfur doped TiO₂, which were calcined at 550 °C (KT5), 575 °C (KT6), 600 °C (KT7) and 625 °C (KT8) for three hours, with a heating profile of 300 °C/h, versus experimental time (days).

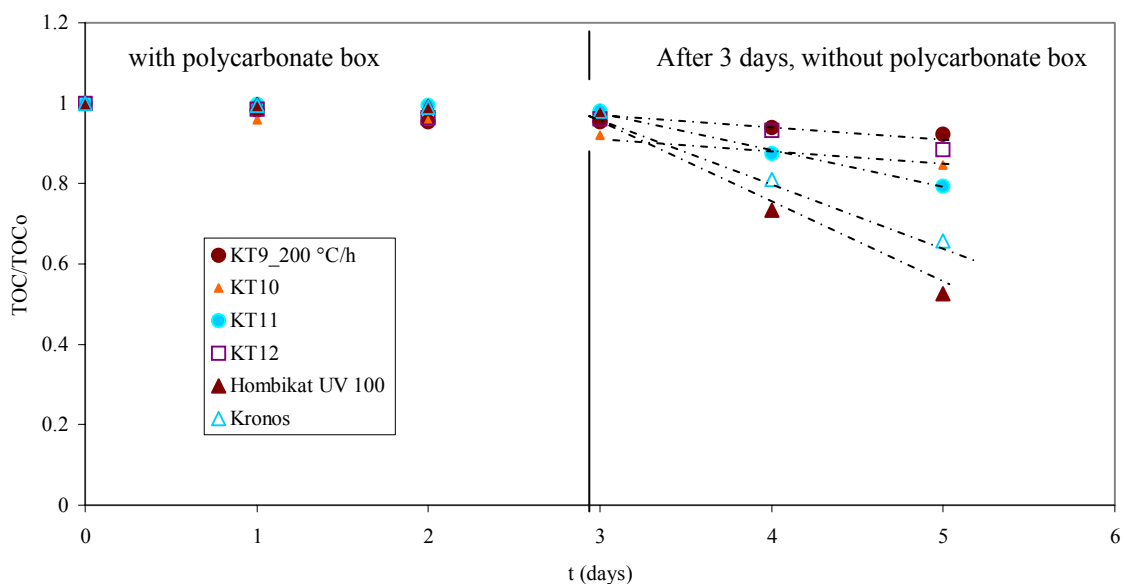


Fig. 55. Plot of TOC mineralization by DCA- degradation for the photocatalysts: Hombikat UV 100, Kronos and sulfur doped TiO₂, which were calcined at 550 °C (KT9), 575 °C (KT10), 600 °C (KT11) and 625 °C (KT12) for three hours with a heating profile of 200 °C/h, versus experimental time (5 days).

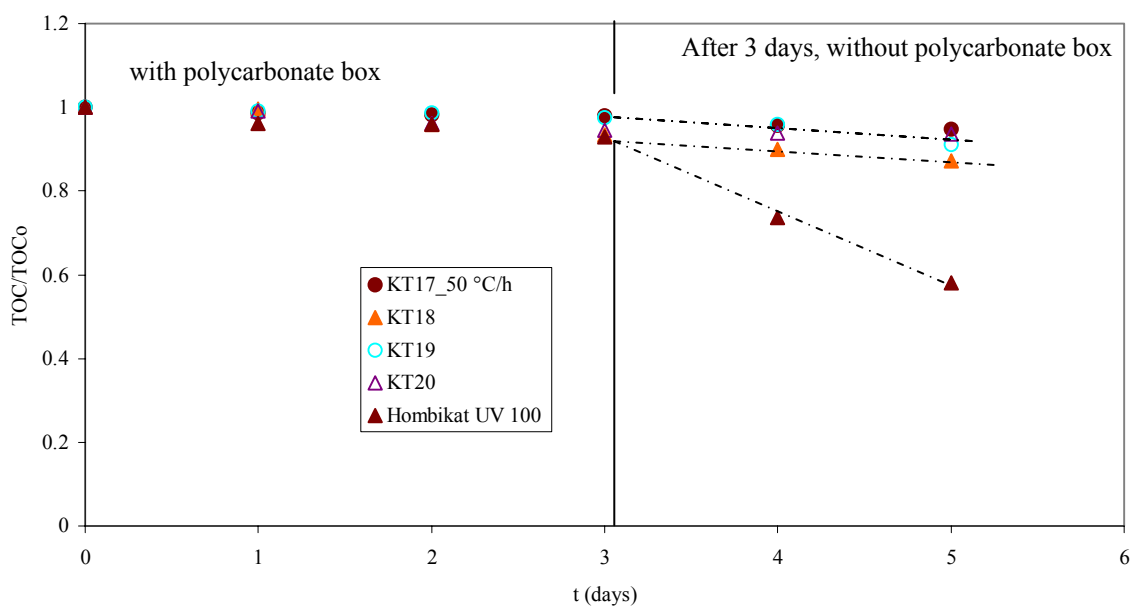


Fig. 56. Decrease of TOC values for the catalysts: Hombikat UV 100, Kronos and sulfur-doped TiO₂, which were calcined at 550 °C (KT17), 575 °C (KT18), 600 °C (KT19) and 625°C (KT20) for three hours (with a heating profile of 50°C/h) versus experimental time (days).

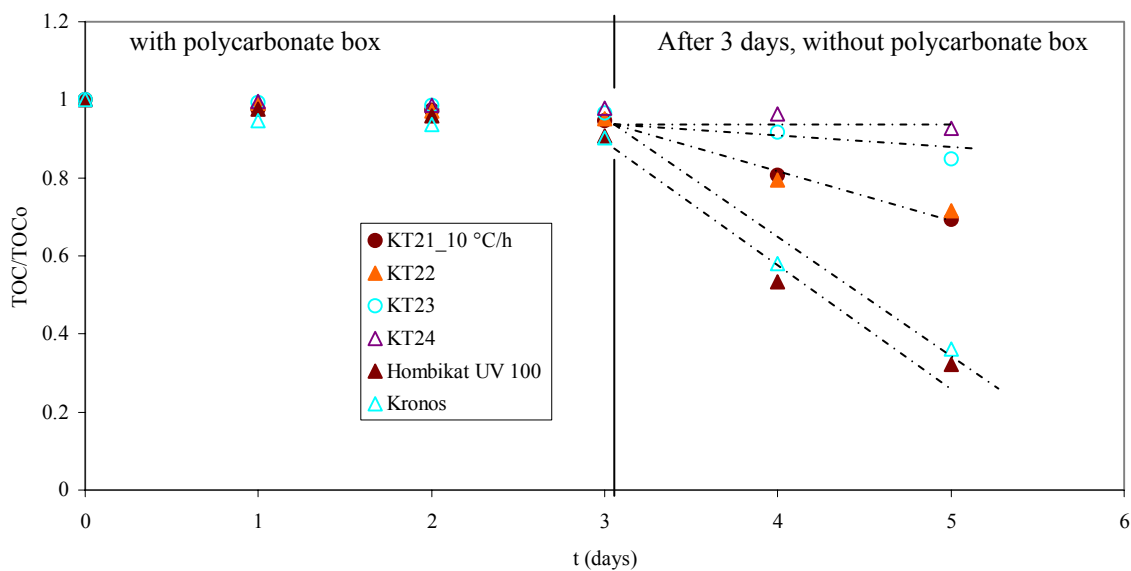


Fig. 57. Decrease of TOC values for the catalysts: Hombikat UV 100, Kronos and sulfur-doped TiO₂, which were calcined at 550 °C (KT21), 575 °C (KT22), 600 °C (KT23) and 625°C (KT24) for three hours with a heating profile of 10 °C/h versus experimental time (days).

11.2 List of figures

- Fig. 1. Scheme of the elementary processes at a semiconductor particle upon irradiation⁷... 12
- Fig. 2. Scheme of simplified mechanism of indirect photocatalysis upon irradiation¹⁰. 16
- Fig. 3. Photodegradation of 4- Chlorophenol (4-CP) on pure titania by visible light illumination in the presence of Fe^{3+} or oxygen as electron acceptors¹¹ 16
- Fig. 4. Simplified schematic of newly formed extra energy levels for doped semiconductors¹⁵. 19
- Fig. 5. Energetic positions of valence band, conduction band and band gap energies of semiconductors vs. NHE and Vacuum level in aqueous solution at $pH = 7^{37}$ 20
- Fig. 6. Crystal structure of the three TiO_2 - modifications: a) rutil, b) anatase and c) brookite. 21
- Fig. 7. Simplified schematic of different methods to activate titanium (IV) dioxide in the visible light region: sensitized ($h\nu_4$ explained in section 5.3.), doping with transition metals or non metal ion doping ($h\nu_2$ and $h\nu_3$)^{10, 18}. 23
- Fig. 8. Photonic efficiencies (%) of Hombikat UV 100⁴⁸ as function of a) catalyst loading, b) pollutant concentration, c) pH value, d) light intensity for the DCA- degradation (1 mM). Experimental conditions: 1 mM DCA, $pH = 3$, catalyst loading 5 g/L, 10 mM KNO_3 , $\lambda > 320$ nm. 26
- Fig. 9. Scheme of difference between Gram -positive and -negative bacteria's cell wall structure.^{60, 61} 28
- Fig. 10. Plot of the Reflectance spectra of the commercial titania powder Hombikat UV 100 as a function of wavelength. 37

<i>Fig. 11. Plot of transformed Kubelka Munk function versus Photon energy (eV) for the commercial catalysts Hombikat UV 100.</i>	38
<i>Fig. 12. The pH-stat titration system employing Metrohm instruments⁶⁹.</i>	42
<i>Fig. 13. Spectra of the filters WG 320, GG 420, GG 495, showing the transmission as a function of the wavelength.</i>	43
<i>Fig. 14. DCA- degradation set-up for indoor experiments.</i>	45
<i>Fig. 15. Transmittance- spectra of polycarbonate material employing UV- Spectrometer. Only visible light can penetrate this material.</i>	45
<i>Fig. 16. Picture of the illumination chamber</i>	46
<i>Fig. 17. Emission spectrum of the lamp ibv L18W742 Coolwhite measured at a distance of 20 cm., with three maxima emissions by the corresponding wavelengths of 365 nm, 406 nm and 439 nm. The incident photon fluxes (I_{hv}) were calculated by the integrated wavelengths values obtaining $2.77E-07 \text{ mol/ m}^2*s$, $7.40 E-07 \text{ mol/ m}^2*s$ and $2.06 E-05 \text{ mol/ m}^2*s$, respectively.</i> 47	47
<i>Fig. 18. Photocatalytic disinfection E. coli -set- up and -scheme.</i>	49
<i>Fig. 19. Sulfur doped TiO₂ photocatalysts calcined at different temperatures 550 °C (KS3) 625 °C (KS6), 650 °C (KS7) and 700 °C (KS8), prepared following the synthesis in section 6.1.2.</i>	54
<i>Fig. 20. XRD patterns for the sulfur doped TiO₂ photocatalysts.</i>	55
<i>Fig. 21. Plot of the Reflectance spectra (a, c and e) and transformed Kubelka Munk function (b, c, f) of sulfur doped TiO₂ prepared with a molar ratio 1:4, calcinated for 3 hours at different temperatures 550 °C, 575 °C, 600 °C and 625 °C and temperature ramps 10 °C/h, 50 °C/h and 100 °C/h, respectively.</i>	59

Fig. 22. Plot of TOC-concentration as a function of the illumination time (h) by DCA-degradation. Experimental conditions: 1mM DCA dissolved in 200 mL distilled water, KNO_3 (10 mM) under $\text{pH} = 3$ and 0.5 g/L catalyst (titania precursors: titanium (IV) isopropoxide and titanium (IV) butoxide calcined at different temperatures 500 °C, 600 °C and 700 °C, respectively) illuminated for 3 hours, under UV- illumination conditions (light intensity $I_{UV(A)}$ 15.5 W/m^2)..... 62

Fig. 23. Plot of TOC-concentration versus irradiation time (h). Experimental conditions: Degradation of DCA (1 mM) in an aqueous solution of KNO_3 (200 mL) at $\text{pH} = 3.0$, 0.5 g/L of photocatalyst (commercial photocatalysts and the sulfur doped TiO_2 calcined at 500 °C (KS2), 600 °C (KS5) and 700 °C (KS8) for three hours), $\lambda_{\text{ex}} \geq 320 \text{ nm}$, $I_{UV(A)} = 190 \text{ W}/\text{m}^2$ 64

Fig. 24. Plot of TOC- reduction versus irradiation time (h). Experimental conditions: Degradation of DCA (1 mM) in an aqueous solution of KNO_3 (200 mL) at $\text{pH} = 3.0$, 0.5 g/L of photocatalyst (commercial photocatalysts and the sulfur doped TiO_2 calcined at 500 °C (KS2), 600 °C (KS5) and 700 °C (KS8) for three hours), $\lambda_{\text{ex}} \geq 420 \text{ nm}$, $I_{UV(A)} = 3.7 \text{ W}/\text{m}^2$ 66

Fig. 25. Reduction of TOC- concentration versus experimental time (h). Experimental conditions: Degradation of DCA (1 mM) in an aqueous solution of KNO_3 (200 mL) at $\text{pH} = 3.0$, 0.5 g/L of photocatalyst (commercial photocatalysts and the sulfur doped TiO_2 calcined at 600 °C (KS5) for three hours), $\lambda_{\text{ex}} \geq 495 \text{ nm}$ 67

Fig. 26. Plot of TOC-reduction versus experimental time (h). Experimental conditions: 1mM DCA dissolved in 200 mL distilled water KNO_3 (10 mM) and 0.5 g/L (the commercial Hombikat UV 100 and Kronos and the sulfur doped TiO_2 catalysts calcined at different temperatures 300 °C (KS1), 500 °C (KS2), 550 °C (KS3), 575 °C (KS4), 600 °C (KS5), 625 °C (KS6), 650 °C (KS7), 700 °C (KS8), 750 °C (KS9) for three hours) during 4 hours under solar illumination $I_{UV(A)} = 9.9 \text{ W}/\text{m}^2$ 69

- Fig. 27. Plot of TOC-reduction versus experimental time (days). Experimental conditions: 1mM DCA dissolved in 200 mL distilled water, KNO_3 (10 mM) and 0.5 g/L commercial photocatalyst Hombikat UV 100 and Kronos, reaction time of 5 days, under indoor illumination conditions mean value $I_{UV(A)} = 0.5 \text{ W/m}^2$ 71
- Fig. 28. Plot of TOC-reduction versus experimental time (days). Experimental conditions: 1mM DCA dissolved in 200 mL distilled water, KNO_3 (10 mM) and 0.5 g/L photocatalyst (sulfur doped TiO_2 photocatalysts calcined at 500 °C (KS3) and 750 °C (KS8), respectively) reaction time 5 days, under indoor illumination conditions mean value $I_{UV(A)} = 0.5 \text{ W/m}^2$.. 71
- Fig. 29. Plot of TOC-reduction versus experimental time (days). Experimental conditions: 1mM DCA dissolved in 200 mL distilled water, KNO_3 (10 mM) and 0.5 g/L photocatalyst (sulfur doped TiO_2 calcined at 600 °C (KS5) and 575 °C (KS4), respectively) reaction time 5 days, under indoor illumination conditions mean value $I_{UV(A)} = 0.5 \text{ W/m}^2$ 72
- Fig. 30. Layout of catalysts position 74
- Fig. 31. Plot of TOC-reduction versus experimental time (h). Experimental conditions: 1mM DCA dissolved in 200 mL distilled water, KNO_3 (10 mM) and 0.5 g/L catalyst (with a molar ratio of 1:4) with a reaction time of 5 days, under indoor illumination conditions..... 75
- Fig. 32. Normalized TOC-values versus illumination time (hours) Mean values and standard deviation calculated for Hombikat UV 100 (2.03) and the sulfur doped TiO_2 catalyst (0.16) calcined at 500 °C (KS2) for 3 hours, for the degradation of DCA under indoor illumination conditions: 1mM DCA dissolved in 200 mL distilled water, KNO_3 (10 mM) and 0.5 g/L catalyst, reaction time 5 days, $I_{UV(A)} = 0.4 \text{ W/m}^2$ 76
- Fig. 33. TOC- removal for the DCA-degradation versus experimental time (days). Experimental conditions: 1mM DCA dissolved in 200 mL distilled water, KNO_3 (10 mM) and 0.5 g/L photocatalyst (a) synthesized with a molar ratio of titanium (IV) isopropoxide and thiourea 1:6, calcined for 3 h. b) calcined for 7 h with a reaction time of 5 days under indoor illumination conditions..... 78

Fig. 34. TOC-mineralization of DCA for the photocatalysts: Hombikat UV 100, Kronos and sulfur doped TiO_2 , which were calcined at 550 °C (KT13), 575 °C (KT14), 600 °C (KT15) and 625 °C (KT16) for three hours with 100 °C/h as calcinations program versus experimental time (5 days), $I_{UV(A)} = 0.4 \text{ W/m}^2$ 80

Fig. 35. Plot of relative rates versus temperature profiles for the sulfur doped TiO_2 photocatalysts calcined at 550 °C, 575 °C, 600 °C and 625 °C, respectively under different temperature profiles 10 °C/h, 50 °C/h, 100 °C/h, 150 °C/h, 200 °C/h, 300 °C/h and 400 °C/h. 81

Fig. 36. Plot of TOC- decrement for DCA- degradation study versus illumination time (h) under artificial illumination conditions: 1mM DCA dissolved in 200 mL distilled water, KNO_3 (10 mM) and 0.5 g/L commercial catalyst illuminated for 19 hours ($I_{UV(A)} = 0.3 \text{ W/m}^2$). 83

Fig. 37. Decrease of TOC- values versus illumination time (h) for the sulfur doped TiO_2 photocatalysts calcined at 550°C (KT21), 575°C (KT22), 600°C (KT23) und 625°C (KT24) for three hours (10°C/h as calcination ramp), with an UV (A) light intensity of 0.3 W/m^2 84

Fig. 38. TOC-mineralization versus illumination time (h) under artificial illumination conditions. Experimental conditions: 1mM DCA dissolved in 200 mL distilled water, KNO_3 (10 mM) and 0.5 g/L catalyst (sulfur doped TiO_2 photocatalysts with a molar ratio of 1:4 and 100 °C/h as heating profile for different calcination temperatures 550 °C (KT13), 575°C (KT14), 600 °C (KT15) and 625 °C (KT16)) illuminated for 19 hours, UV (A) light intensity value of 0.3 mW/m^2 and the distance from the lamps to the reactors 60 cm. 85

Fig. 39. Plot of TOC-removal for DCA- degradation study versus experimental time (h) under artificial illumination conditions: 1mM DCA dissolved in 200 mL distilled water, KNO_3 (10 mM) and 0.5 g/L catalyst (with a molar ratio of 1:6) illuminated for 19 hours, UV(A) light intensity value of 0.3 W/m^2 and distance of 60 cm (reactor-lamp). 86

Fig. 40. Plot of photonic efficiency values as function of the different sulfur doped TiO_2 catalysts a) molar ratio 1:4 (Photocatalysts KT21- KT24) and 1:6 (Photocatalysts KT21A- KT24A) b) heating profile 10°C/h (KT21- KT24) and 100°C/h (KT13- KT16). 88

Fig. 41. Plot of TOC-removal for DCA- degradation study under indoor illumination conditions versus experimental time (days): 1mM DCA dissolved in 200 mL distilled water, KNO_3 (10 mM) and 0.5 g/L lanthanum-doped TiO_2 photocatalyst (calcined at 400°C (KL1), 500°C (KL2), 600°C (KL3) and 700°C (KL4), with 0.4% Lanthanum content) illuminated for 5 days with a UV (A)-light intensity of 0.4 W/m^2 90

Fig. 42. Plot of TOC- decrement for DCA- degradation study under indoor illumination conditions versus experimental time (days): 1mM DCA dissolved in 200 mL distilled water, KNO_3 (10 mM) and 0.5 g/L lanthanum doped TiO_2 catalyst (calcined at 400°C (KL5), 500°C (KL6), 600°C (KL7) and 700°C (KL8), with 0.9% lanthanum content) illuminated during 5 days with a UV (A)-light intensity of 0.4 W/m^2 91

Fig. 43. Disinfection achieved by phototreatment of a model bacteria suspension (*Escherichia coli*) with an ampicillin concentration of 75 mg/L dissolved in 5 L of a physiological salt solution for a total period of 3 hours. 93

Fig. 44. Plot of first order kinetics of *E. Coli* disinfection using ampicillin concentration of 75 mg/L dissolved in 5 L of a physiological salt solution for a total period of 3 hours. 94

Fig. 45. Plot of the change of CFU versus time, experimental conditions: aliquot of *E. Coli* with a concentration of ampicillin 75 mg/L dissolved in 5 L of a physiological salt solution, illumination performed with the lamp TQ718 for a total period of 3 hours. 95

Fig. 46. Plot of first order kinetics of *E. coli* disinfection using ampicillin concentration of 75 mg/L dissolved in 5 L of a physiological salt solution for a total period of 3 hours. 96

- Fig. 47. Disinfection achieved by photocatalytic treatment of a model bacteria suspension (*Escherichia Coli*). Experimental conditions: aliquot of *E. coli* with a concentration of ampicillin 75 mg/L and a concentration of catalyst Degussa P25 ranging from 0.1 to 2 g/L, dissolved in 5 L of a physiological salt solution, illumination performed with the lamp TQ718Z4 for 3 hours..... 98
- Fig. 48. Plot of C.F.U. rates versus Catalyst Degussa P25 concentration (g/L). Experimental conditions: aliquot of *E. coli* with a concentration of ampicillin 75 mg/L and a concentration of catalyst Degussa P25 ranging from 0.1 to 2 g/L, dissolved in 5 L of a physiological salt solution, illumination performed with the lamp TQ718Z4 for 3 hours..... 99
- Fig. 49. Study of TOC-degradation (%) determined by TOC (%) - measurements for commercial catalysts Sachtleben Hombikat UV 100, Kronos, Degussa P25 and Toho and for the sulfur doped TiO₂ catalysts calcined at 550 °C, 575 °C, 600 °C and 625 °C with 10 °C/h calcination ramp under artificial light illumination conditions..... 101
- Fig. 50. Study of TOC-degradation (%) in comparison to different experimental illumination conditions and different photocatalysts such as Kronos, Hombikat UV 100 and the sulfur doped TiO₂ calcined at 600 °C..... 101
- Fig. 51. Plot of TOC-reduction versus experimental time (days). Experimental conditions: 1mM DCA dissolved in 200 mL distilled water, KNO₃ (10 mM) and 0.5 g/L photocatalyst (sulfur doped photocatalysts calcined at 550°C (KS2) and 700 °C (KS9), respectively) reaction time 5 days, under indoor illumination conditions. 116
- Fig. 52. Plot of TOC-reduction versus experimental time (days). Experimental conditions: 1mM DCA dissolved in 200 mL distilled water, KNO₃ (10 mM) and 0.5 g/L photocatalyst (sulfur doped TiO₂ calcined at 625 °C(KS6) and 650 °C (KS7), respectively) reaction time 5 days, under indoor illumination conditions. 117

Fig. 53. Plot of TOC removal for the catalysts Hombikat UV 100, Kronos and sulfur doped TiO_2 , which were calcined at 550 °C (KT1), 575 °C (KT2), 600 °C (KT3) and 625 °C (KT4) for three hours, 400 °C/h as calcination profile versus experimental time (days). Experimental conditions: 1mM DCA dissolved in 200 mL distilled water, KNO_3 (10 mM) and 0.5 g/L photocatalyst (synthesized with a molar ratio of titanium (IV) isopropoxide and thiourea) with a reaction time of 5 days. 117

Fig. 54. Plot of TOC removal for the catalysts Hombikat UV 100, Kronos and sulfur doped TiO_2 , which were calcined at 550 °C (KT5), 575 °C (KT6), 600 °C (KT7) and 625 °C (KT8) for three hours, with a heating profile of 300 °C/h, versus experimental time (days). 118

Fig. 55. Plot of TOC mineralization by DCA- degradation for the photocatalysts: Hombikat UV 100, Kronos and sulfur doped TiO_2 , which were calcined at 550 °C (KT9), 575 °C (KT10), 600 °C (KT11) and 625°C (KT12) for three hours with a heating profile of 200 °C/h, versus experimental time (5 days). 118

Fig. 56. Decrease of TOC values for the catalysts: Hombikat UV 100, Kronos and sulfur-doped TiO_2 , which were calcined at 550 °C (KT17), 575 °C (KT18), 600 °C (KT19) and 625°C (KT20) for three hours (with a heating profile of 50°C/h) versus experimental time (days). 119

Fig. 57. Decrease of TOC values for the catalysts: Hombikat UV 100, Kronos and sulfur-doped TiO_2 , which were calcined at 550 °C (KT21), 575 °C (KT22), 600 °C (KT23) and 625°C (KT24) for three hours with a heating profile of 10 °C/h versus experimental time (days). 119

11.3 List of tables

<i>Table 1. Overview of different photocatalysis applications³⁻⁵ .</i>	11
<i>Table 2. List of the synthesized undoped photocatalysts and their different calcination temperatures.</i>	31
<i>Table 3. The different molar ratios and calcination temperatures chosen for the synthesis of the sulfur- doped TiO₂ photocatalysts.</i>	32
<i>Table 4. The experimental conditions of different lanthanum-concentrations, calcination temperatures and heating rates for the preparation of lanthanum- doped TiO₂ photocatalysts.</i>	34
<i>Table 5. Physical properties of different types of commercial TiO₂ catalysts used in this study.</i>	35
<i>Table 6. Complex mediums recipe.</i>	50
<i>Table 7. LB-Endo Agar Mediums recipe.</i>	50
<i>Table 8. Elemental analysis and band gap values of the undoped TiO₂ materials.</i>	51
<i>Table 9. Elemental analysis of the prepared sulfur doped TiO₂ samples from Table 2.</i>	52
<i>Table 10. Summary of the experimental band gaps obtained for the sulfur doped TiO₂ photocatalysts.</i>	56
<i>Table 11. Elemental analysis of the lanthanum doped TiO₂ photocatalysts showing a range of lanthanum concentrations and different calcination temperatures.</i>	60

<i>Table 12. Experimental band gap values calculated by Kubelka Munk function from diffuse reflectance spectra. Section 6.3.4. explains how it is possible to calculate the experimental band gap values. The samples were measured as powders and BaSO₄ was taken as the background reflectance spectrum.</i>	<i>61</i>
<i>Table 13. Photonic efficiencies and initial DCA- degradation rates calculated for the undoped samples and for the commercial catalysts Hombikat UV 100.</i>	<i>63</i>
<i>Table 14. Photonic efficiencies and DCA- rates calculated for the commercial and sulfur doped TiO₂ catalysts with a wavelength ≥ 320 nm and a light intensity UV (A) value of 190 W/m².</i>	<i>65</i>
<i>Table 15. Initial DCA- rates calculated for the commercial and self made catalysts with a wavelength value of 420 nm (the photonic efficiencies were calculated with a corresponding light intensity $I_{UV(A)} = 3.7$ W/m²) and 495 nm.</i>	<i>67</i>
<i>Table 16. The initial DCA-rates for the different photocatalysts have been determined following a kinetic of zero order. The relative rates have been calculated for each photocatalysts in relation with the initial DCA-rate of Hombikat UV 100, which was taken as standard.....</i>	<i>69</i>
<i>Table 17. The initial DCA- rates of the sulfur doped TiO₂ photocatalysts are shown, following a kinetic of zero order. The relative rates have been calculated for each photocatalysts in relation with the DCA-rate of Hombikat UV 100, which was taken as standard. For the calculation of photonic efficiencies it is assumed that every day has only 14 hours solar illumination $I_{UV(A)} = 0.5$ W/m².</i>	<i>72</i>
<i>Table 18. The calculated photonic efficiencies and DCA-rates for Hombikat UV 100 and sulfur doped TiO₂ catalyst (KS2) (during the last two days of the illumination experiments without the polycarbonate box, taking into account that one day has only 14 hours solar illumination).</i>	<i>75</i>

<i>Table 19. Photonic efficiencies calculated (during the last two days without the polycarbonate box) from the mean values of Hombikat UV 100 and the sulfur doped TiO₂ catalyst (KS2): 1mM DCA dissolved in 200 mL distilled water, KNO₃ (10 mM) and 0.5 g/L catalyst, with a reaction time of 5 days, I = 0.4 W/m².....</i>	76
<i>Table 20. Photonic efficiencies calculated during the last two days without the polycarbonate box, taking into account that every day has only 14 hours illumination (I_{UV(A)} = 0.4 W/m²) for Hombikat UV 100, Kronos and the sulfur doped TiO₂ catalyst (calcined in the range from 500 °C to 750 °C), with a molar ratio of 1:6 (titanium (IV) isopropoxide to thiourea).....</i>	78
<i>Table 21. DCA- degradation rates of the sulfur doped TiO₂ catalysts which were calcined for three hours at different temperatures: 550°C, 575 °C, 600 °C and 625 °C, and with different temperature profiles 10°C/h, 50°C/h, 100°C/h, 200°C/h, 300°C/h and 400°C/h. The DCA- degradation rates for the commercial catalysts (Hombikat UV 100 and Kronos VLP 7001) are also included.</i>	80
<i>Table 22. Photonic efficiencies of the sulfur doped TiO₂ catalysts which were calcined for three hours at different temperatures: 550°C, 575 °C, 600 °C and 625 °C, and with different temperature profiles 10°C/h, 50°C/h, 100°C/h, 200°C/h, 300°C/h and 400°C/h.....</i>	81
<i>Table 23. The DCA-rates, DCA- relative rates and photonic efficiencies for the commercial catalysts and for the sulfur doped TiO₂ catalysts which were calcined for three hours at different temperatures 550°C, 575°C, 600°C and 625°C, calcination profiles (10°C/h and 100°C/h) and sulfur molar ratios (1:4 and 1:6 in relation to titanium (IV) isopropoxide and thiourea). The relative rates have been calculated in relation to the DCA- degradation rate of Hombikat UV 100.....</i>	87
<i>Table 24. List of the lanthanum doped TiO₂ catalysts which have been tested.</i>	89
<i>Table 25. DCA-rates, relative rates and photonic efficiencies for the lanthanum doped TiO₂ photocatalysts in dependence of the lanthanum concentration. The relative rates were calculated in relation to the Hombikat UV 100 rate corresponding to each run.</i>	91

Table 26. Comparison of initial rate constants for E. Coli inactivation with R^2 values greater than 0.90, (except for the measurement without TiO_2 catalyst) and using the lamp TQ718Z4 UV (A), obtained from exponential regression. 94

Table 27. Total rate constants for E. Coli inactivation with R^2 values obtained from exponential regression. 96

11.4 Curriculum Vitae

Personal dates:

Name: Marta Pilar Bello Lamo
Date of birth: 20th February, 1978 in Zaragoza (Spain)
Nationality: Spanish
Marital Status: single

Studies:

1996-2002 Licenciada en Ciencias Químicas (Chemistry Graduation) at the Faculty of Science in Zaragoza (Spain)

Sept. 2002- Jan.2002 Doctorate courses at the Faculty of Science in Zaragoza

Feb. 2003 -Aug.2003 Scholarship *SOCRATES-ERASMUS* at the TU Carolo-Wilhemina, Braunschweig, Institute of analytic and inorganic Chemistry (Head of teamwork Prof. Dr. P. G. Jones)

Nov.2003- Sept.2004 Practical training and Diploma Thesis in Volkswagen (Wolfsburg, Germany) at the Department of active gases treatment
 Diploma Thesis: „Untersuchungen von Einflussgrößen auf die Aktivität der NO_x-Speicherkatalysatoren für die Anwendung in Dieselfahrzeugen“

April 2005 Practice in the Institute of technical Chemistry at the Faculty of Science in Hannover (Germany) (Head of teamwork Prof. Dr. D. Bahnemann)

Since Juni 2005- PhD work at the Gottfried Wilhelm Leibniz University Hannover by Prof. Dr. D. Bahnemann about Photodetoxification of water by modified and unmodified TiO₂ in cooperation with BASF AG (Ludwigshafen, Germany)